Photocatalytic Degradation Studies using Nanocomposite of Co and N Co-doped TiO_2 Nanotubes and Reduced Graphene Oxide

Name: Tanzeela Akram

Reg. No. 00000117199

This thesis is submitted as a partial fulfillment of the requirements for the degree of

MS in Chemistry

Supervisor: Dr. Habib Nasir

Co-supervisor: Dr. M. Zahid Rana

Department of Chemistry
School of Natural Sciences (SNS)
National University of Sciences and Technology (NUST)
H-12, Islamabad, Pakistan
2017

FORM TH-4

National University of Sciences & Technology

MS THESIS WORK

We hereby recommend that the dissertation prepared under our supervision by: TANZEELA AKRAM, Regn No. 00000117199 Titled: Photocatalytic Degradation Studies using Co and N codoped TiO_2 Nanotubes and Reduced Graphene Oxide Nanocomposite be accepted in partial fulfillment of the requirements for the award of **MS** degree.

Examination Committee Members

1. Name: DR. ZAHIDA MALIK Signature:

2. Name: DR. FAHAD EHSAN Signature:

3. Name: DR. TARIQ MAHMOOD Signature:

Co-Supervisor's Name: DR. M. ZAHID RANA Signature:

Supervisor's Name: PROF. HABIB NASIR Signature:

Head of Department

29-08-17
Date

COUNTERSINGED

Date: 29/8/17

Dean/Principal

THESIS ACCEPTANCE CERTIFICATE

Certified that final copy of MS thesis written by **Ms. Tanzeela Akram**, (Registration No. **00000117199**), of **School of Natural Sciences** has been vetted by undersigned, found complete in all respects as per NUST statutes/regulations, is free of plagiarism, errors, and mistakes and is accepted as partial fulfillment for award of MS/M.Phil degree. It is further certified that necessary amendments as pointed out by GEC members and external examiner of the scholar have also been incorporated in the said thesis.

Signature: _____

Name of Supervisor: Prof. Habib Nasir

Date: 29-08-17

Signature (HoD): _____

Date: 29-08-17

Signature (Dean/Principal): _____

Date: 29/8/17

In the name of ALLAH whose worth can't be described by the speakers. (Nehj-ul-Balagha)

Dedicated to

My loving Parents Zareena Akram, M. Akram and brother Usama Akram

Acknowledgements

At first sight, I praise Allah, the almighty for providing me this opportunity and granting me the capability to proceed successfully. No doubt without his help and guidance no one can find righteous path.

"The price of success is hard work, dedication to the job
at hand and the determination that whether we win or
lose, we have applied to the best of ourselves to the task at hand."
(Vince Lombardi)

I express my cordial thanks to my thesis advisor, ***Dr. Habib Nasir*** *for his encouragement, thoughtful guidance and gracious comments. Without his help, I wouldn't have been able to complete my thesis. I would like to pay gratitude to my co-supervisor* ***Dr. M. Zahid Rana*** *and his team for his cooperation, assistance in characterization and delivery of chemicals and* ***NESCOM*** *for providing me fellowship. I am also thankful to all faculty members of the department for teaching me useful courses which helped me a lot during my research phase specially* ***Dr. Zahida Malik*** *and* ***Dr. M. Fahad Ehsan.*** *I greatly acknowledge the facilities and technical support provided by the other NUST schools like* ***IESE***, ***SCME*** *and* ***SMME***.

Finally, I would like to express my gratitude to all my righteous friends and seniors ***Sadia bibi***, ***Hadia Zahoor***, ***Huma Khizar***, ***Nitasha Komal***, ***Maryam Tahir*** *and* ***Memoona Qamar*** *for their loyal support, guidance, encouragement and prayers. Last but not the least, I express my profound gratitude to my family for providing me support and continuous encouragement.*

Tanzeela Akram

Abstract

Many types of dyes are used in textile industries and the contaminated water is expelled as it is without any treatment for the removal of dyes and harmful reagents which pose threats to human and animal health because some dyes are dangerous to chronic level. They have many short-term impacts such as skin sensitization and nausea to lingering impacts like cancer. Photocatalysis is an advanced technique from nanochemistry having many applications in daily life which cover areas from clean energy production and self cleaning surfaces to environmental protection. In this research, TiO_2 and graphite were used for the preparation of TiO_2 nanotubes and graphene oxide, respectively. TiO_2 nanotubes were prepared by hydrothermal method and Hummers' method was used for the graphene oxide synthesis. Co-doping of cobalt and nitrogen was done on TiO_2 catalysts which resulted in narrowing of band gap with increase in efficiency and thus making the process more economical. Urea and cobalt nitrate were used as nitrogen and cobalt dopant precursors, respectively. Nitrogen concentration was kept constant and cobalt was taken in 4 different concentrations i.e 0.2, 0.4, 0.6 and 0.8 g. The obtained catalysts were characterized by FT-IR, DRS, SEM, TGA, BET, XRD and EDX for the investigation of attached functional groups, band gap, morphology, thermal stability, surface area, phase and composition, respectively. Additionally the effects of doped amount of cobalt ions on the optical properties and photocatalytic activity of co-doped TiO_2 nanotubes were investigated. Methyl orange was selected for the degradation study. The results exhibited that photocatalytic performance of 4-CoN-TNT is best amongst all in the visible light. It shows efficiency of 88%. To further improve the efficiency the best catalyst was selected for the nanocomposite preparation with reduced graphene oxide. Hydrothermal method was used for nanocomposite formation and in situ reduction of graphene oxide was carried out. Again the degradation study was carried out against methyl orange. The efficiency was increased up to 93%.

Table of Contents

List of Figures

List of Tables

Abbreviations and Acronyms

BET (Brunauer-Emmett-Teller)

DMMP (Dimethyl methyl phosphonate)

DRS (Diffuse Reflectance Spectroscopy)

EDX (Energy Dispersive X-Ray Spectroscopy)

GO (Graphene Oxide)

FTIR (Fourier Transform Infrared Spectroscopy)

MO (Methyl Orange)

rGO (Reduced Graphene Oxide)

SEM (Scanning Electron Microscopy)

TNT (Titania Nanotubes)

UV-Vis (Ultra Violet-Visible Spectroscopy)

XRD (X-Ray Diffraction)

Chapter 1: Introduction

Introduction

Earth is home of millions of species but humans are dominating all and the problems we are facing today regarding climatic changes to health problems are all created by us. There are a lot of chemicals which are intentionally released to the environment without knowing their hazardous affects. And because of these chemicals we are not only harming ourselves but also other creatures of this planet. There is a need to find routes for the degradation of these pollutants for a healthier environment.

Here in this research work we have focused on the photocatalytic degradation of some hazardous chemicals.

1.1. Titania TiO_2

1.1.1. Polymorphs and properties

Titanium dioxide (TiO_2) is most widely studied metal oxide and scientists show much interest toward titania because of its versatile applications specially in photochemistry. Mostly its three crystalline forms are studied which are anatase, rutile and brookite [1] as shown in figure 1.1.

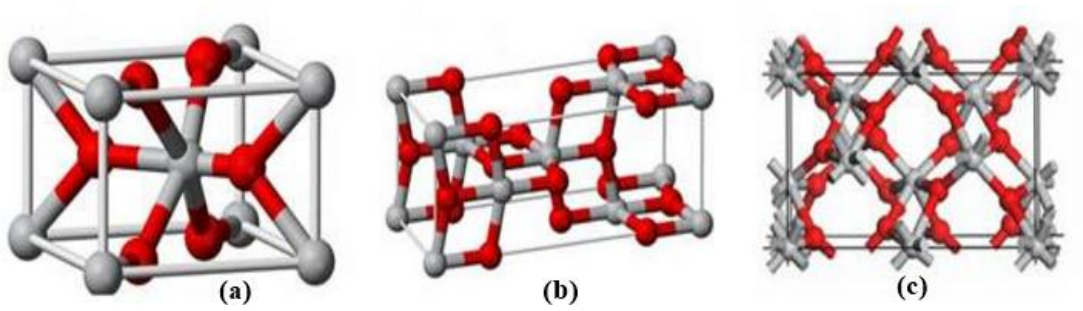

Figure 1.1 Crystal structures of polymorphs of titanium dioxide (a) rutile, (b) anatase and (c) brookite [2]

Brookite is the trivial form of TiO_2 for researchers because it's difficult to synthesize in laboratory and in nature it is not present in profusion [3]. Rutile is a well known form of TiO_2, abundantly available naturally and can easily be synthesized in laboratory [2]. Low efficiency of rutile makes it less useful as a photocatalyst. Anatase form is the most relevant form of titania in regard to photochemistry, specially because of its suitable band gap and other facinating properties [2, 4]. Table 1.1 summarizes some of the properties of the three phases of titania.

Table 1.1 Physical properties of three crystalline forms of TiO_2 [3]

Polymorph	Crystal Structure	Band gap	Refractive index	Density (g/cm^3)
Anatase	Tetragonal	3.19 eV	2.52	3.79-3.84
Rutile	Tetragonal	3.00 eV	2.72	4.13-4.26
Brookite	Orthorhombic	3.11 eV	2.63	3.99-4.11

1.2. Broad applications of titania

1.2.1. Sunscreens

TiO_2 is chemically stable and serves as a function of blocker for UVA (ultraviolet light 315-400 nm) and UVB (280-315 nm) radiations. TiO_2 has large band gap and absorbs ultraviolet light and due to this property its is used in many cosmetics as sunscreen [5].

In the presence of ultraviolet light and water, hydroxyl radicals are produced by TiO_2 which are considered as carcinogenic so titania particles should be coated with silica or alumina to restrain the contact of hydroxyl radicals with skin [6].

1.2.2. Pigment

Due to the white opaque appearance of titania it is used as a pigment. Also used as white coatings on solids, as white color in liquid paints and also as opacifier (making substances more opaque) [7].

1.2.3. Self cleaning glass

A thin transparent layer of anatase is coated on glass [8]. When light falls on the glass TiO_2 is activated. Electrons are excited and when these electrons come in contact with water, they result in the production of hydroxyl radicals. These hydroxyl radicals are responsible for the degradation of organic molecules [9, 10].

1.2.4. Gas sensor

TiO_2 is used as sensor for hydrogen gas because electric resistance of titania changes when it comes in contact with different concentrations of hydrogen gas other gas sensors can also be made [11, 12].

1.2.5. Paper industry:

Due to the white and opaque appearance of TiO_2 it is used in paper industry to enhance the paper opacity [13].

1.2.6. Semiconductors

Titanium dioxide is very common naturally occurring semiconductor. Its wide band gap and photo-stability makes it the most important semiconductor in the field of photochemistry and thus having vast applications including photo water splitting [14], dye sensitized solar cells (DSSCs) and Photo-degradation of different compounds [15-18]. The last one is concerned with the application in this study.

1.3. Nanostructured TiO_2

With the emergence of nanochemistry scientists also have studied nanoparticles of TiO_2 and found numerous applications which are basically related to large surface area and semiconducting properties. Many morphologies of titania have been developed by different scientists as shown in figure 1.2.

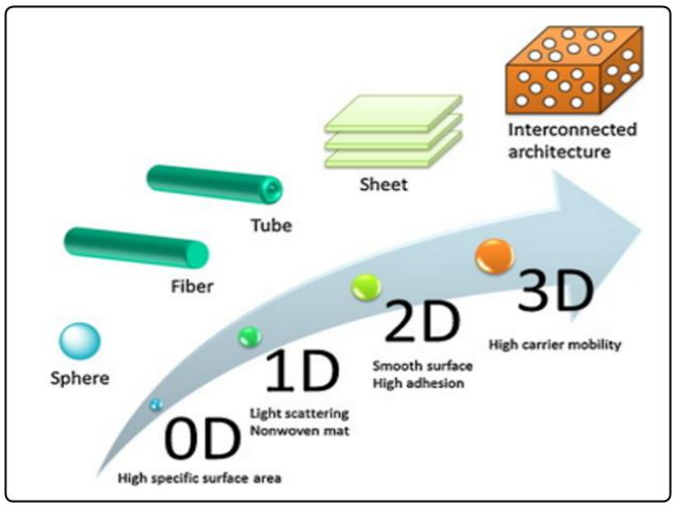

Figure 1.2 Different morphologies of TiO_2 [19]

1.3.1. TiO_2 nanospheres

When we study about TiO_2 nanostructures, maximum literature is about nanospheres. There alluring properties were reported in many research articles [20, 21]. TiO_2 nanospheres mostly posses a high surface area and pore volume which makes them quite suitable for the photocatalytic activity because the accessible surface area is increased in this way. The light harvesting properties are also increased as more light can access the interior of these materials [19].

1.3.2. TiO_2 nanotubes

In 1998 Kasuga and his coworkers for the first time synthesized titania nanotubes by hydrothermal method [22]. Since the discovery scientists are exploring different applications of titania nanotubes from dye sensitized solar cells to photocatalysis. Efforts have been made to understand the mechanism of titania nanotubes formation but scientists are not agreed on one point in this regard as different hypothesis were suggested by different scientists [23]. Mechanism of formation of nanotubes is discussed in detail in section 1.4.3.4.

These structures expected to have large pore volume and specific surface area and high surface to volume ratio, thus result in the reduction of electron hole pair recombination [24].

1.3.3. TiO_2 nanosheets

Nanosheets are often seen as flake shaped materials in scanning electron microscope (SEM). They mostly have smooth flat surface [25]. Nanosheets are of very small thickness mostly less than 10 nm and lateral size may range up to several micrometers. Because of their small thickness, smooth surface and photocatalytic property they are mostly used as coating for making self cleaning glasses [26].

1.4. Synthesis techniques of TiO_2 nanotubes

Scientists have adopted different techniques for the synthesis of TiO_2 nanotubes which are as follows and discussed in detail one by one;

- Electrochemical anodization
- Template assisted sol gel technique
- Alkaline hydrothermal method

1.4.1. Electrochemical anodization

In this technique electrochemical cell is used having one anode and cathode as shown in figure 1.3. Cathode is mostly made up of platinum (inert metal) and anode is made up of highly pure (99.9%) titanium foil. Hydrofluoric acid is mostly used as electrolyte [27-29].

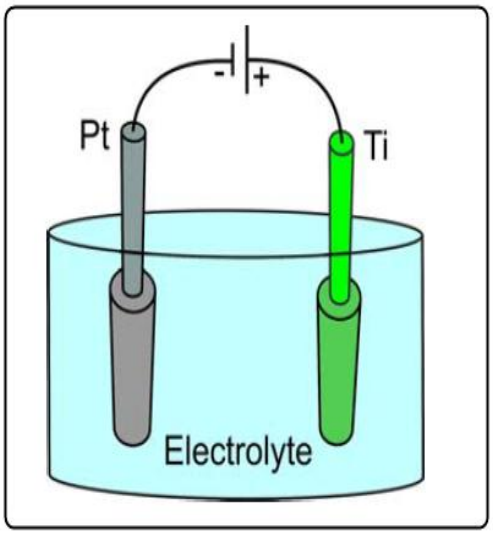

Figure 1.3 Electrochemical cell for preparation of TiO_2 nanotubes [30]

Different voltages applied and time of the process affects the morphology of TiO_2. Three operations are occurring concurrently which result in the formation of nanotubes in anodization process [29].

- TiO_2 formation by the oxidation of titanium (as titanium foil is used in the cell as anode).
- Field assisted dissolution of titanium ions in the electrolyte of the cell.
- Because of the etching by fluoride ions chemical dissolution of Ti and TiO_2.

1.4.2. Template assisted sol gel technique

This technique involves three major steps [31]

- Nanostructured template selection.
- Using a relevant technique (i.e. sol gel) for the deposition of the precursor on template.

- Removal of the precursor after acquiring certain morphology from the template by using different techniques i.e. etching and dissolution. Diagrammatic representation of these three steps is shown in figure 1.4.

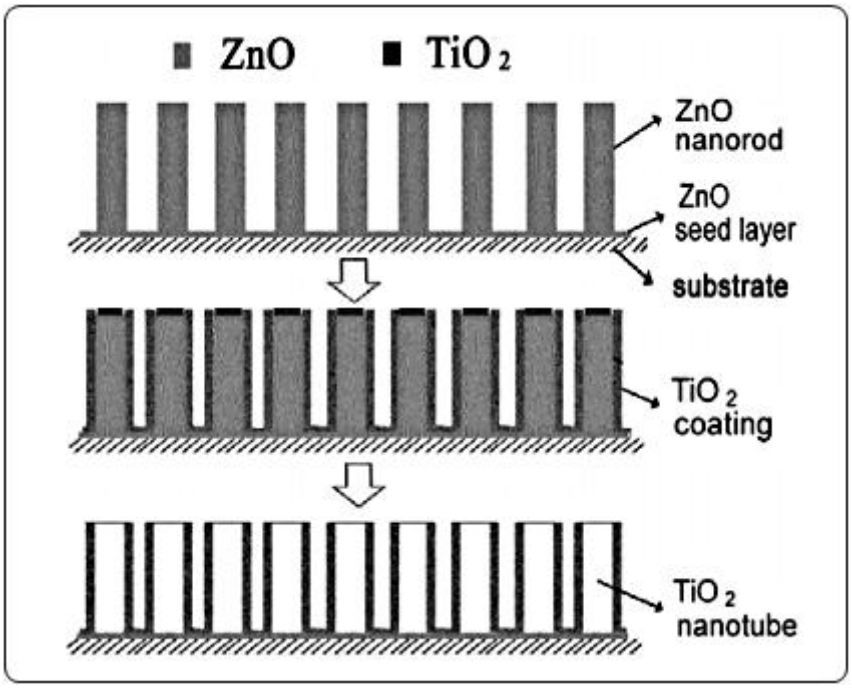

Figure 1.4 Diagrammatic representation of template assisted technique [31]

1.4.3. Alkaline hydrothermal synthesis

1.4.3.1. History

By the end of 20th century carbon nanotubes gained much interest after its discovery by lijima [32]. Much research was carried out on developing nanotubes which have remarkable novel properties. At that time many scientists work on the synthesis of metal oxides nanotubes such as Al_2O_3 [33], MoO_3 [34], V_2O_5 [35], SiO_2 [33] using different methods. Kasuga and his coworkers for the first time synthesized TiO_2 nanotubes from hydrothermal method in 1998 [22]. Since then researchers are working to enhance the properties of titania nanotubes as they have many applications from dye sensitized solar cells [36] to photocatalytic degradation studies [37].

1.4.3.2. Steps involved in hydrothermal synthesis of TiO_2 nanotubes

This method is quite simple and involves easily manageable steps which are as follows;

- Preparation of highly concentrated alkaline solution.
- Making a dispersion of TiO_2 powder in alkaline solution by continuous stirring.
- Autoclave reaction at certain temperature (110-150 degree Celsius) and duration (24-72 hours).
- Washing with dilute HCl and deionized water.
- Drying and calcination.

1.4.3.3. Parameters affecting the morphology and formation of nanotubes

There are many parameters which affect the morphology and formation of nanotubes which are illustrated in figure 1.5.

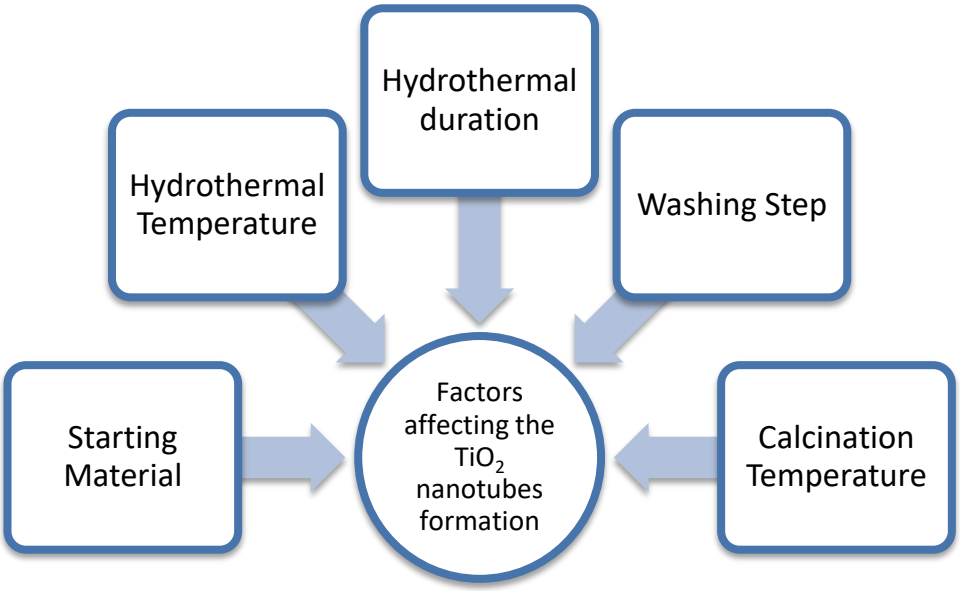

Figure 1.5 Parameters affecting the morphology and formation of nanotubes [23]

1.4.3.4. Formation Mechanism of Titania naotubes

Since the discovery of TiO_2 nanotubes scientists have been studying the mechanism of formation of nanotubes. Great diversity is seen in different scientists opinion. According to some scientists because of the highly concentrated alkaline solution Ti-

O-Ti bonds were disrupted which result in the formation of new Ti-O-Na bonds because titanium ions were exchanged with sodium ions. After the hydrothermal treatment obtained material is washed with dilute acidic solution and de-ionized water respectively. This step is pledged with the replacement of sodium ions by hydrogen ions forming Ti-OH bonds. Up to this step nanosheets of titania were formed. Dehydration results in the formation of Ti-O-Ti and Ti-O…H-O-Ti bonds whose outcome is hydrogen bonding which in return cause the decrease in bond distance of two titanium ions. As a consequence folding of sheets occurs, forming tube like structures [38]. Proposed mechanism for the formation of TiO_2 nanoubes is shown in figure 1.6.

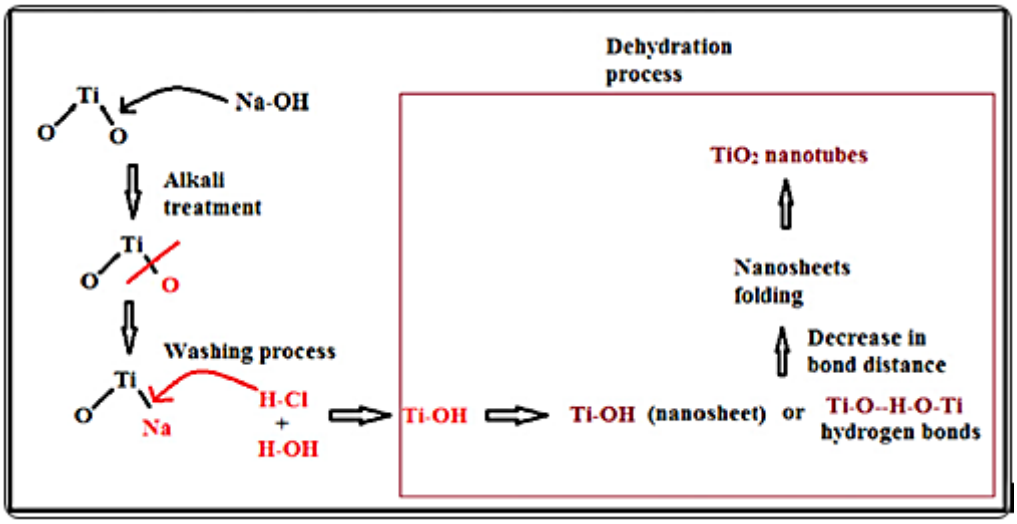

Figure 1.6 Proposed mechanism for the formation of TiO2 nanoubes [23]

Advantages of hydrothermal method [23]:

- Low energy requirement.
- Comparatively non polluting setup.
- High yield.
- Mostly pure phase is obtained.
- Simple and easy to handle.

1.5 Photocatalysis

Photocatalysis is stimulation of a chemical reaction in the presence of light. Photocatalyst and light are the key components of photocatalysis. Catalysts are actually responsible for lowering the activation energy without taking part in the. chemical reaction as shown in figure 1.7 but when we specifically talk about a

photocatalyst its play its role only in the presence of light and thus these reactions are often called as photo initiated catalytic reactions

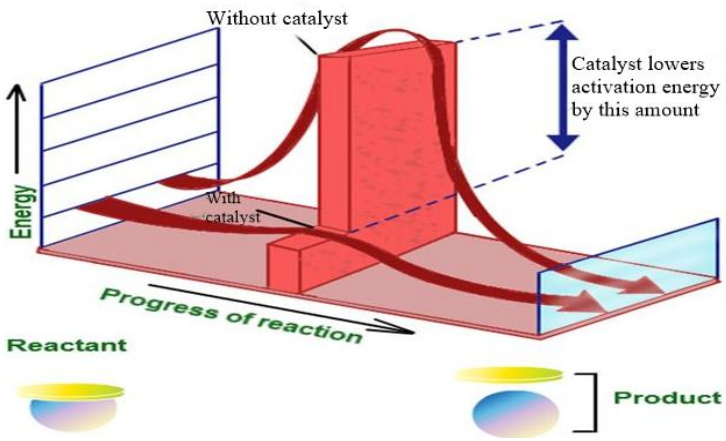

Figure 1.7 Diagramatic representation of catalyst activity

Photocatalysis is an advanced technique from nanochemistry which has many applications in daily life that's why scientist's interest in this field is continuously increasing. Applications of photocatalysis cover areas from clean energy production [39, 40] and self cleaning surfaces [41, 42] to environmental protection [43, 44].

1.5.1. Main steps involved in photocatalysis

The main steps involved in the photocatalysis are as follows [45]:

i. Photon absorption and e^-/h^+ generation
ii. Oxidation of donor specie
iii. Reduction of acceptor specie
iv. Recombination of e^-/h^+

For the practical application of the photocatalyst, reduction and oxidation are two crucial steps because real chemistry is involved in these steps as illustrated in the figure 1.8

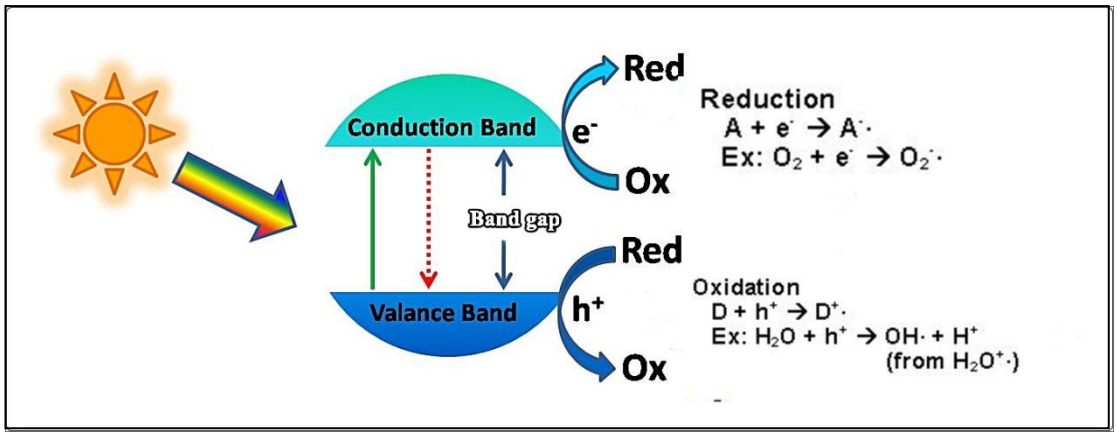

Figure 1.8 Schematic representation of a photocatalyst [46]

1.6. TiO_2 as a photocatalyst

Titanium dioxide is a white powder. The d-electron configuration of titanium is d^0 because titanium is in IV oxidation state. The white color of titanium dioxide can also be explained due to lack of metal centered and d-d transitions. Charges are transferred to metals from ligands when light is absorbed. In the case of TiO_2 electrons are transferred from oxygen to vacant d orbitals of titanium, in short from valence band to conduction band [47].

High activity of TiO_2 nanoparticles as a photocatalyst is based on following:

- High surface area because more the surface area more will be the quantity of absorbed pollutants which we want to degrade.
- Less electron hole pair recombination because more the oxidation and reduction causing species more will be the efficiency of the catalyst.

1.7. Mechanism of photocatalysis in TiO_2

When TiO_2 absorbs photon of energy equal to or more than its band gap, e^-/h^+ are formed.

$$\mathbf{TiO_2 + hv \longrightarrow h^+ + e^-}$$

When these electrons reach the surface of a catalyst they react with the atmospheric oxygen.

$$\mathbf{O_2 + e^- \longrightarrow `O_2^-}$$

Now holes are left behind due to which surface of the catalyst is positively charged so it absorbs moisture from the air and hydroxyl radicals are produced.

$$h^+ + H_2O \longrightarrow H^+ + OH^-$$

$$h^+ + OH^- \longrightarrow \text{`}OH$$

Two competing phenomenas were occurring during this process, one is the formation of electron hole pair and the other is the recombination of them [47]. The radicals produced in these reactions are highly active and are responsible for the decomposition of unwanted bacteria and hazardous materials.

1.8. Moving to visible light absorption capability

TiO_2 has a large band gap (~3.2 eV) due to which it is UV light active. Tuning of a band gap can make titania visible light active. There are some methods by which researchers are able to tune the properties i.e. band gap and photocatalytic activity of the titania some of them are discussed in detail below [47].

1.8.1. Doping

The main flaw in using titania as a photocatalyst is the large band gap and e^-/h^+ recombination [48] and because of large band gap titania is ultraviolet light active. Doping is one of the approaches by which these flaws can be minimized. The main goal of doping is to decrease the band gap and limit electron hole pair recombination which sequels to visible light active titania.

Doping is influential parameter which greatly affects the behavior of a photocatalyst. It is parallel to introducing impurities but in a different way. Scientists have doped titania by different elements including metallic and non metallic ones [49-52]. Here in this work we are interested in metallic doping. Doped metallic species restrict the electron hole pair recombination because they act as electron scavengers and thus life time of charges increases ultimately result in the increase of photocatalytic activity of the catalyst [51, 53].

1.8.2. Co-doping

Co-doping is enhanced form of doping in which semiconductor is doped with two elements instead of one. Co-doping just like as doping improves the activity of the photocatalyst by narrowing the band gap and restricting electron hole pair

recombination.

It is reported in many papers that co-doping is better than simple doping [49, 54-57]. Behnajaday and Eskandarloo reported the comparison of doped and co-doped titania. They mono-doped TiO_2 with copper and silver and then for the sake of comparison they co-doped TiO_2 with these metals and according to the study co-doping presented high photocatalytic activity [58].

1.9. Phase transformation

Anatase is less stable as compare to rutile almost at all temperatures. The temperature at which calcination process takes place during post treatment of the catalysts greatly affects the phase of TiO_2. The morphology of nanotubes is also affected by the high temperature calcinations process. From many studies it was concluded that 400 degree Celsius is the optimum temperature to restore the nanotube morphology and anatase phase [49, 55, 56]. But there are some reports which assure that up to 600 degree Celsius there is no significant phase transformation of anatase to rutile. Above 600 degree Celsius the morphology of nanotubes is also disturbed [59].

1.10. Applications of TiO_2 as a photocatalyst

Applications of TiO_2 have increased many folds in the last decade. TiO_2 is a versatile photocatalyst and has applications in many fields because of its high efficiency and stability. Figure 1.9 illustrates wide applications of TiO_2.

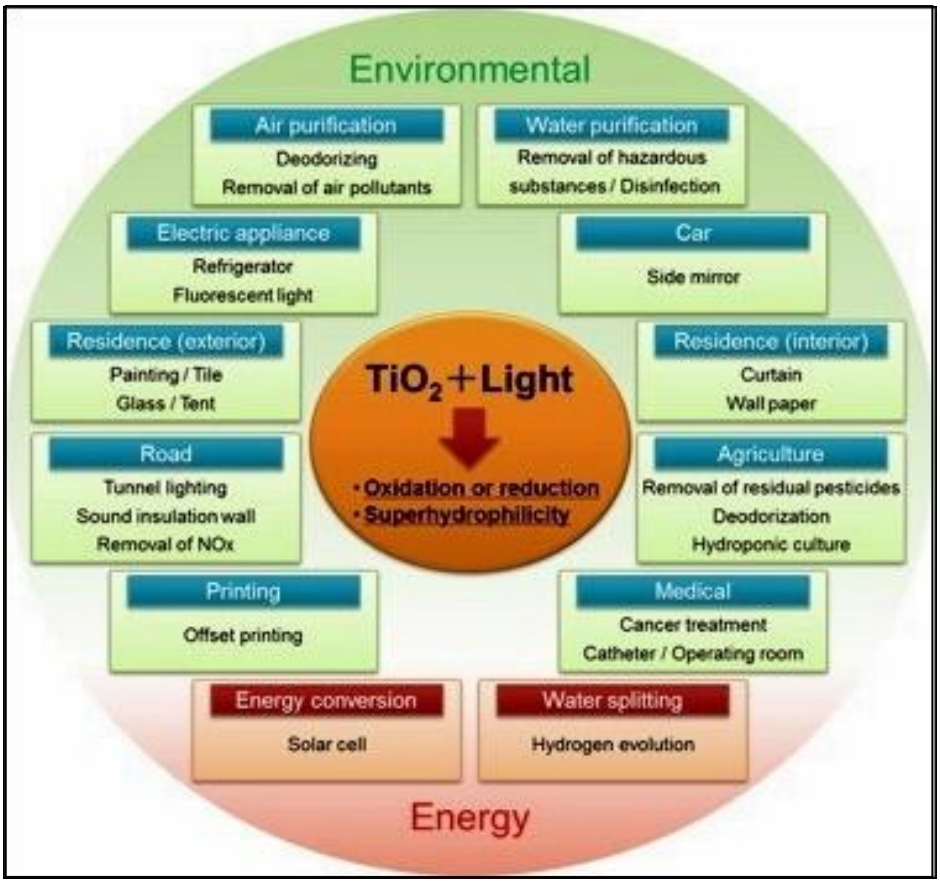

Figure 1.9 Different applications of TiO_2

1.11. Water purification by photocatalysis

Semiconductor photocatalysis for the waste water treatment has recently emerged and gained much interest. Many reports are published so far on this topic [52, 60]. An ideal photocatalyst for water purification must have the following properties [61]

- Chemically inert
- Ease to produce and use
- Activated by sunlight
- Non toxic

No catalyst fulfills all of the requirements but TiO_2 is the most promising catalyst. That's why scientists are working on this semiconductor to make it more efficient. Here in this research we are also interested in working on TiO_2 because of its fascinating properties [61].

1.12. Dyes

Dyes are sort of pigments which are used to color different substances but mostly used on fibers and leather made products. Dyes are aromatic organic compounds and have affinity for the particular substances. Most of the dyes are used in the form of aqueous solutions [62]. The solubility of dyes in water is because of the auxochromes i.e. -OH, -Cl, -Br, $-NO_2$, -COOH, -NHR, $-NH_2$ etc. Auxochromes have the ability to ionize in water thus making dyes soluble and these groups are also responsible to intensify colors of dyes. Auxochromes can be classified on the basis of their charge and nature i.e. acidic or basic [63].

1.12.1. What makes the dyes colored?

Dyes are organic aromatic compounds but they pose colors because;

- They have color bearing groups (chromophores).
- They have a conjugated system.
- They exibit resonance of electrons.
- They absorb light in visible region [63].

1.12.2. Classification of dyes

Broadly dyes are classified as natural and synthetic dyes. Animals and plants are the sources of natural dyes. Like Tyrian purple and madder are natural dyes extracted from sea snails and madder root respectively. Synthetic dyes are classified as non-azo dyes and azo dyes. Azo dyes are further classified as acidic, basic, reactive, disperse, sulphur and vat dyes. Synthetic dyes can also be classified as basic and acidic based on their nature [64]. Figure 1.10 shows the flow chart representing the classes of dyes.

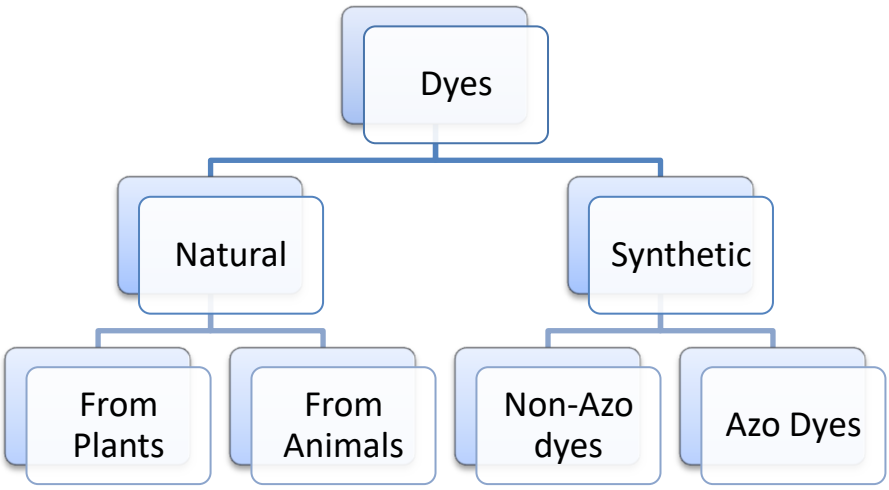

Figure 1.10 Flow chart representing classification of dyes

1.12.3. Hazards of dyes

Following are the severe hazards of dyes [65, 66]:

- Mostly dyes are water soluble and cause water pollution when expelled in rivers un-administratively from the industries.
- Dyes affect the absorption and reflection of sunlight from water thus affects the underwater photosynthetic activity.
- Many dyes are carcinogenic.
- Some dyes cause respiratory sensitization when lungs are exposed to dye dust for long time.
- Transparency of water bodies are greatly affected by the small amount of dyes which are even undetectable by human eye.
- Some dyes can cause irritation to the skin.

1.12.4 Methyl orange

Methyl orange is an orange color dye and mostly used as pH indicator as it changes its color from orange to yellow when present in more basic solutions.

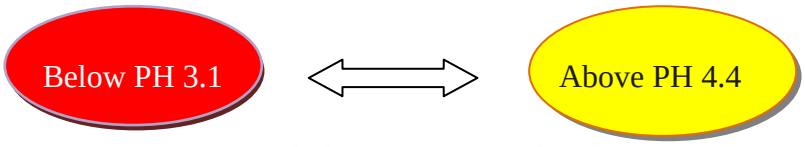

Methyl orange a pH indicator

The molecular structure of methyl orange is changed when the pH of the solution is changed which is indicated by the change in color of methyl orange. In acidic conditions hydrogen ion is attached to the nitrogen atom of N=N bond thus changing the molecular structure [67] as shown in figure 1.11 and 1.12.

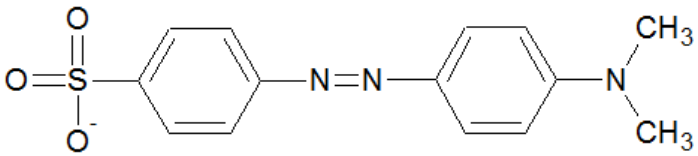

Figure 1.11 Yellow form of methyl orange

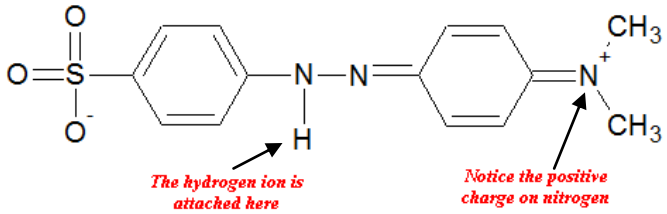

Figure 1.12 Red form of methyl orange

1.12.5 Mechanism of dye degradation by a photocatalyst

More than 7×10^5 tons of dyes are produced annually [68]. Most of them are not naturally degradable and are carcinogenic so their discharge in water is of great concern for the marine and human life. Photocatalytic degradation is a convenient way to degrade these chemicals.

Photocatalysts have the potential to generate some oxidative species when illuminated by light. These oxidative species mostly include hydroxyl radicals and singlet oxygen and these species have the ability to destroy a lot of organic molecules, dyes, pesticides and contaminants.

Proposed reaction pathway of degradation of dye using TiO_2 is illustrated in figure 1.13. First of all dye is adsorbed on the surface of photocatalyst. This step is mostly done in lab by the continuous stirring of a catalyst and dye in a suitable solvent for

some time in dark. In the second step when the photo catalyst is illuminated with light electrons jump from valence band to conduction band which results in the formation of holes in valence band of TiO_2. Here begins the main chemistry of a photocatalyst, holes may react with water molecules and form hydroxyl radicals and on the other side electrons are able to react with oxygen to form superoxide free radicals. These radicals (hydroxyl and superoxide) are very much reactive species and are responsible for the degradation of the dye after some intermediate steps. Some inorganic minerals may form out of these dyes. This is a cyclic process so after completion of one cycle photocatalyst go back to its original form to carry out another cycle. But studies reveal that after some cycles photocatalysts are no more efficient to degrade more species like dyes or pesticides because their own structure may be destroyed in the process and chemically they are no more active [52, 68].

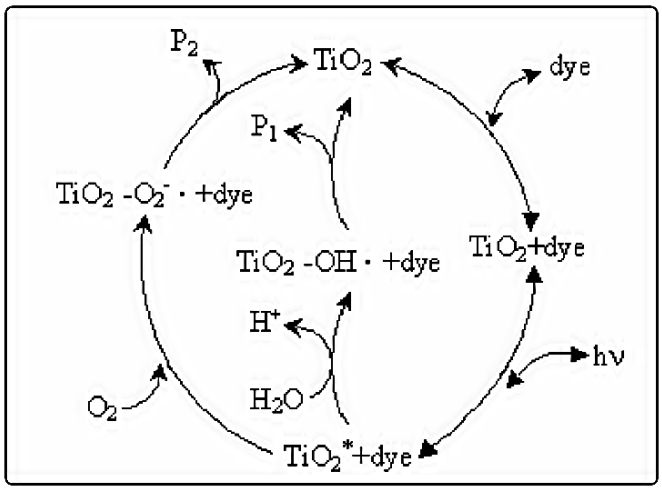

Figure 1.13 Mechanism of degradation of dye by a photocatalyst [69]

1.13. Pesticides

Pesticides are chemical compounds that are used to kill insects, pests and weeds. They usually have severe effects on central nervous system and thus cause the death of insects but large exposure to humans is also dangerous. Even some pesticides are harmful in low quantity like organochlorine pesticides. Man is using pesticides from ages without knowing the harmful and long term effects of them. When pesticides are present in water they became extremely dangerous for the cattle and human consumers. So, controlled quantity of pesticides should be released in environment according to the need.

1.13.1. DMMP as a pesticide

The current work is about the degradation of DMMP. Dimethyl methylphosphonate (DMMP) belongs to class organophosphates, having a chemical formula $C_3H_9O_3P$. The reaction between alcohol and phosphoric acid produce organophosphates which have severe effects on nervous system [70]. DMMP is used as pesticide from decades because it kills the pesticides and insects but scientists have devised other biological methods to protect the crops from weeds pests and insects which are quite safe and environment friendly. Table 1.2 represents the properties of DMMP.

Table 1.2 Properties of DMMP

Formula	$C_3H_9O_3P$
Boiling point	181ºC
Melting point	-50º C
Density	1.145 g/ml
Molar mass	124.08 g/mol
Appearance	Colorless liquid
Solubility in water	Slowly hydrolysis
Main hazards	Toxic

1.14. Chemical Warfare Agents

Many weapons of mass destruction were created after World War II but chemical warfare agents were the most ferocious one. They are more dangerous than explosives. As explosion is localized and caused by a shear force. The use of chemical warfare agents is considered as barbarous but still we see nerve gas attacks in past few years. They have devastating effects on humans as well as on other living beings. CWAs are actually incapacitating agents which alter the normal functioning of the body [71].

Effects of all CWAs to the body are not alike. They vary according to the nature of chemical. According to the chemical structure they are classified as arsenicals, organophosphorus, organoflourine and organosulphur compounds. There chemical nature is not same so they have different physiological effects on human body and thus classified accordingly as [71]:

- Nerve agents
- Blistering agents
- Choking agents (pulmonary agents)
- Riot-control agents (tear gases)
- Bloods agents (cyanogenic agents)
- Psychomimetic agents
- Toxins

1.14.1. Nerve agents

As the name indicates they affect the nervous system. All of them are synthetic and listed as most threatening chemicals. They are more toxic than any other chemical warfare agents and have the ability to cause death even in few minutes depending upon the concentration [72]. All of them are colorless liquids in the pure form. Depending upon the volatility and stability they are classified as G-agents and V-agents. V-agents are more stable ones having low volatility [71].

The mode of action of most of them is similar. In our body there are billions of neurons. The region where one nerve ends and the other nerve outset is known as synapse. It is actually in the form of small cavity like region as shown in fig. 1.14. The two nerves communicate by the neurotransmitters. When nerve impulse reaches the end of pre-synaptic nerve it releases neurotransmitters like acetyl choline. These chemicals are received by the receptors present on the post synaptic nerve. After the message transmission there are some enzymes which cause the degradation of these neurotransmitters like for acetyl choline, acetylcholinesterase is present which is responsible for the degradation of acetyl choline. Nerve agents actually block the sides of these enzymes and thus they are no more able to degrade the particular neurotransmitter for which it is meant as shown in fig. 1.15. As a result post synaptic nerve is triggered aggressively and nerve impulse communication occurs in uncontrolled way resulting many problems in body like constriction of eye pupil, running nose, watery eyes, extreme sweating, urination, increased production of saliva, abnormal heart rate, blood pressure, muscular twitches, cramps, inhibition of respiratory center and eventually death [71].

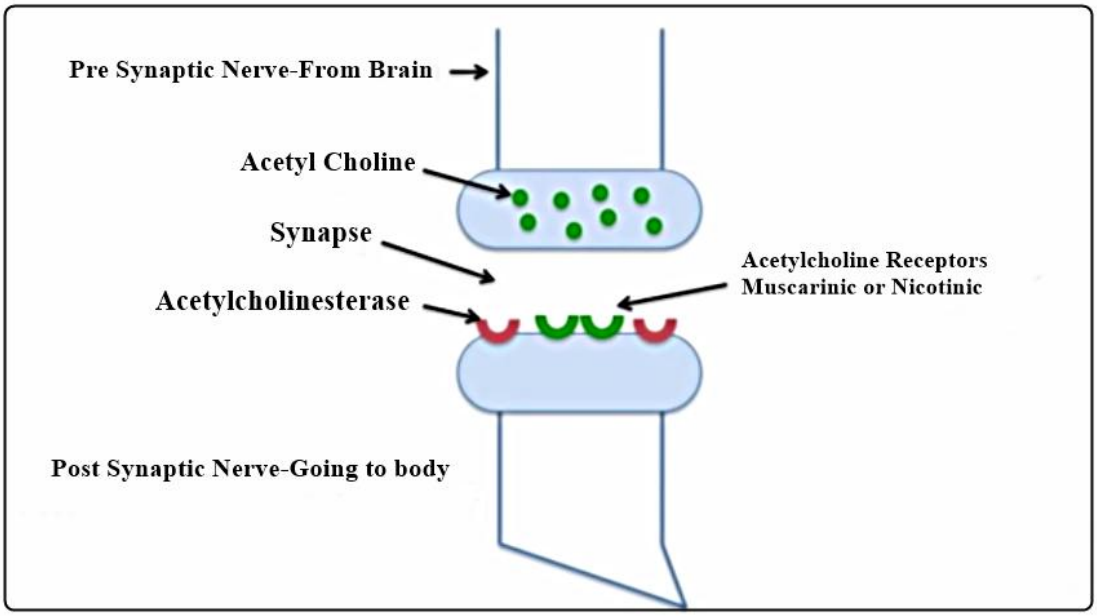

Figure 1.14 Pictorial representation of a nerve communication system

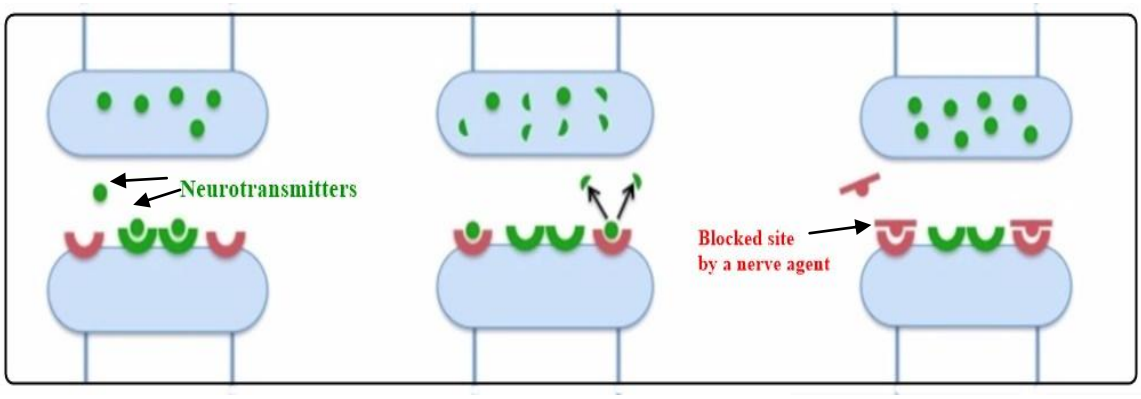

Figure 1.15 Schematic representation how nerve agent work

1.14.2. DMMP as a nerve agent simulant

Decontamination of these extremely toxic chemicals is necessary in some conditions. Different physical and chemical methods have been devised for this purpose as nerve agents have incapacitating effects on humans which are irreversible. Studying nerve agents directly can be fatal for this purpose scientists choose some simulants which are like some of the nerve agents in properties and chemical nature but are less toxic in comparison [73]. DMMP is also a simulant of sarin (a nerve agent) [74]. In our study we used sarin simulant DMMP for studying the photocatalytic degradation.

1.15. Graphene

Carbon exists in many allotropic forms as shown in figure 1.16. Some of them are well known like diamond and graphite and have wide applications in diverse areas because of their hardness and softness respectively. Fullerens [75] and carbon nanotubes [32] are two other forms of carbon recently discovered and are attaining great interest of scientists.

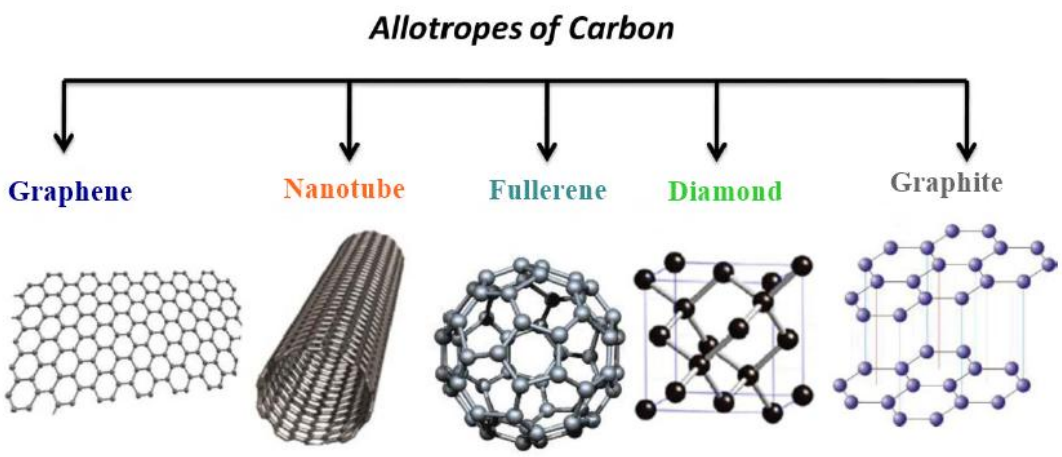

Figure 1.16 Allotropes of carbon

There is another two dimensional allotrope of carbon known as graphene. At the University of Manchester, Andre Geim and Kostya Novoselov isolated the one atom thin layer of graphite known as graphene in 2004 using top down approach [76] as illustrated in figure 1.17. For their pioneer work they were awarded noble prize 6 years after their research work, in 2010.

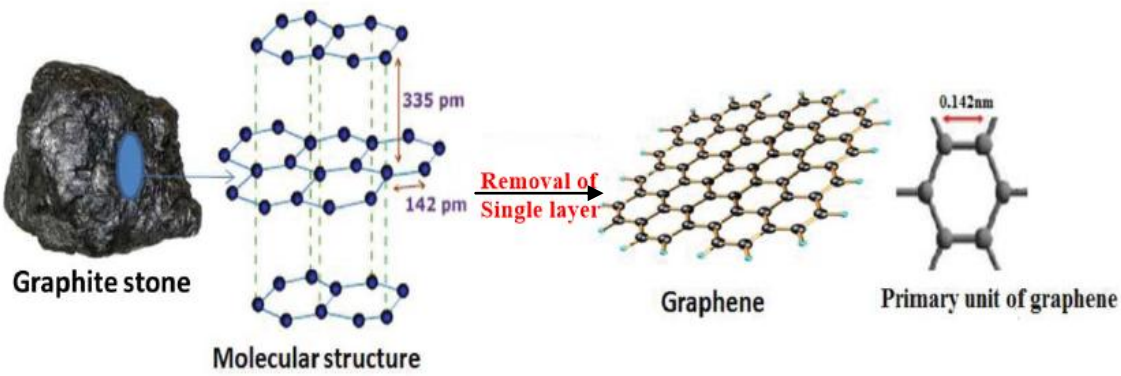

Figure 1.17 How graphene was formed

Graphene is 2D allotrope of carbon and is considered as the building block of many allotropic forms of carbon like stacking of these sheets form 3D graphite form, rolling of this sheet can form 1D single wall carbon nanotube and rapping gives the 0D bucky ball structure.

1.16. Graphene oxide

Graphene oxide is the oxidized form of graphene. It is produced by the oxidation and exfoliation of graphite. The oxidation of graphitic layers results in the attachement of various functional groups on the carbon planes. These intercalated functional groups result in the weakening of the van der waals forces present between carbon planes. Figure 1.18 clearly show the difference between graphene and graphene oxide.

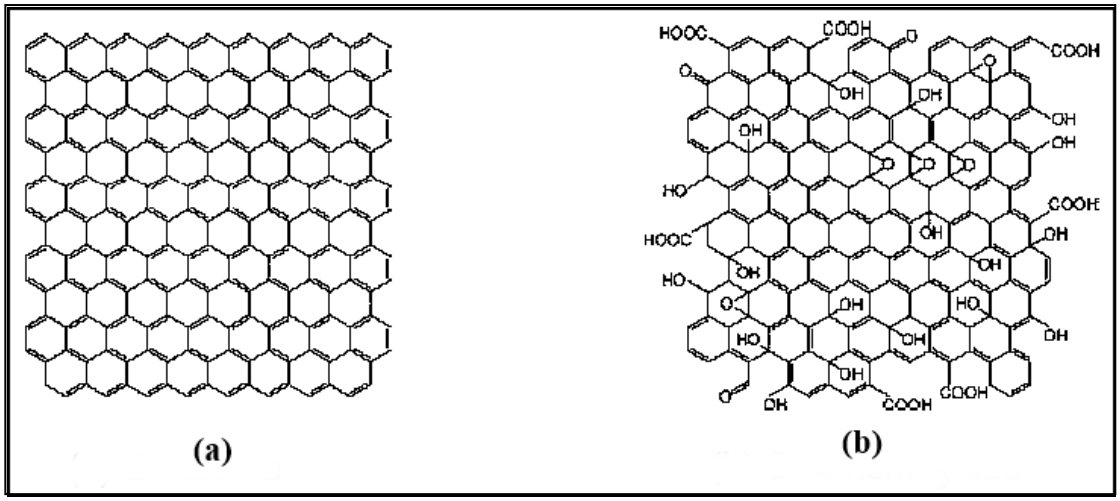

Figure 1.18 (a) Graphene and (b) Graphene oxide

There are two types of carbon atoms in graphene oxide: Carbon atoms bonded to different functional groups and the carbon atoms involved in the formation of aromatic rings. The ratio of these two types of carbon atoms or regions illustrates how much oxidation is done. The functional groups are actually present on both sides of the plane [77]. Hydrophilic nature of graphene oxide is because of these functional groups so stable aqueous dispersions can be made. Water molecules form hydrogen bonding with the covalently bonded oxygen molecules of GO [78, 79]. Figure 1.19 illustrates the hydrogen bonding between oxygen functionalities and water molecules.

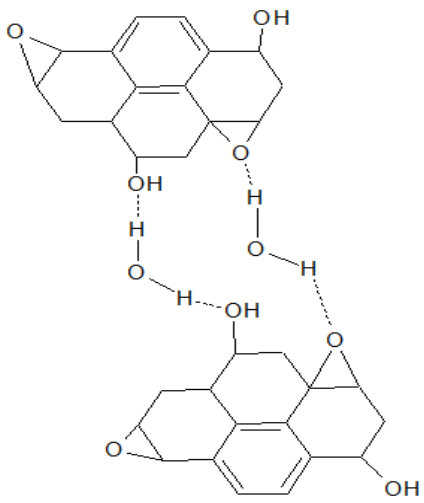

Figure 1.19 Hydrogen bonding between grapheen oxide layers [78]

1.17. Synthesis route of Graphene/ Inorganic nanostructure composite

1.17.1. In-Situ chemical synthesis

This method is very much suitable for the preparation of graphene/inorganic nanostructure composite [80]. The very first step for the synthesis of nanocomposite by this technique is the interaction between positively charged metal atoms and negatively charged electron cloud of oxygen atoms bonded with GO [81].

1.17.2. Microwave heating

Microwave heating is quite different from ordinary heating so use of this technique for the synthesis of nanostructures is more dependent on the properties of material being used rather than process conditions. For a very short time highly localized heating results in the formation of very fine particles [82, 83].

1.17.3. Hydrothermal and solvothermal techniques

It is a well known technique for the synthesis of nanostructures at high temperature and pressure. The process is carried out in a closed system and mostly the solvent used is water so this technique is considered as environmental friendly. Highly pure crystals can be formed in bulk amount depending on the capacity of the vessel of autoclaves so this method gains a lot of interest by the researchers. There are many reports for the synthesis of graphene/inorganic nanostructures composites based on this technique: CuO/graphene [84], ZnO/graphene [85] and SnO_2/graphene [86].

It is not compulsory to use water as a solvent some other solvents can also be used like ethanol, methanol etc. If the reaction medium is not based on water then this technique is known as solvothermal technique.

1.18. Applications of graphene/inorganic nanocomposites

1.18.1. Sensor

In literature there are a lot of examples of graphene based sensors [87-89]. These sensors are mostly less time consuming and cheap. Nanostructures have large surface area and high chemical and thermal stability when decorated on the surface of graphene sheets so the composite formed have remarkable properties to use as a gas sensor [90, 91].

1.18.2. Supercapacitor

Supercapacitors are different from ordinary capacitors as they exhibit high energy density [92]. In 1957 supercapacitors were introduced for the first time publically [93]. Areas in which we require rapid charge discharge cycles we use supercapacitors rather than simple capacitors because they are mostly meant for short term energy storage. The use of titania in these supercapacitors as electrode has proven to increase the capacitance [94-96].

1.18.3. Photocatalysis

Our world population is increasing day by day which results in increment of pollutants in the environment. Various sectors are involved in this like agriculture human waste and above all industries. 783 million people in the world do not have approach to fresh and clean water for drinking due to which death rate because of diseases caused by unhealthy drinking is increasing [97]. So, photocatalysis is an easy and safe approach to degrade the pollutants in air as well as in water to get healthy clean environment around the world. There are many photocatalysts known which degrade the pollutants among them TiO_2 gain much interest but it has some draw backs which are discussed in previous sections. Related draw backs can be minimized by the graphene/TiO_2 nanocomposite formation.

When light falls on a photocatalyst i.e. TiO_2 the photocatalyst become excited and the electrons jump from valence band to conduction band, these electrons are then

transferred to the graphene sheets thus resulting in the less electron hole pair recombination. Fig. 1.20 portrays this phenomenon clearly.

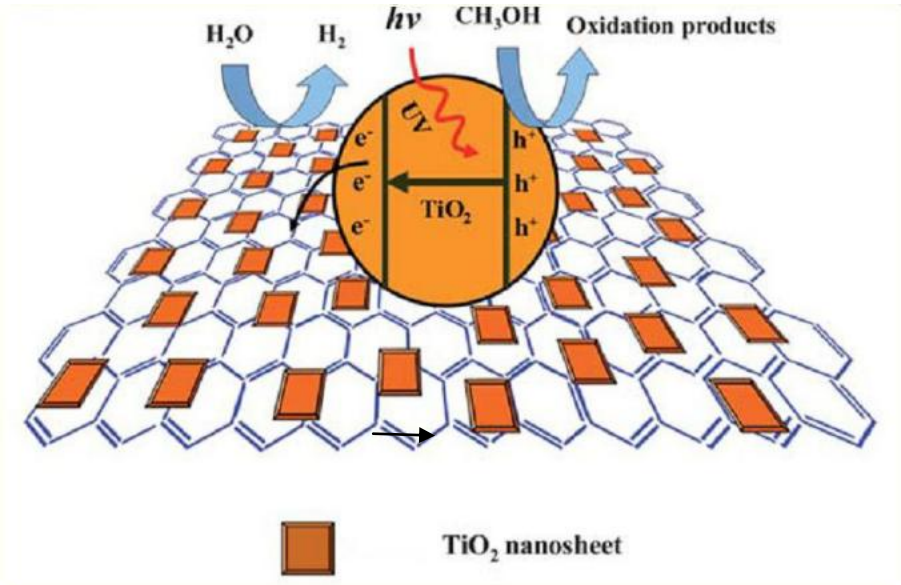

Figure 1.20 Functioning of graphene/TiO_2 nanocomposite [98]

1.19. Structure and objectives of thesis

This thesis describes an effort to produce TiO_2 nanotubes using hydrothermal synthesis. Major task of the present work was to make titania visible light active by doping, co-doping and nanocomposite formation side wise controlling the morphology.

Chapter 1 includes the introduction about the research work done. Chapter 2 summarizes different reports related to this work. Methods and techniques of experimentation and description of characterization techniques are described in chapter 3. In chapter 4 results and discussions are listed side wise the degradation study. Finally conclusion is engrossed in chapter 5.

Detailed objectives of this work are:

- Preparation of titania nanotubes.
- Doping and codoping of these nanotubes to decrease the band gap in order to make titania visible light active and more efficient against pollutants degradation.
- Characterization of prepared catalysts.

- By carrying the photocatalytic degradation studies against methyl orange sorting out the best catalyst.
- Preparation of nanocomposite of the best catalyst with graphene oxide in order to further improve its activity against any dye or pesticide degradation.
- Degradation study of DMMP (a warfare agent simulant and pesticide).

Chapter 2: Literature Survey

This chapter includes reports in literature related to this work. This chapter is devised into seven sections. In section 2.1 photocatalysis is discussed generally, section 2.2 is about TiO_2 naotubes and having subsections including different methods for the synthesis, section 2.3 includes reports about nitrogen doped TiO_2 nanotubes, section 2.4 is about cobalt doped nanotubes, co-doping related reports are discussed in section 2.5, section 2.6 is explaining different reports about graphene oxide and titania composites and in the last section reports about degradation of methyl orange was discussed.

2.1. Photocatalysis

Photocatalysis is the stimulation of a chemical reaction in the presence of light. When light having energy equal to or more than the band gap of the catalyst is interacted with catalyst the catalyst become activated. Electrons jump from valence band to the conduction band. This excitation results in the formation of the e^-/h^+. These electron hole pairs are responsible for the degradation or breakdown of certain chemicals or pollutants. Following is the reaction mechanism of whole process;

$$\text{Catalyst} + \text{Photon} \longrightarrow \text{holes}^+ + \text{electrons}^-$$

$$\text{holes}^+ + \text{electrons}^- \longrightarrow \text{energy}$$

$$H_2O + \text{holes}^+ \longrightarrow {}^{\cdot}OH + H^+$$

$$O_2 + \text{electrons}^- \longrightarrow O_2^{\cdot -}$$

$${}^{\cdot}OH + \text{substrate} \longrightarrow H_2O + CO_2$$

$$O_2^{\cdot -} + H^+ \longrightarrow {}^{\cdot}OOH$$

$${}^{\cdot}OOH + {}^{\cdot}OOH \longrightarrow H_2O_2 + O_2$$

$$O_2^{\cdot -} + \text{substrate} \longrightarrow CO_2 + H_2O$$

$${}^{\cdot}OOH + \text{substrate} \longrightarrow CO_2 + H_2O \text{ [99]}$$

2.2. TiO_2 nanotubes as a photocatalyst

In 1990's Iijima discovered carbon nanotubes [32]. This discovery unfolded new routes in material science sector. Many scientists successfully prepared nanotubes of different materials. TiO_2 nanotubes were prepared by Kasuga in 1998 by the hydrothermal method [22]. After its discovery many scientists devise different methods for the synthesis of titania nanotubes. Scientists are more interested in this morphology because these structures are expected to have large pore volume and specific surface area and high surface to volume ratio, thus result in the reduction of electron hole pair recombination [24]. Here are some reports related to the synthesis methods of titania nanotubes.

2.2.1. Anodization method

In this technique electrochemical cell is used having one anode and cathode. Cathode is mostly made up of platinum (inert metal) and anode is made up of highly pure (99.9%) titanium foil.

Dawei Gong, Craig A. Grimes and Oomman K.Varghese 2001 reported the synthesis of TiO_2 nanotubes from anodization method for the first time. Fabrication of titania nanotubes was done by anodic oxidation of titanium foil in electrolytic cell. Hydrofluoric acid was used as an electrolyte. Nanotubes were properly aligned in the form of arrays. One end of these tubes was open and the other end was closed. The diameter of nanotubes was from 25-65 nm. Diameter of nanotubes was identified as dependent on the applied voltage, as the voltage was increased diameter was also increased but the length was independent of the voltage applied [100].

Qi Li and Jian Ku Shang, 2009 successfully synthesized titania nanotubes from anodization method. Titanium foil was used for the preparation of nanotubes. Prior to anodization titanium foil was sonicated in ethanol, acetone and de-ionized water respectively. Glycerin and DI water in the volume ration of 9:1 was used as electrolyte. Glycerin was used because it resists the change in pH and thus promotes the smooth nanotubes formation. NH_4F and NH_4Cl were also added to electrolyte and the final concentrations of both were 0.36 M and 0.25 M respectively. FESEM analysis was done after different time intervals from 30 minutes to 3 hours and results revealed that after 30 minutes no proper nanotubes was seen but 3 hrs anodization show complete nanotubes formation [101].

2.2.2. Sol-gel method

T. Maiyalagan, B. Viswanathan and U. V. Varadaraju, 2006 synthesized TiO_2 nanotubes by simple sol-gel template assisted method. Alumina membranes were used as template and titanium isopropoxide was used as a precursor for the synthesis of nanotubes. Titanium isopropoxide and 2-propanol was used in the ration of 1:20 and alumina template membrane was dipped in the solution. After air drying and heating in the furnace alumina template was dipped in 3 M solution of NaOH. NaOH and dissolved anodic alumina was then removed by several washings with distilled water. TiO_2 nanotubes formed in this process are straight and dense having outer diameter of 200nm [102].

Zhuowei Cheng and Zhiqi Gu et al., 2016 reported the synthesis of TiO_2 nanotubes by a combination of sol gel and hydrothermal method. Titanium butoxide $Ti(O\text{-}Bu)_4$ was used as a precursor of TiO_2 nanotubes. After preparation of a solution of titanium butoxide and precursors of dopants the solutions were mixed together by drop wise addition and after achieving complete hydrolysis final solution was aged for 6 hours and then dried at 80 ºC. Obtained gel was then mixed with 10M NaOH and suitable solvents. Hydrothermal heating at 130 ºC for 48 hrs was applied to the mixture. Obtained sample was then washed with HCL and deionized water to obtain 7 pH. After drying and calcinations TiO_2 nanotubes were obtained [103].

2.2.3. Hydrothermal method

In 1998 Kasuga discover titania nanotubes. He used hydrothermal method for the synthesis. Later on many scientists followed his procedure and study different parameters affecting different properties of titania nanotubes. Here are some reports related to hydrothermal synthesis of nanotubes.

G. H. Du, Q. Chen et al., 2001 successfully prepared TiO_2 nanotubes by hydrothermal method. They have used tetrabutyl titanate for the preparation of TiO_2 crystals. The hydrothermal temperature was set at 130 ºC for 24-72 hours. According to TEM analysis nanotubes have the diameter of 8-10 nm and length is up to several hundred nanometers. They have calculated the atomic ratio of O/Ti which varies from tube to tube. The nanotubes they have prepared are multi walled analogous to carbon nanotubes and the spacing between each shell is 0.75 nm [104].

Xiaoming Sun and Yadong Li, 2003 prepared titania nanotubes under hydrothermal conditions. They optimize the temperature from 100-180 ºC for more than 48 hours. The nanotubes they have prepared have the inner diameter of 5 nm and outer diameter is of 10 nm and the length is ~300 nm. Nanotubes were dispersed in alcohol using ultrasonicator which results in the transition of morphology. Mechanism of the formation of nanotubes was also studied and according to them for the stability of framework sodium ions play vital role and ion substitution have significant effect on many properties of nanotubes specially the optical properties are affected [105].

Chien-Cheng Tsai and Hsisheng Teng, 2004 synthesised the titania nanotubes from TiO_2 nanoparticles by using hydrothermal method. They studied the effect of temperature on nanotubes. Duration of autoclave heating was fixed (24 hours). Temperature was optimised from 110-150 ºC. According to these scientists hydrothermal temperature have significant effect on the structure of nanotube and anatase to rutile transformations at high temperatures. Surface area increases with the increase in temperature up to certain extent. Maximum surface area i.e. 400 m^2/g was obtained at 130 ºC. And according to their discovery size of nanotubes can be modified by changing the pH of washing solution [106].

Dmitry V. Bavykin and Valentin N. Parmon et al., 2004 studied the effect of different hydrothermal conditions on the structure of titania nanotubes. They study the temperature range from 120-150 ºC and according to their study the diameter of nanotubes increases with increase in temperature. When temperature was increased further it results in the formations of non hollow TiO_2 nanofibers, having diameter ~75 nm. The ratio of weight of TiO_2 to the volume of NaOH solution also have a significant effect on average diameter of nanotubes. When TiO_2 to NaOH molar ratio is increased it results in the increase in average diameter of nanotubes and decrease in surface area [107].

B Poudel and W Z Wang et al., 2005 reported the titania nanotubes transformation into nanowires. They have successfully prepared titania nanotubes of outer diameter 9 nm, wall thickness of about 2.5 nm and length of about 600 nm by simply using the hydrothermal method. When calcination was done above 650 ºC the nanotubes were transformed to nanowires. According to them highly crystallized nanotubes were only prepared in optimized conditions. The purity and crystallinity of nanotubes is affected

by the volume filling fraction of autoclave and the concentration of the acid used for washing after hydrothermal reaction [108].

Mohd Hasmizam Razali and Ahmad-Fauzi Mohd Noor et al., 2012 studied the effect of pH of washing solution on the nanotubes formation. Sodium titanate nanotubes were prepared when the pH of washing solution is 12 and hydrogen titanate nanotubes were obtained when the pH is 7. Thermal stability was also monitored. Sodium titanate nanotubes were stable up to 500 ºC and above 700 ºC this nanotube morphology was changed to nanorods. Titania naotubes were formed from hydrogen titanate nanotubes when heated up to 300 ºC for 2 hours. When the temperature was increased up to 500 ºC the small segments were produced from large nanotubes and at 700 ºC nanotubes morphology was totally collapsed and small nanoparticles were formed [109].

Kalithasan Natarajan and R. I. Kureshy et al., 2016 synthesized the TiO_2 nanotubes from TiO_2 nanoparticles. Simple hydrothermal method was used. Hydrothermal temperature was set at 130 ºC for 48 hours. Calcination was done at two different temperatures i.e. 250 ºC and 450 ºC. They have used the titania naotubes for the degradation of indigo carmine dye under UVLED irradiation. According to their kinetic study, degradation of the dye follows first order kinetics. The effect of morphology on band gap was studied and according to the analysis and calculations band gap is not affected by morphology as titania nanotubes has the same band gap as of the simple titania nanoparticles [110].

2.3. Nitrogen doped TiO_2 nanotubes

Nitrogen doping in the TiO_2 lattice succeed to persuade new band states in the band gap of titania which results in the absorption edge shifting to visible region [111]. In the past few years enough work was done on nitrogen doping.

Here are some related reports;

Hiromasa Tokudome and Masahiro Miyauch, 2004 prepared nitrogen doped TiO_2 nanotubes by wet process. For the preparation of TiO_2 nanotubes simple hydrothermal method was used. Nitrogen doping was done by immersing the undoped nanotubes in ammonia solution (1.0 M) for 15 hours. According to the report nitrogen from ammonia substitute the oxygen atoms in the lattice of TiO_2. By doping nanotubes

become visible light active. The activity of the catalyst was checked against degradation of gaseous isopropanol and even in water activity of the catalyst was not decreased [50].

Jiaqing Geng and Dong Yang et al., 2009 prepared TiO_2 nanotubes by hydrothermal method. Hydrothermal temperature was set at150 ºC for 72 hours. After nanotubes preparation nitrogen doping was done by dispersing nanotubes in guanidine carbonate. They use these nitrogen doped nanotubes for the degradation of methylene blue in artificial solar light and concluded that doped nanotubes show higher efficiency then the undoped ones [111].

Dong Lin and Cao Guo-xi et al., 2009 prepared TiO_2 nanotutbes by anodization method. For the growth of oxide nanotube arrays titanium foil was used as a substrate. Titanium foil was used as cathode in the electrolytic cell. For nitrogen doping the as prepared nanotubes were soaked in aqueous ammonia solution and annealed in ammonia atomosphere. Nitrogen from ammonia is responsible for doping in the titania lattice. According to the analysis nitrogen doped nanotubes show highly ordered structures and has less phase transformation at high temperature. Degradation of methyl orange was studied under visible light using these doped and undoped nanotubes and the results revealed that doped nanotubes show better activity [112].

Yue-Kun Lai and Jian-Ying Huang et al., 2010 fabricated highly ordered nitrogen doped TiO_2 nanotubes using anodization method. 1 molar ammonia solution was used for nitrogen doping. The effect of different annealing temperatures was also studied on the morphology, photoabsoption and photoelectrochemical properties. According to this study above 450 ºC nanotubes structures started collapsing and morphology was disturbed. They studied the degradation of methyl orange. Nitrogen doped catalysts show better results then undoped catalysts. The intermediates forms during the degradation of methyl orange as shown in figure 2.1 were analyzed by liquid chromatography and mass spectrometry [113].

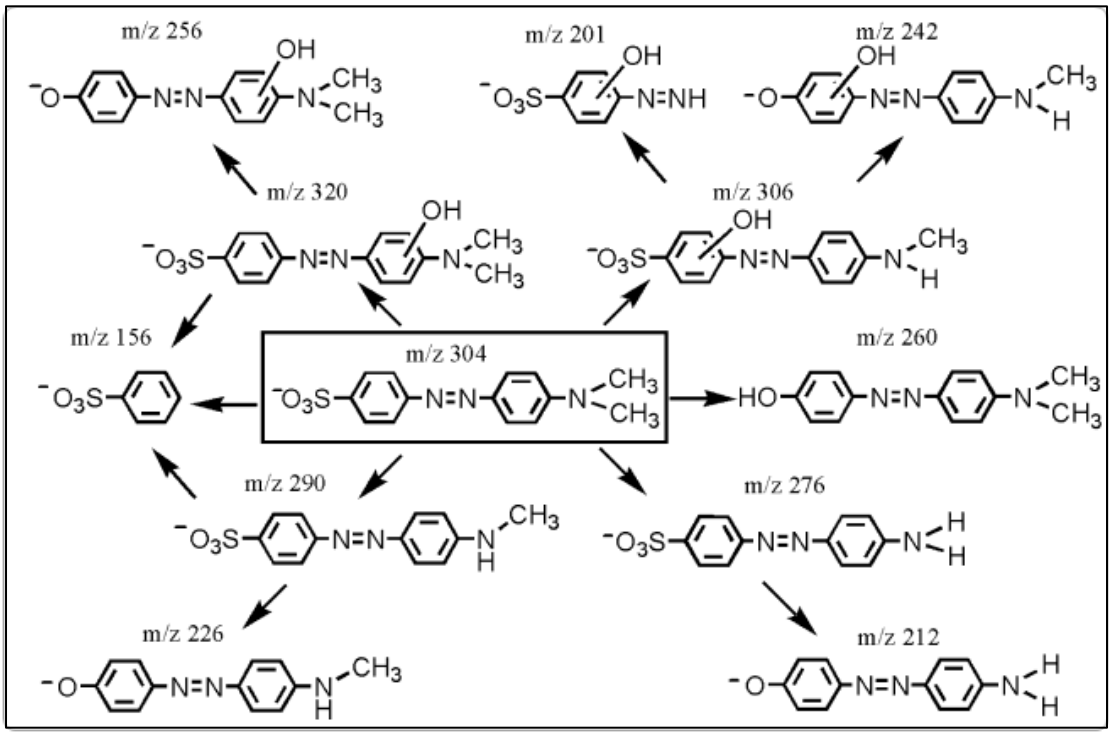

Figure 2.1 Proposed intermediate products during degradation of methyl orange [113]

Jingjing Xu and Yanhui Ao et al., 2010 synthesized TiO_2 nanotubes by anodization method. Hydrazine hydrate was used for nitrogen doping. The atomic ratio of nitrogen to titanium was 8/25 which was calculated by EDX. Photoelectrochemical and photocatalytic properties of doped and undoped catalysts were studied. According to the results photocurrent of undoped nanotubes was nearly half as that of nitrogen doped nanotubes. Photocatalytic degradation of a dye was studied and according to the study 99% dye was degraded in 105 minutes by the doped nanotubes side wise undoped nanotubes are able to degrade only 59% dye in same time period [114].

Rajini P Antony and Tom Mathews et al., 2012 prepared vertically aligned nanotube arrays by anodization method. Titanium foil (1 × 1 cm) and urea was used as precursor of titania nanotubes and nitrogen respectively. It is a single step electrochemical synthesis which is cost effective and efficient. Nitrogen doping was confirmed by XPS. By the incorporation of nitrogen in the lattice band gap of titania is reduced due to which alteration in many properties were observed. Here in this work enhancement of field emission in doped nanotubes was reported [115].

Cheng-Ching Hu, Tzu-Chien Hsu and Shan-Yu Lu, 2013 prepared nitrogen doped TiO_2 nanotubes by a one step cohydrothermal synthesis. Urea was used for nitrogen

doping. XPS confirm the Ti-N-O and Ti-O-N bonds in the lattice which assure the successful doping of nitrogen. Rhodamine B was used to study the photocatalytic activity of the catalysts. According to the study as the nitrogen concentration increases the photocatalytic activity also increases up to a certain limit and after that nitrogen doping had no effect. Morphology was also affected by the increase in urea loading; the nanotubes transforms themselves to agglomerated particles after certain concentration of urea [116].

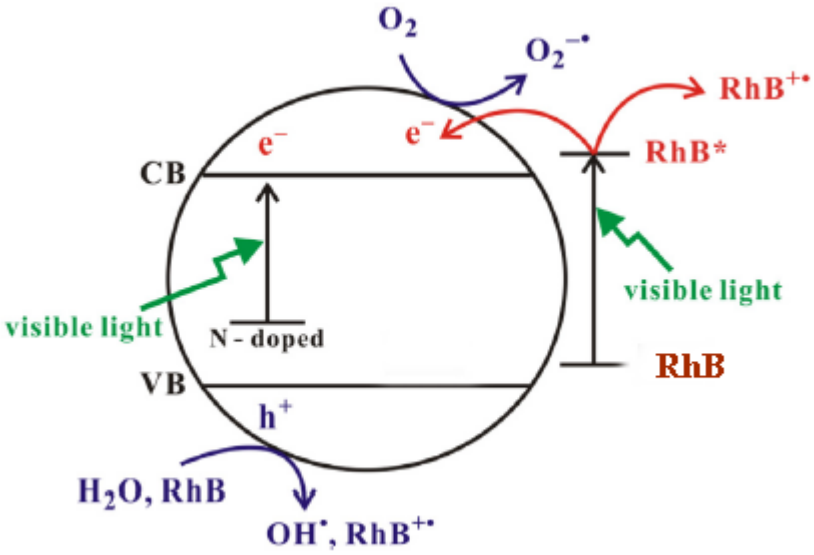

Figure 2.2 Illustration of degradation of rhodamine B by the nitrogen doped catalyst [116].

2.4. Cobalt doped TiO_2 nanotubes

The main goal of doping is to decrease the band gap and limits electron hole pair recombination which sequels to visible light active titania. Doping is influential parameter which greatly affects the behavior of photocatalyst. Doping is parallel to introducing impurities but in a different way.

Here are some reports related to cobalt doping:

Chien-Te Hsieh and Wen-Syuan Fan et al., 2009 synthesized cobalt doped titania naotubes by using cobalt nitrate as precursor of cobalt. Cobalt doping was done by simply adding 0.01 M solution of cobalt nitrate side wise other reported chemicals in the autoclave. The hydrothermal temperature was set at 135 ºC for 24 hours. Cobalt doping and nanotubes formation occur simultaneously. Nanotubes synthesized have high porosity and specific surface area as compare to the precursor i.e. TiO_2 powder.

The activity of cobalt doped and undoped TiO_2 nanotubes were checked against degradation of a basic dye BV 10 and they concluded that cobalt doped nanotubes show better results then undoped [37].

Jung-PinWang, Hsi-Chi Yang and Chien-Te Hsieh, 2012 synthesized highly porous cobalt doped TiO_2 nanotubes by hydrothermal method. Commercially available TiO_2 powder and 0.01 molar solution of cobalt nitrate was used as precursor of titania nanotubes and cobalt doping respectively. The outer diameter of nanotubes was 10-15 nm and length of several hundred micro meters. Cobalt doping results in narrowing of band gap and enhances the photocatalytic ability of the catalyst. The activity of catalysts was checked against the degradation of methylene blue under fluorescent lamp. Doped nanotubes show better activity as compared to simple titania nanotubes [52].

V.C. Ferriera, M.R. Nunes et al., 2013 reported the synthesis of homogeneous cobalt doped TiO_2 naotubes by a novel chemical route. Metallic cobalt powder and titanium trichloride was used as starting materials. From these chemicals greenish grey doped titania powder was formed which was used as precursor for the synthesis of titania nanotubes. For the nanotubes synthesis simple hydrothermal method was used. Doping shift the absorption edge of catalysts to the visible region and thus making the photocatalyst visible light active. Methylene blue was used to study the activity of doped and undoped catalysts. Undoped nanotubes show less activity as compared to doped ones [117].

Xiao Zhao and Zhengqing Cai et al., 2016 reported the preparation of cobalt doped titania nanotubes by hydrothermal method. Cobalt chloride hexahydrate ($CoCl_2.6H_2O$) was used for cobalt doping. Hydrothermal temperature was set at 150 ^{o}C for 48 hours. Doped cobalt ions were responsible for the narrowing of band gap i.e. 2.8 eV from 3.2 eV and thus converting TiO_2 to visible light active catalyst. Degradation of Phenanthrene was checked by these catalysts under solar light irradiation. Doped catalysts show better activity as compared to undoped ones. In addition, the cobalt doped catalysts had good reusability and could be gravity separated [51].

Jicai Liang and Cuiyu Hao et al., 2016 prepared cobalt doped nanotubes by a combination of co-precipitation and hydrothermal method. Titanous sulphate $Ti(SO_4)_2$ was used as titanium source and cobalt nitrate hexahydrate $(CoNO_3)_2.6H_2O$ was used as cobalt source. This study concluded that there is no change in lattice structure of TiO_2 by the minor addition of dopants and new lattice structures are also not formed. Degradation of methylene blue was studied under ultraviolet light. The best degradation rate was 97.2% which was achieved when the cobalt doping content was 1.3% [53].

2.5. Codoped TiO_2 nanotubes

Co-doping is enhanced form of doping in which semiconductor is doped with two elements instead of one. Co-doping just like as doping improves the activity of the photocatalyst by narrowing the band gap and restricting electron hole pair recombination. Mostly semiconductors are doped in a way that one element is responsible for narrowing of band gap and other element (mostly a transition metal) serves as function of electron donor.

Fan Dong,Weirong Zhao and Zhongbiao Wu, 2008 prepared C,N and S co-doped TiO_2 nanotubes by nanoconfinement effect. Commercially available TiO_2 powder was used as precursor for TiO_2 nanotubes synthesis. For doping of C, N and S thiourea was used. Simple hydrothermal method was used for the synthesis of nanotubes. Hydrothermal temperature was set at 150ºC for 48 hours. Four molar ratios of Ti/thiourea were set i.e. 1:0, 1:1, 1:2, 1:3. To check the activity of prepared samples, photocatalytic degradation of toluene was studied. Molar ratio 1:1 show the best results in visible and ultraviolet light [54].

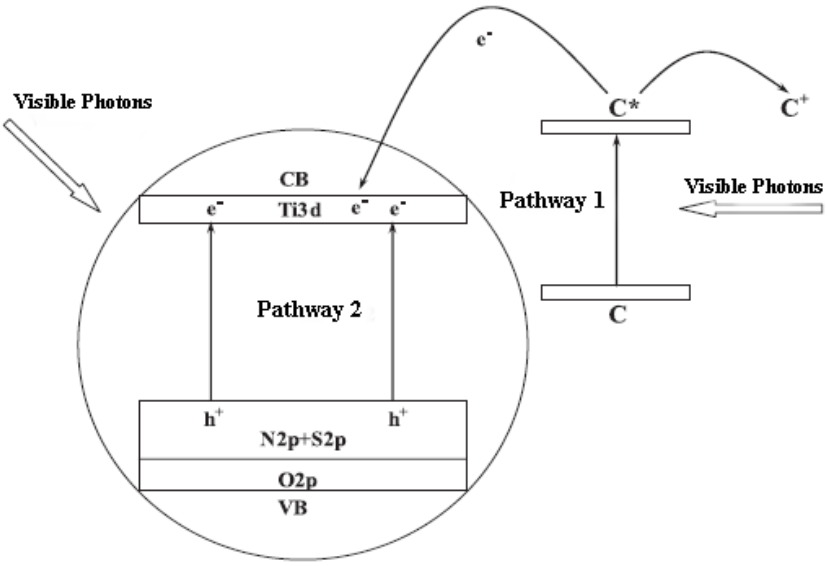

Figure 2.3 Schematic illustration of electron hole pair generation in visible light [54]. C, N and S refer to doped elements.

Jinmin Fan and Zhihuan Zhao et al., 2015 prepared chromium and nitrogen co-doped TiO_2 nanotubes by two step process; hydrothermal synthesis and post impregnation method. The autoclave was heated at 160 ºC for 24 hours. Urea and chromium nitrate was used as precursor of nitrogen and chromium respectively. Different concentrations of chromium were used in the preparation. XPS analysis confirms the successful doping of both dopants. Degradation of methyl orange was carried out to check the activity of different catalysts. The degradation rate was up to 97.16% by the catalyst when the concentration of chromium was 1.06% [57]. Pictorial illustration of dye degradation by catalysts is shown in figure 2.4.

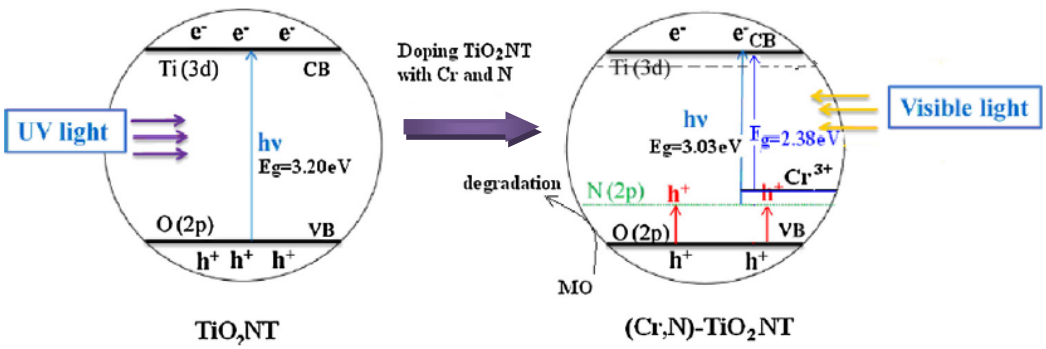

Figure 2.4 Illustration of the proposed mechanism for the degradation of methyl orange over codoped and un-doped catalysts [57].

Sreenivasan Koliyat Parayil1 and Abdul Razzaq et al., 2015 synthesized carbon and nitrogen co-doped TiO_2 nanotubes by hydrothermal method. Urea was used as a source of carbon and nitrogen for doping. Concentration of dopants was varied to check the best suitable concentration for photocatalysis. In 0.1 g of TiO_2 nanotubes 0.1, 0.3, 0.6 and 1g of urea was mixed and ground well for doping. These catalysts were used for the conversion of CO_2 to CH_4. Sample having 0.6 g of urea show the best results. According to the report more the concentration of dopants less will be the surface area. That's why more dopant concentration doesn't increase the activity of the catalyst further [56]. Figure 2.5 show the schematic illustration how nanotubes are responsible for the conversion of CO_2 to CH_4

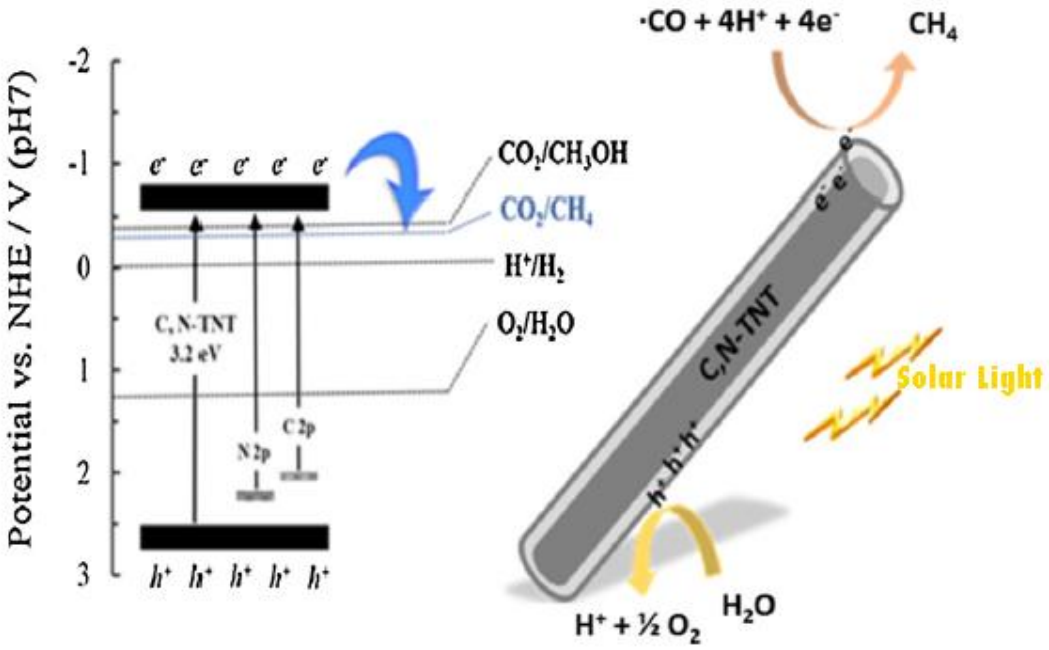

Figure 2.5 Schematic illustration how nanotubes are responsible for the conversion of CO_2 to CH_4 [56].

Ruey-an Doong and Chun-Yi Liao, 2016 synthesized copper and nitrogen co-doped nanotubes by microwave assisted hydrothermal method. After hydrothermal reaction the slurry was heated to 150 ºC for 3 hours at 600 W. For Copper and nitrogen doping copper nitrate solution was used. XPS analysis confirms the doping of copper in zero valent stage. Nitrogen is responsible for the enhancement of visible light activity and copper serve as electron donor specie. The activity of catalysts was checked against

degradation of bisphenol A (BPA) under ultraviolet and visible light. Cu and N co-doped catalyst show better photocatalytic activity then undoped catalyst [118].

2.6. TiO_2/Graphene oxide composite

Peng Song and Xiaoyan Zhang et al., 2012 synthesized nanocomposite films composed of graphene oxide and TiO_2 nanotubes by using an easily manageable impregnation method. TiO_2 nanotubes were prepared from simple anodization method and modified Hummers method was used for the synthesis of graphene oxide. TiO_2 nanotubes were immersed in graphene oxide suspension for 5 hours to prepare TiO_2/GO nanocomposite.

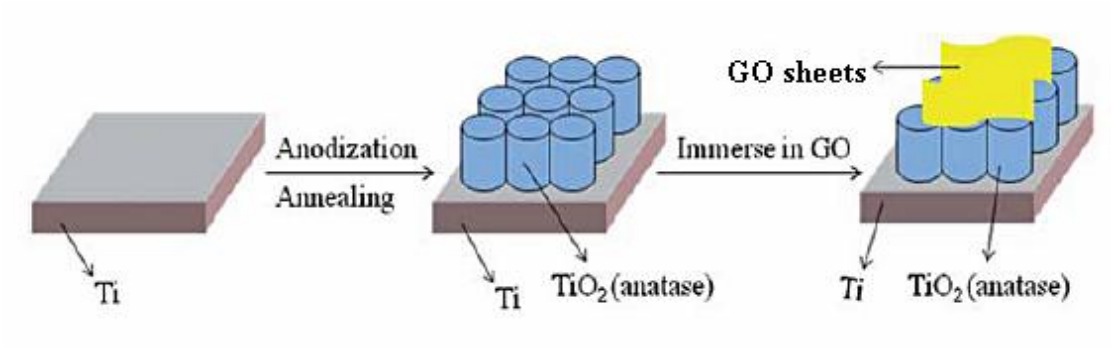

Figure 2.6 Schematic illustration for the synthesis of TiO_2/GO nanocomposite [119].

Visible light photoelectrochemical response was enhanced and photoconversion efficiency was also increased 15 times when TiO_2 nanotubes were decorated by graphene oxide. Degradation of methyl blue was studied to check the photocatalytic activity of TiO_2/GO nanocomposite and simple TiO_2 nanotubes. Nanocomposite show better activity as compare to titania nanotubes [119].

Wei Liu and Xinzhi Wang et al., 2014 prepared nanocomposite of graphene and TiO_2 nanotubes. Graphene oxide was prepared by modified Hummers method and titania nanotubes was synthesized by hydrothermal method. Hydrothermal temperature was set at 135 ºC for 72 hours. For the preparation of nanocomposite of graphene and titania nanotubes again hydrothermal method was used. Ascorbic acid was used as a reducing agent. Autoclave temperature was maintained at 120 ºC for 4 hours. TEM analysis confirms the nanocomposite formation.

Under light methylene blue have a self decomposition phenomenon that's why authors refused to use this dye. RBK5 dye was used to study the photocatalytic

activity of the catalysts. Results clearly depicted that TiO_2/GN nanocomposite show better activity than simple titania nanotubes [120].

Hong Tao and Xiao Liang et al., 2015 successfully synthesized graphene and titanium dioxide nanotubes composite. Graphite Oxide was prepared by modified Hummers method which was used as a precursor of graphene and TiO_2 nanotubes were synthesized from hydrothermal method. For the preparation of nanocomposite suspension of graphite oxide and titania nanotubes was made and again hydrothermal treatment was applied for 4 hours at 120 ºC. Degradation of acetaminophen was studied to check the photocatalytic activity of prepared catalysts.

In the preaparation of nanocomposite as the GO loading was increased photocatalytic activity was also increased but up to a certain limit, beyond that limit activity started decreasing because of the obstruction of light. According to the report 5% GO loading is the best suitable ratio for maximum activity of the catalyst. Both high and low doasage of GO affect the performance of catalyst. More the concentration of catalyst more will be the adsorption sights available but after a specific concentration (o.4g/L) the activity was decreased due to the shield of light because of dark color of the catalyst. pH also had a significant effect on the degradation of acetaminophen. pH value from 3 to 7 doesn't drastically affect the degradation process but at pH 11 the efficiency of the catalyst was greatly dropped [121].

Meng Wei and Junmin Wan et al., 2015 reported the fabrication of Titania nanotubes co-sensitized with copper (II) meso-tetra(4-carboxyphenyl)porphyrin (CuTCPP) and reduced graphene oxide nanosheets. Graphene oxide was prepared by modified Hummers method. Nanocomposite of graphene oxide and titania nanotubes was made by hydrothermal method. Hydrothermal conditions were set at 135'C for 24 hours. Heating reflux process was used to sensitize RGO-TNT by CuTCPP. CuTCPP has a vital role in the photon capturing and expanding the absobtion region to visible light portion. The activity of prepared catalysts was checked against degradation of methylene blue. 5%CuTCPP/rGO-TNT show the best results for the degradation and even after six cycles maximum dye was degraded with this catalyst [122].

Qi Lai, Xue-ping Luo and Shi-fu Zhu, 2016 synthesized hybrids of graphene oxide and titania nanotubes. Modified Hummers method was used for the synthesis of graphene oxide. Titania nanotubes and GO-TNT hybrids were formed simultaneously

by a simple hydrothermal method. Autoclave was heated at 130ºC for 40 hours. Reduction of graphene oxide occurs in hydrothermal treatment and reduced graphene oxide was formed. As titania nanotubes formation and reduction of graphene oxide occurs simultaneously, it results in the insertion of oxygen containing groups in the titania layer structure. Calcination was done at different temperatures and best results were achieved at 350 ºC. Samples calcined at this temperature had more crystallinity and show better degradation of methylene blue [123].

Huidi Liu and Yaling Wang et al., 2015 synthesized reduced graphene oxide and titania nanotubes nanocomposites. For the preparation of titania nanotubes hydrothermal method was used and modified Hummers method was followed for the synthesis of graphene oxide. Nanocomposite was also prepared by hydrothermal method. Autoclave was heated at 120 ºC for 12 hours. Figure 2.7 depicts the nanocomposite functioning for the degradation of hazardous components. Different weight ratios of GO to TNT was used i.e. 1%, 2% and 5%. The activity of catalysts was checked against degradation of rhodamine B and Cr (VI) under ultraviolet light. For the degradation of rhodamine TNT-2%rGO show best results but in case of the degradation of Cr(VI) TNT-5%rGO show best results [124].

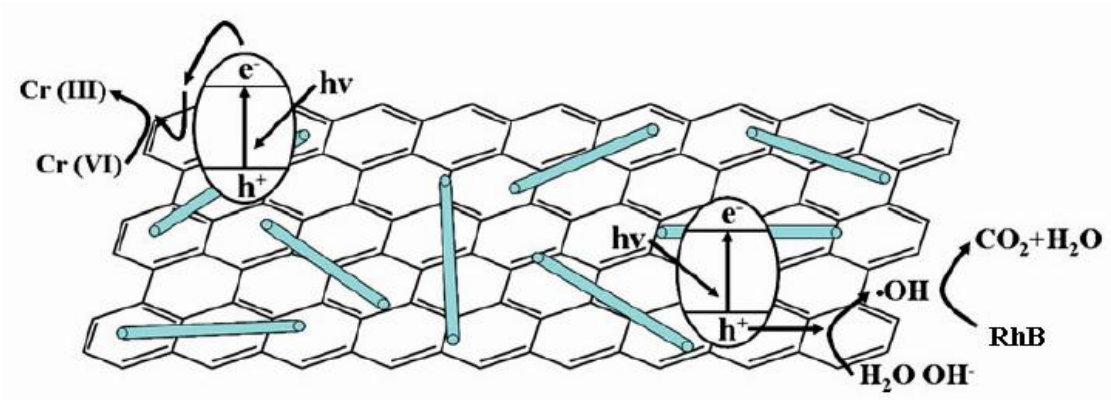

Figure 2.7 Schematic illustration of degradation of rhodamine B dye and Cr(VI) [124].

2.7. Photocatalytic degradation of DMMP

Studying nerve agents directly can be fatal for this purpose scientists choose some stimulants which are like some of the nerve agents in properties and chemical nature but are less toxic in comparison. DMMP is also a simulant of sarin (a nerve agent).

Decontamination of these extremely toxic chemicals is necessary in some conditions. Different physical and chemical methods have devised for this purpose as nerve agents have incapacitating effects on humans which are irreversible.

Here are some reports related to degradation of DMMP by photocatalysis;

K.E. O'shea, I. Garcia, and M. Aguilar, 1997 used different types of TiO_2 powders to degrade dimethyl methylphosphonate (DMMP) and diethyl methylphosphonate (DEMP). Degussa P25 show best results. Intermediate products were also investigated. Methyl phosphonic acids and low molecular weight organic acids were mainly formed during degradation. Carbon dioxide and phosphate were formed on complete mineralization. Side wise sonication, dissolved oxygen, increase in the amount of titania and addition of H_2O_2 cause the significant increase in the rate of degradation [125].

Timothy N. Obee and Sunita Satyapal 1998, used TiO_2 coated glass substrate for the degradation of dimethyl methylphosphonate (DMMP). Different concentrations of DMMP in air (between 1 to 90 ppm) were used. Products as a result of degradation of DMMP were identified. According to the study carbon monoxide and carbon dioxide were identified in gas phase. Methyl phosphonic acid and phosphate were recognized on the catalyst and due to these species catalyst was deactivated in short time. But an interesting thing was discovered that if the deactivated catalyst was washed with water the activity was completely regained and partially regained when exposed to ultraviolet light [126].

Yi-Chuan Chen and Alexandre V. Vorontsov et al., 2003 reported the degradation of dimethyl methylphosphonate (DMMP) by TiO_2. They have studied the effect of sonication in the degradation of DMMP. Sonicator having frequency of 20 kHz was used. Increment in the degradation process was recorded in the presence of ultrasound waves. Increment is not only because of deagglomeration of TiO_2 nanoparticles but also due to the elevated mass transport of reagent. Same types of intermediates were formed in simple photocatalysis and sonophotocatalysis [127]. Figure 2.8 show the scheme of DMMP degradation.

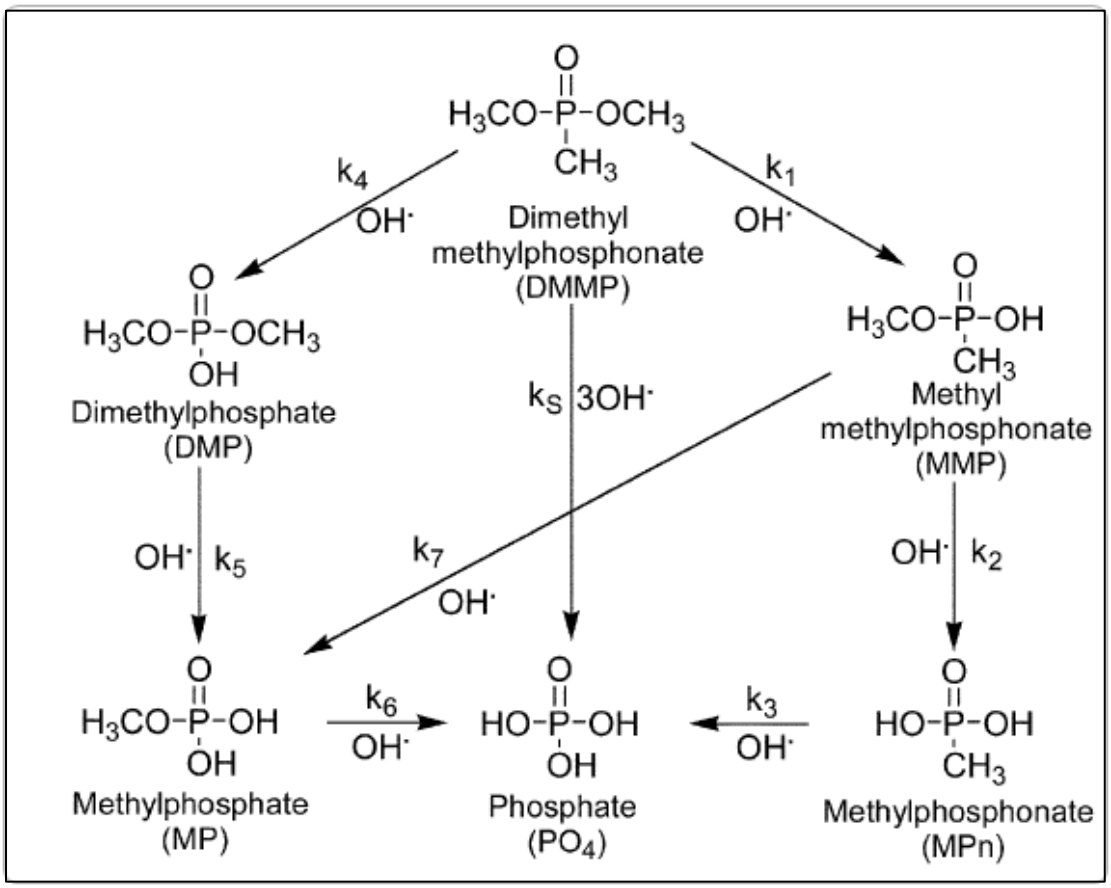

Figure 2.8 Scheme of DMMP degradation [127]

Chapter 3 Experimental Work

This chapter explains all the practical work which was performed for the synthesis of graphene oxide, titanium dioxide nanotubes, co-doping of nanotubes with nitrogen and cobalt and nanocomposite of co-doped titania nanotubes and graphene oxide. This chapter also explains the details of different techniques used for the characterization of as prepared nanocatalysts.

3.1. Synthesis of graphene oxide

Graphene oxide was prepared at the start of practical work of research. Hummers' method was used for the synthesis of GO.

3.1.1. Materials

Graphite powder (Sigma Aldrich), Sodium nitrate (BDH), Ptassium permanganate (Sigma Aldrich), Hydrogen peroxide (Merck), Sulphuric acid (95 % Sigma Aldrich), Hydrochloric acid (37% Sigma Aldrich).

3.1.2. Procedure for the synthesis of graphene oxide

Hummers method was followed for the synthesis of graphene oxide. Graphite flakes (2 g) and sodium nitrate (2 g) were mixed in 50 ml sulphuric acid in a 1000 ml beaker. Beaker should be kept in an ice bath to maintain the temperature below 5 ºC with continuous stirring. After 2 hours stirring potassium permanganate (6 g) were added slowly because the addition of $KMnO_4$ cause rise in temperature so ice bath was not removed and temperature should be maintained below 15 ºC. Here greenish color of the mixture was observed. After the addition of $KMnO_4$ ice bath was removed and mixture was kept under stirring for 2 days. After two days stirring the chocolaty thick mixture was observed. Then 100 ml of water was added drop wise because concentrated H_2SO_4 was present in mixture and addition of water cause rise in temperature. Temperature should be maintained below 98 ºC. Further 200 ml water was added here drop wise addition is not required. After addition of water brown colored suspension was observed. Finally 10 ml of hydrogen peroxide (H_2O_2) was added slowly. The final appearance was yellowish brown. Mixture was centrifuges at 6000 rpm and washed with 0.1 molar HCl and finally with deionized water several times to maintain the neutral pH. Product was vacuum oven dried at 35 ºC for 24

hours. Dark brown to blackish flakes were obtained. Grinding was done for further use and stored in an air tight vial.

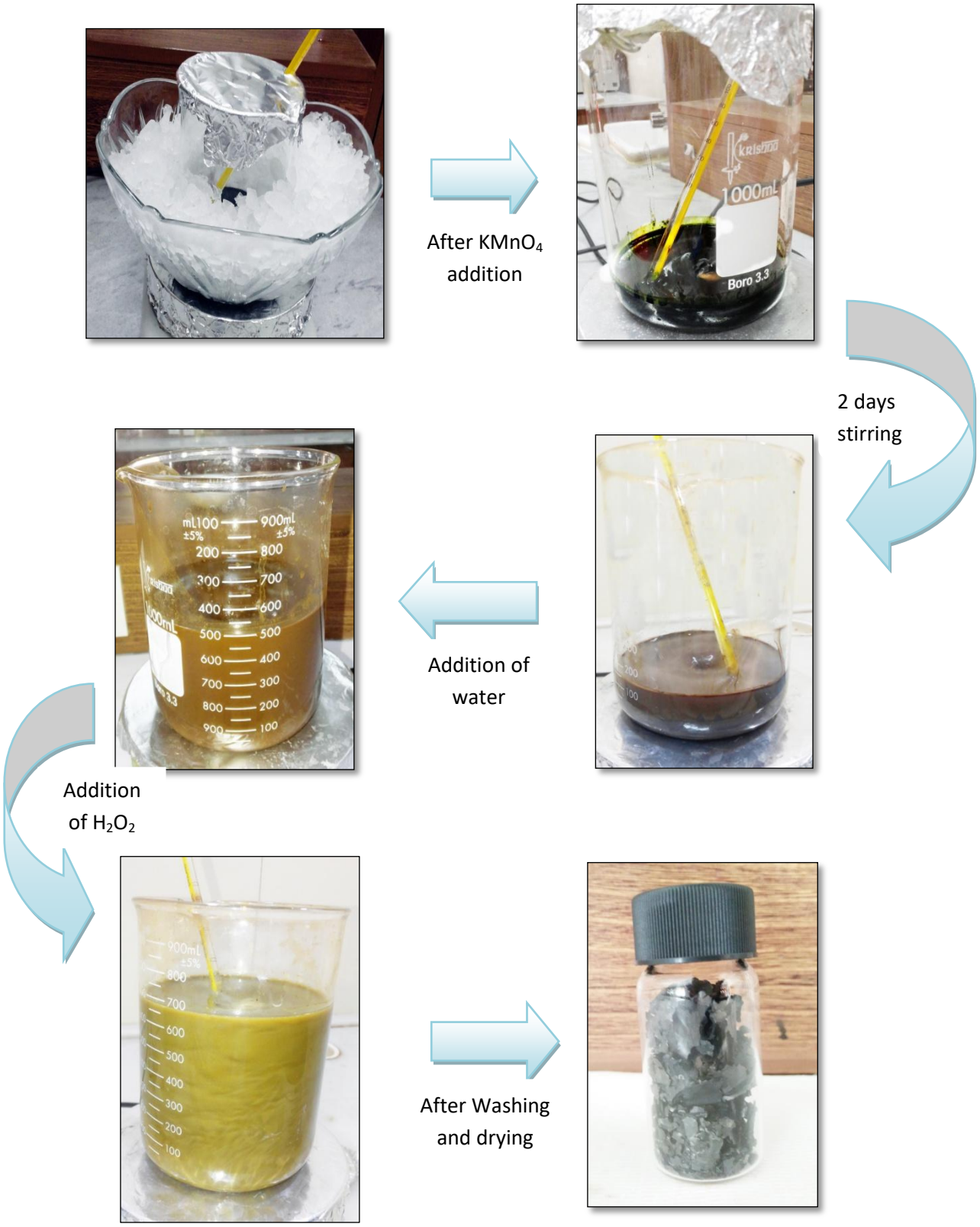

Figure 3.1 Schematic representation for preparation of graphene oxide

3.2. Synthesis of TiO_2 nanotubes (TNTs)

Second step was the synthesis of titania nanotubes. Simple hydrothermal method was used for the synthesis of nanotubes.

3.2.1. Materials

Titanium dioxide powder (Merck), sodium hydroxide (Merck), hydrochloric acid (37% Sigma Aldrich), urea (Sigma Aldrich), cobalt nitrate (Merck).

3.2.2. Procedure for the synthesis of TiO_2 nanotubes

First of all 100 ml of 10 M NaOH solution was prepared. 3 g of TiO_2 powder was added to this solution with continuous stirring. Stirring was done for more 30 minutes, followed by hydrothermal treatment of the mixture at 130 ºC for 72 hours. After hydrothermal reaction precipitates were separated by centrifugation and washed with 0.1 M HCl solution and deionized water several times to attain the final pH 7. After washing sample was vacuum dried at 80 ºC for 6 hours. Calcination was done at 400 ºC for 2 hours. Obtained white color fluffy solid sample was stored in a glass vial as shown in figure 3.2.

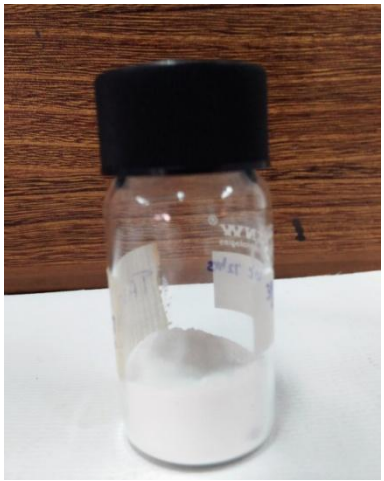

Figure 3.2 Prepared sample after hydrothermal reaction.

After the confirmation of morphology of naonotubes by SEM nitrogen and cobalt doping was done. Percentage of nitrogen doping was fixed as selected after literature survey which value is reported as best but cobalt doping was done in different percentages. The procedure of doping and co-doping is explained below.

3.2.3. Procedure for nitrogen doping

First of all 100 ml of 10 M NaOH solution was prepared. 3 g of TiO_2 powder was added to this solution with continuous stirring. After stirring of 30 minutes urea was added and mixture was stirred for more 30 minutes, followed by hydrothermal treatment of the mixture at 130 ºC for 72 hours. After hydrothermal reaction precipitates were separated by centrifugation and washed with 0.1 M HCl solution and deionized water several times to attain the final pH 7. After washing, sample was vacuum dried at 80 ºC for 6 hours. Finally annealing was done at 400 ºC for 2 hours.

3.2.4. Procedure for Cobalt and nitrogen co-doping

The nitrogen doped nanotubes of TiO_2 obtained from the above experiments were then doped with cobalt by using cobalt nitrate hexahydrate ($Co(NO_3)_2.6H_2O$) by the following procedure.

First of all 30ml of $Co(NO_3)_2.6H_2O$ solution was prepared with varied concentrations i.e. 0.6 mM, 1.35 mM, 2.06 mM and 2.75 mM (0.2g , 0.4g, 0.6g and 0.8g in 30 ml water) as shown in figure 3.3.

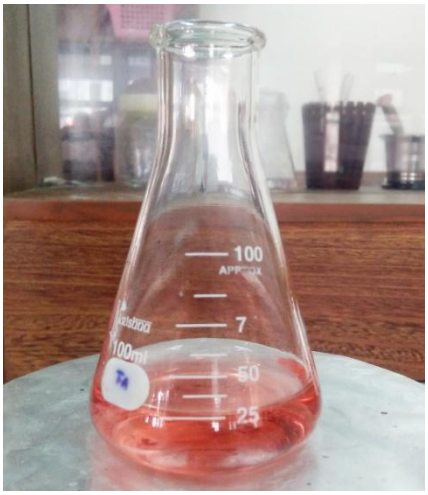

Figure 3.3 30 ml solution of cobalt nitrate hexahydrate

1 g of nitrogen doped nanotubes were dispersed in the solution. Color of the dispersion changes from pink to green. After stirring of 24 hours mixture was dried in vacuum oven at 80 ºC for 4 hours. After drying, annealing was done at 400 ºC in a heating furnace as shown in figure 3.4. After calcinations green colored final product was obtained in the form of powder. Figure 3.5 show variation in color with the increase in dopant concentration.

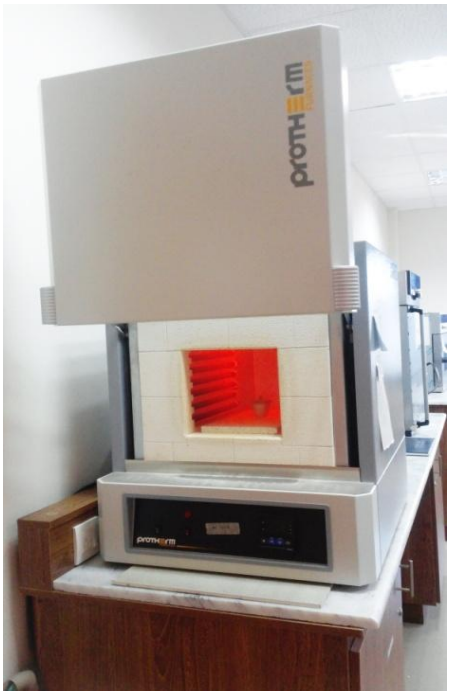

Figure 3.4 Furnace for calcination of samples present at SNS, NUST, Islamabad

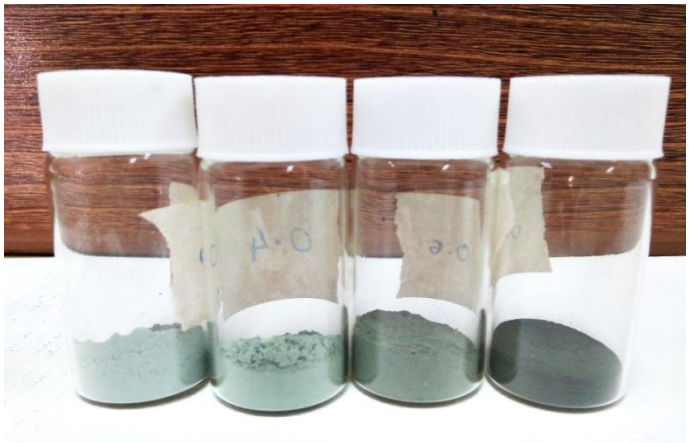

Figure 3.5 Prepared N and Co co-doped titania nanotubes samples.
From left to right concentration of cobalt is increasing as depicted by the darkening of sample color.

Here is the table depicting the details about all prepared samples including sample composition, urea loading cobalt, nitrate hexahydrate loading and annealing temperature.

Table 3.1 Indices of samples and experimental details

Sample ID	Sample Composition	TiO_2:Urea (Mass ratio)	TiO_2:$Co(NO_3)_2.6H_2O$ (Mass ratio)	Annealing Temp.
B-TiO_2	Bulk TiO_2	-	-	-
TNT	Titania nanotubes	-	-	400 ºC
N-TNT	Nitrogen doped titania nanotubes	1:2	-	400 ºC
1-CoN-TNT	Co and N codoped titania naotubes	1:2	1:0.2	400 ºC
2-CoN-TNT	Co and N codoped titania naotubes	1:2	1:0.4	400 ºC
3-CoN-TNT	Co and N codoped titania naotubes	1:2	1:0.6	400 ºC
4-CoN-TNT	Co and N codoped titania naotubes	1:2	1:0.8	400 ºC

3.3. Synthesis of rGO/CoN-TNTs nanocomposite

After the degradation study of a dye by using co-doped TNTs we selected the best catalyst and prepared its nanocomposite with rGO to further enhance the properties and check its degradation capability too.

3.3.1. Materials

As prepared co-doped TiO_2 nanotubes and graphene oxide.

3.3.2. Procedure

Graphene oxide was dispersed in 30 ml of deionized water by probe sonicator. After 30 minutes of sonication co-doped TNTs was added and again sonication was done at low amplitude. Then vigorous stirring was done for 3 hours. The prepared suspension was transferred to autoclave and held at 120 ºC for 12 hours. The product was washed with deionized water several times and dried under air at 60 ºC. The obtained sample is denoted as reduced graphene oxide, co-doped TNTs nanocomposite.

3.4. Characterization of the catalysts

Morphology, crystalline phase, particle size, elemental analysis and surface area was found by using different characterization techniques. Above discussed properties were distinguished under two main types; the structural and optical properties.

3.4.1. Structural properties

Morphology, crystalline phase, topography and elemental analysis are under this heading. Techniques used for studying these properties are as under:

3.4.1.1. Scanning electron microscope

Scanning electron microscopy is fundamental to microstructural or nanostructural study. It is world widely used to obtain the following information:

a) Topographical descriptions
b) Morphology
c) Phase distributions
d) Crystal structure
e) Presence of any defects
f) Elemental composition (with the addition of EDS)

Instrumentation: Electron optical column, vacuum system, signal detection and a display system are the main parts of the instrument as shown in diagram 3.8. Optical column is having magnetic lens, aperture and electron source. A vacuum pump is

attached side wise which creates vacuum inside the chamber. When beam of electron is fired from electron gun, condenser lens confine the electron beam. The condenser lens is also responsible to make the beam coherent. Focusing of the beam is done by objective lens. Interaction of electron beam with sample produces some specific signals which are detected by detectors and display on computer [128]. Figure 3.6 show schematic diagram of SEM.

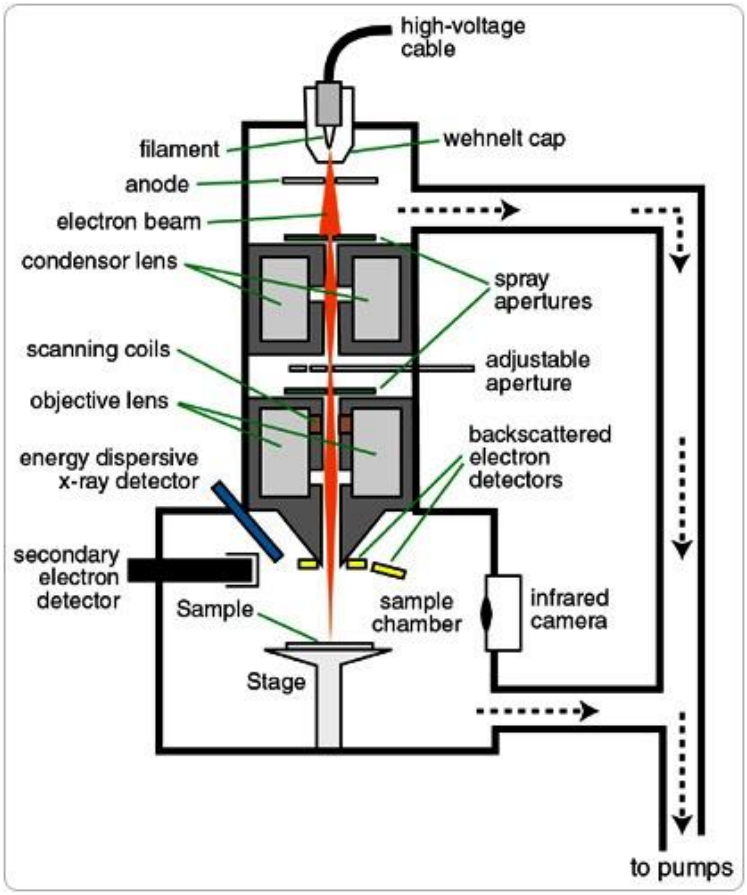

Figure 3.6 Schematic diagram of scanning electron microscope (SEM) [129]

Principle of method: When beam of electrons is generated by an electron gun, it interacts with the sample surface using a potential difference and directed by magnetic fields. When beam of electrons intrude on the surface of sample it interacts with atoms of the sample by different mechanisms. As a result different type of signals are produced which provide information about the sample. Different types of specially designed detectors are present in assembly which are used to sense and collect these signals. Table 3.2 represents some detectors and types of signals.

Table 3.2 Different types of signals generated, detectors and information provided by these signals.

Signal	Detector	Information Provided
Secondary electrons	Everhart-Thornley (ET) Detector	Surface features
Back scattered electrons	Solid state detector	Crystallographic structure and Surface features
X-rays	EDX detector	Compositional analysis and phase analysis

EDX or EDS is analytical technique hyphenated with SEM. From EDX elemental composition of the sample can be easily find out. When highly energetic beam of electrons hit the sample, the atoms produce characteristic x-rays. These x-rays are detected by detectors and displayed in the form of spectrum having specific peaks for each element thus giving the information about elements present in the sample. Figure 3.7 show block diagram of EDS machine.

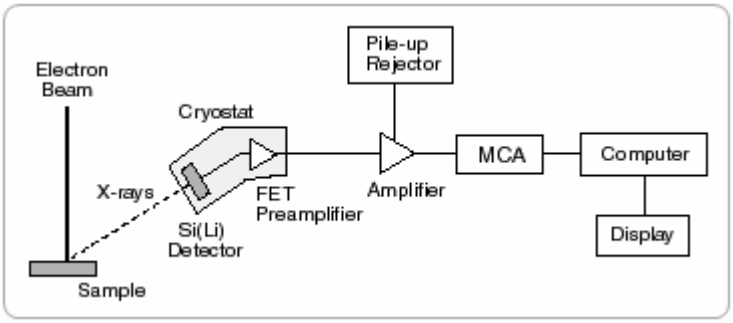

Figure 3.7 Schematic representation of EDS/EDX

SEM used in this study for the characterization of sample is JSM-6490A, made by JEOL, present in School of Chemical and Materials Engineering of NUST, Islamabad as shown in figure 3.8 and for EDS TESCAN machine present at IST, Islamabad was used as shown in figure 3.9.

Figure 3.8 Scanning Electron Microscope present at SCME, NUST, Islamabad

Figure 3.9 Scanning Electron Microscope at IST, Islamabad

3.4.1.2. X-ray Diffractometry (XRD)

XRD is one of the unswerving techniques mostly used for the identification of phases. Quantitative analysis by XRD is also possible as the intensity of any peak refers to the concentration of particular phase in the sample.

Principle of XRD: X-rays have high energy and small wavelength. Wavelength of X-rays (0.5-50Å) is comparable with the distance between atoms in solids. When X-rays strike on atoms of solid sample they are weakly scattered in all directions. As crystals have different lattice planes. Structural details of crystals are ideal to explore only when the scattering from a given family of planes are strong enough that x-rays reflected by each plane arrive at the detector in phase [130].

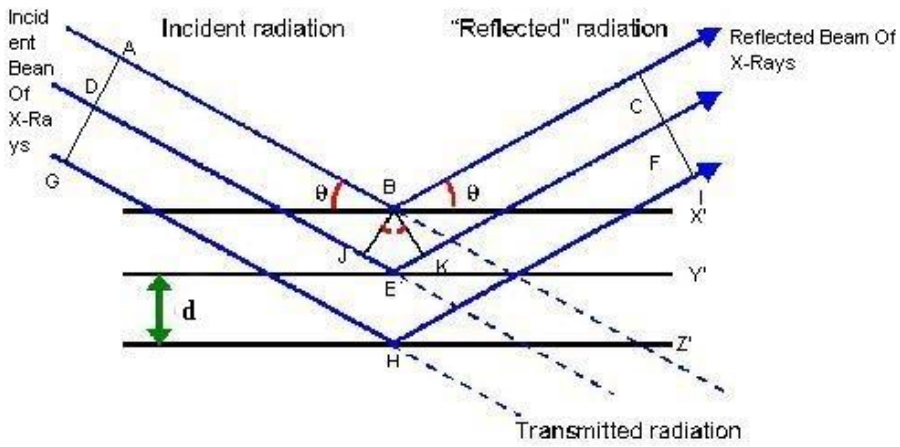

Figure 3.10 Schematic diagram illustrating of diffraction of X-rays from crystal planes

After interacting with atoms the way these rays are diffracted are investigated in XRD analysis. Diffraction occurs on the princilple of Bragg's law which is stated as:

Bragg's Law:

$$2d\sin\theta=n\lambda \qquad \text{…….Equation 1}$$

Where;

d = Inter planes spacing

θ = Incident angle

λ = wavelength of x-rays

n = 1 for a monochromatic radiation

Typically we get a plot having 2θ values on x-axis and intensity on y-axis. The results are then computed to get information about the crystallinity, phase and particle size [130]. The particle size of crystallites can be find out by applying Scherer's formula.

Scherer's formula

$$D = K \lambda / B\cos\theta \qquad \text{...……..Equation 2}$$

Where;

D = Particle size of crystallites

K = 0.9

λ = wavelength of x-rays

B = Full width half maxima (FWHM)

θ = Bragg's angle in degrees

For this study XRD analysis were carried out using STOE powder diffractometer at SCME NUST. It utilizes a monochromatic radiation Cu Kα with wave length of 1.54 Å.

3.4.2.4. Surface area measurement (BET analysis)

Specific surface area and pore size distribution of the sample can be find out by BET analysis (Brunauer, Emmett and Teller). This information is used to predict the efficiency of the catalyst. As more the surface area of the catalyst more will be the adsorption of dye/pesticide (component which we want to degrade) on catalyst and thus resulting in more efficiency.

For BET analysis sample should be completely dried because this technique is only applicable on dry solid samples. Prior to analysis degassing was done to remove any moisture from sample. Other contaminants can also be removed by degassing process. To shorten the degassing time period highest possible temperature was set at which sample may not damage or degrade. Very stable samples have less degassing time but according to IUPAC recommendation 16 hours degassing should be done. After degassing sample is shifted to analysis port. Here sample is cool down by liquid nitrogen. Low temperature is achieved to ensure the maximum interaction between gas molecules and solid sample. Helium gas is passed for the dead run as He is very stable gas and do not adsorb on the sample surface. Then nitrogen gas is passed for adsorption. Sample is heated to get desorption isotherm [131]. Figure 3.11 show the block diagram of BET analyzer.

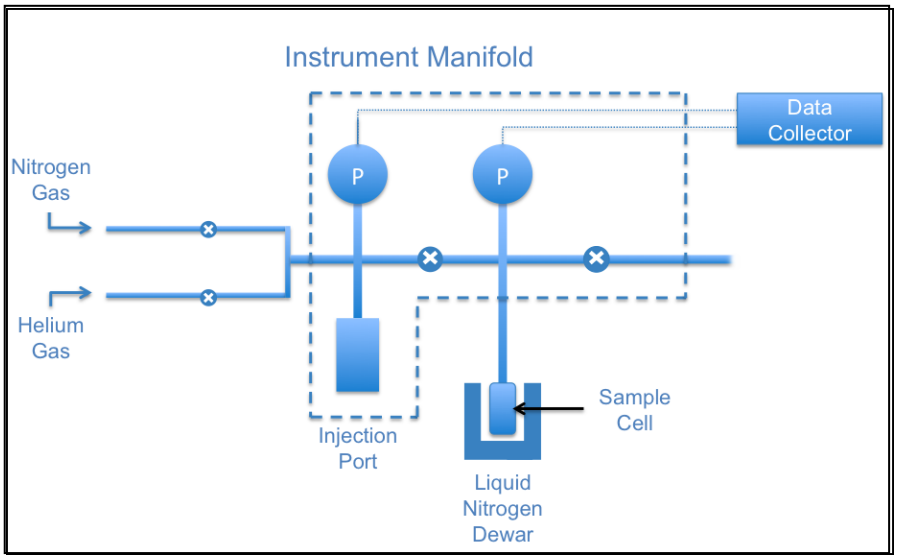

Figure 3.11 Schematic representation of the BET analysis instrument. The degasser is not shown [131]

3.4.2. Optical properties

Optical properties of the samples can be found out by using the following techniques;

3.4.2.1 Infrared Spectroscopy

IR spectroscopy is a non destructive analytical technique which gives us information about the functional groups present in the chemical compound. IR is qualitative as well as quantitative analysis technique.

Infrared spectroscopy is also known as vibrational spectroscopy. Infrared radiations are used in this technique. When IR radiations are absorbed by the molecules of the sample, molecules are excited from ground energy state to higher energy states and thus gaining higher vibrational amplitude. When radiations interact with sample it produces bending and stretching vibrations that match with frequencies of bonds present in the sample. These vibrations are fundamental vibrations. There are two types of fundamental vibrations; Stretching vibrations and bending vibrations. Bending vibrations are of low frequency as compare to stretching vibrations.

There are different methods for the preparation of samples. Powder samples, KBr pelleting and simple solutions are mostly used for analysis. Spectra are obtained having wave number on x-axis and % transmittance or absorbance on y-axis. Characteristic peaks of every functional group give rough idea about the structure of the molecules in the sample.

FTIR used in the study is ALPHA model, SN 200488 present in SNS, NUST, Islamabad as shown in figure 3.12.

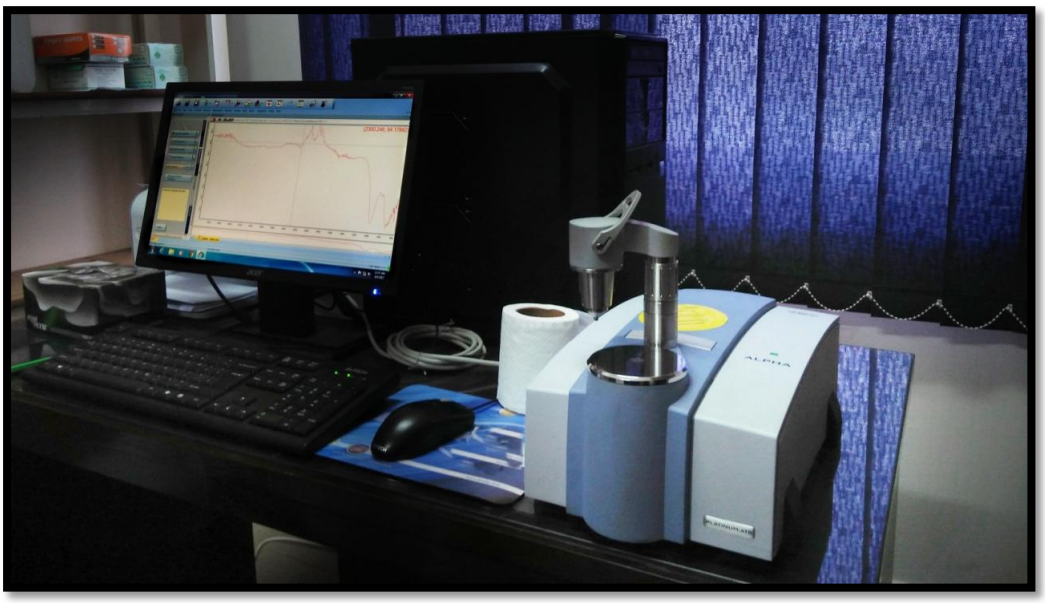

Figure 3.12 FTIR spectrophotometer present at SNS, NUST, Islamabad

3.4.2.2. UV-Visible Spectroscopy

UV-Visible region is having wavelength of radiations from 200-800 nm. Ultraviolet region is from 200-380 nm and above this region lies visible region. Electrons are excited when molecules absorb UV-visible radiations.

This technique is useful for quantitative analysis. As the Beer Lambert Law states that absorbance of a solution has a direct relation with the absorbing species in the solution. It is stated as:

$$\mathbf{A = \epsilon cl} \qquad \text{……Equation 3}$$

Where;

A = Absorbance

ϵ = Molar absorptivity in L $M^{-1}cm^{-1}$

c = Concentration in M L^{-1}

l = Path length in cm

Thus by keeping the path length constant we can calculate the concentration of absorbing species in the solution.

We get a xy graph having absorbance on y-axis and wavelength on x-axis. From this graph band gaps of the catalysts can be find out by constructing tauc plots. Photon energy (hv) versus $(\alpha h\nu)^{1/2}$ graph is first constructed. An extrapolation of a line at particular region in the graph touches the x-axis at a specific value which indicates the value of band gap for a particular semiconductor.

3.4.3. Thermal properties

For the analysis of thermal properties many techniques were devised i.e. differential thermal analysis (DTA), differential scanning calorimetry (DSC), thermogravimetric analysis (TGA) and thermomechanical analysis (TMA).

3.4.3.1. Thermogravimetric analysis (TGA)

Changes in physical and chemical properties of materials as a function of constant increase in temperature are measured by thermogravimetric analysis. TGA give information about both physical and chemical phenomena's. Physical phenomena's include adsorption, desorption, sublimation and vaporization and chemical phenomena's like oxidation, reduction, dehydration and chemisorptions can be studied by this technique.

TGA is related to mass loss or mass gain so properties related to mass can be easily predicted. TGA is very precise about mass change and temperature change. Figure 3.13 Block diagram representing TGA instrumentation.

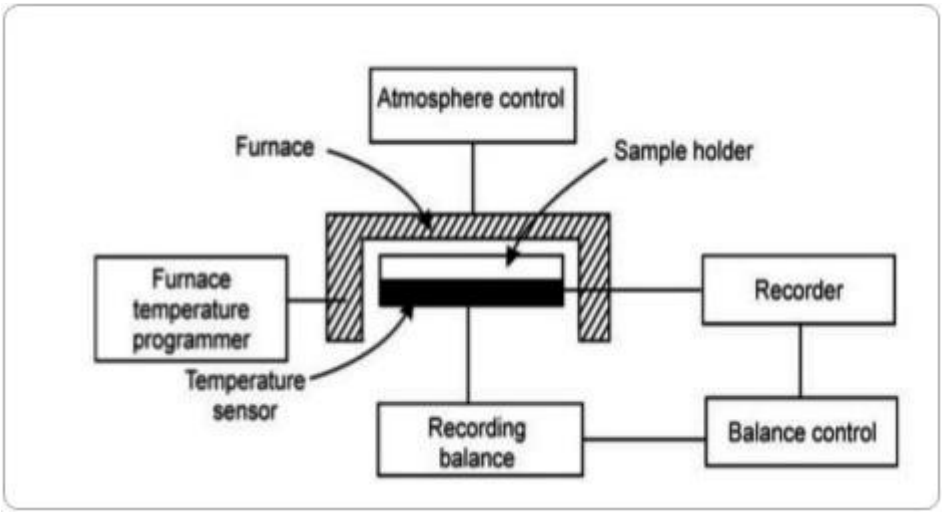

Figure 3.13 Block diagram representing TGA instrumentation.

Chapter 4 Results and Discussion

This chapter explains the chracterization and structural changes of the as prepared doped and co-doped TiO_2 nanotubes and nanocomposite of reduced graphene oxide and TiO_2 nanotubes. Chapter also includes the degradation studies of methyl orange.

4.1. Results of the structural, optical and thermal properties of the catalysts

Structural, optical and thermal properties were studied by analysis of samples by different techniques. Results are explained as under;

4.1.1. Scanning Electron Microscopy (SEM)

SEM images for different samples of catalysts were taken. The images of TiO_2 commercially available powder show that these particles are spherical and are in nanometer range as shown in figure 4.1.

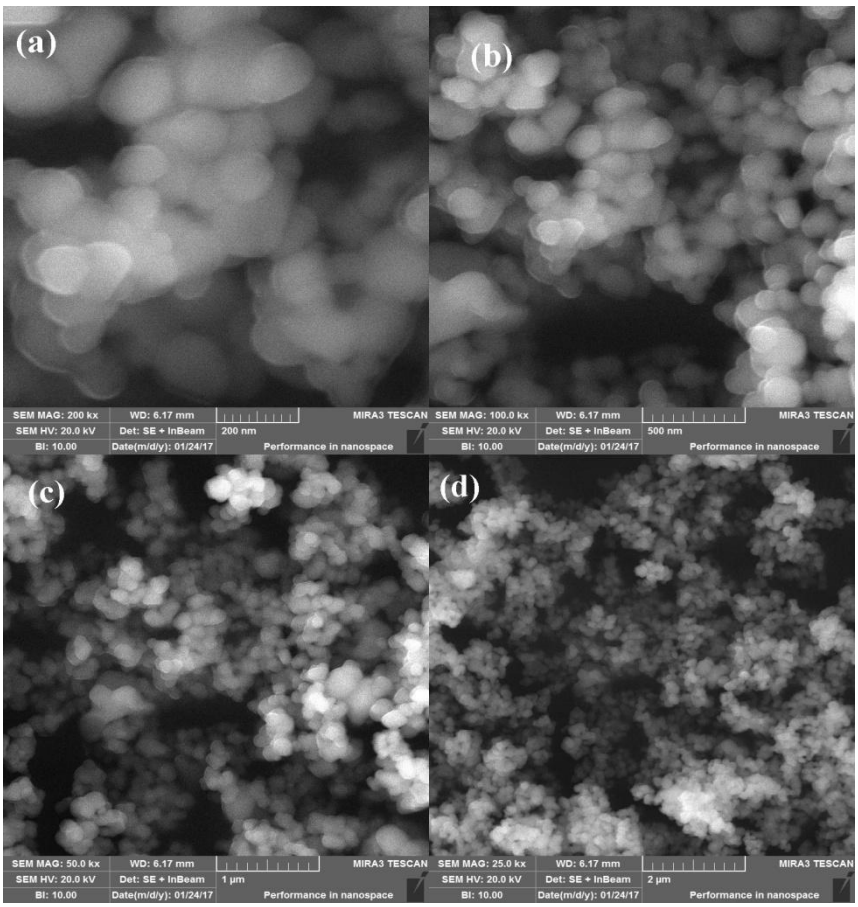

Figure 4.1 SEM images of TiO_2 powder

Figure 4.2 shows SEM images of undoped TiO_2 nanotubes prepared by hydrothermal method. The excessive charging at the end points of tube like structures shows the presence of open ends. Length of these nanotubes is in micrometer range but diameter is in nanometer range.

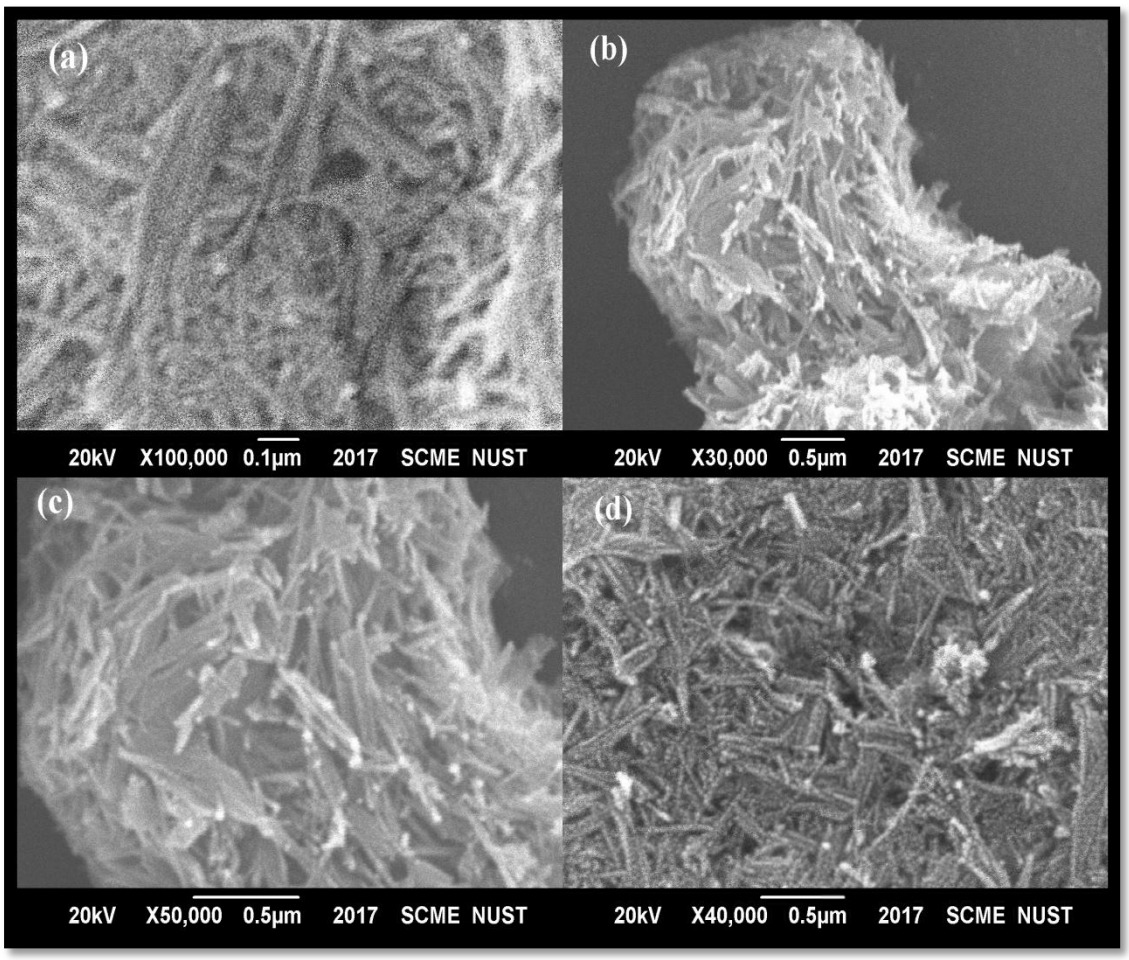

Figure 4.2 SEM images of undoped TiO_2 nanotubes

SEM images of powder samples of nitrogen doped and co-doped TiO_2 nanotubes are shown in figure 4.3 and 4.4 respectively. Reported SEM images of nanotubes in many papers also have woven thread like structures like ours. TEM is the best technique for the complete morphology determination of nanotubes.

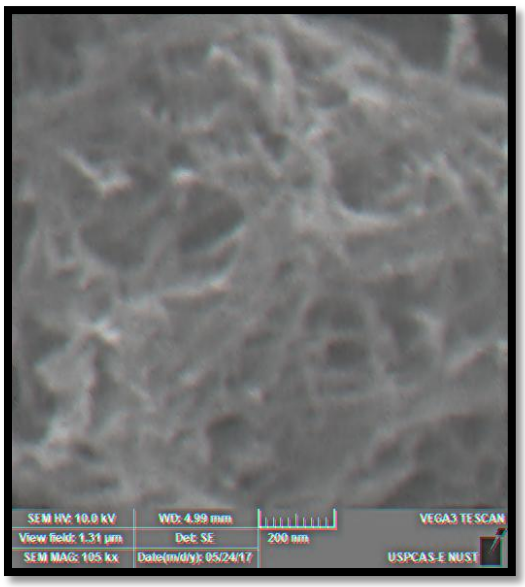

Figure 4.3 SEM image of nitrogen doped TiO_2

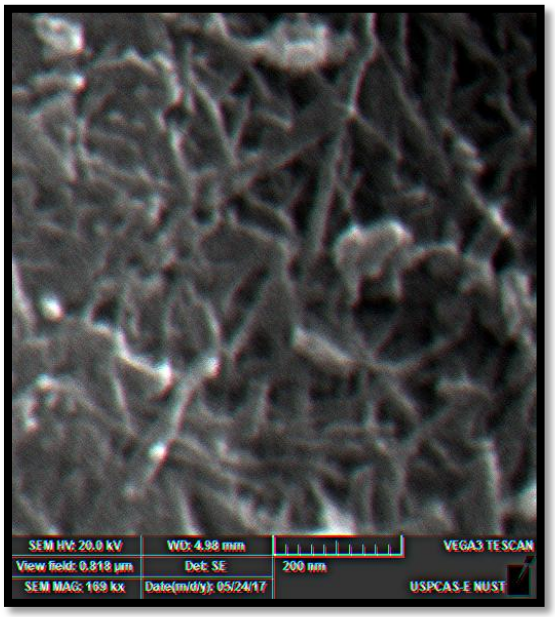

Figure 4.4 SEM image of codoped TiO_2

SEM images of graphene oxide show stacked sheets as shown in Figure 4.5. These sheets are of micrometer size and may have thickness in nanometer range depending on the number of stacked sheets.

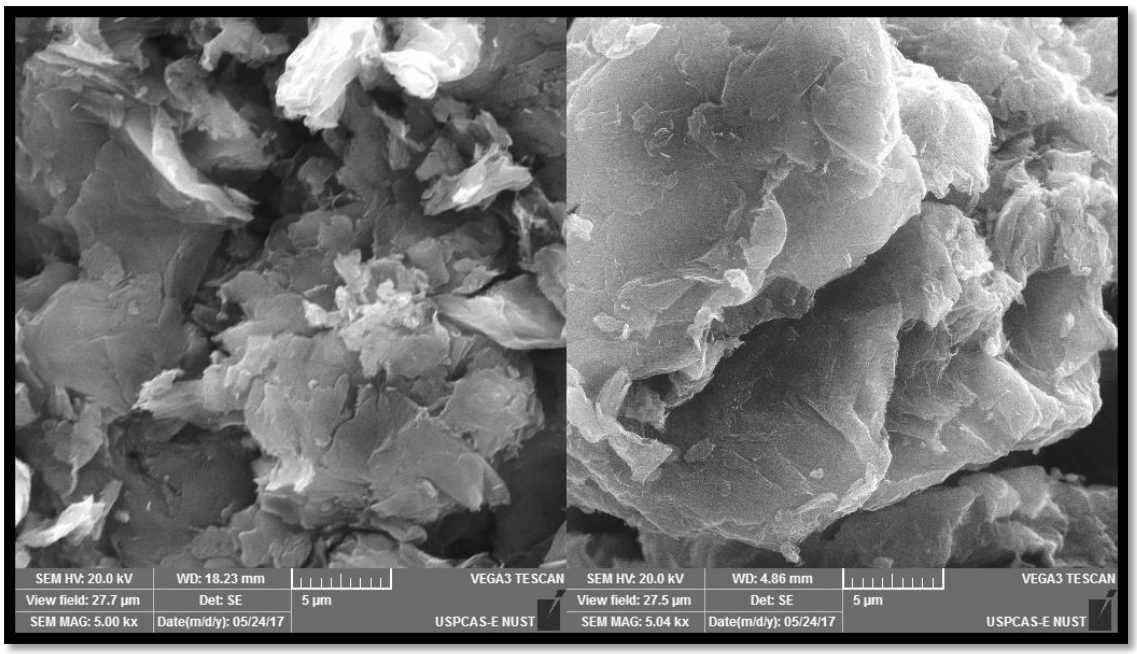

Figure 4.5 SEM images of graphene oxide sheets

4.1.2. Energy dispersive X-ray spectroscopy (EDX)

EDS or EDX is used for the elemental composition detection of the sample. Each element show specific peak in the graph depicting its presence in the sample. In our co-doped sample EDS clearly show peaks of titanium, oxygen and cobalt. Fig 4.6 shows EDS spectra of the catalyst having least composition of cobalt.

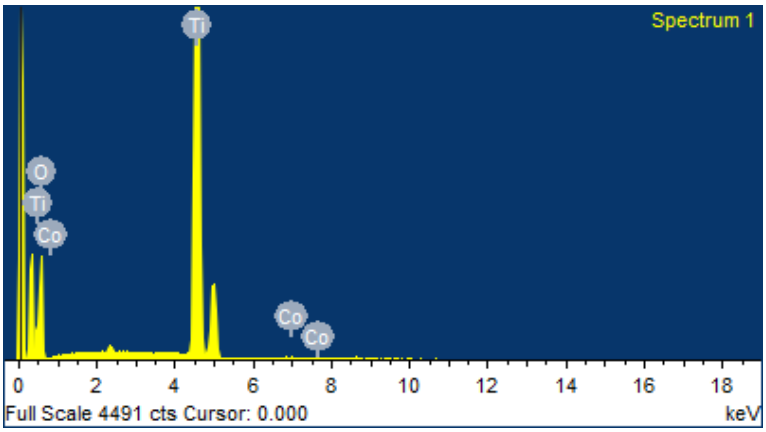

Figure 4.6 EDS spectra of 2-CoN-TNT

Table 4.1 Elemental composition of 2-CoN-TNT

Element	Weight%	Atomic%
O	44.34	70.47
Ti	55.44	29.43
Co	0.22	0.09

4.1.3. X-ray Diffraction (XRD)

XRD spectra of all the prepared samples are stacked in fig. 4.7. In rGO/CoN-TNT all characteristic peaks of anatase phase of TiO_2 with reference to JCPDS card no. 21-1272 were observed. Anatase has characteristic peaks at 25.3º, 37.3º, 47.6º, 53.5º and 55.1º two theta values and all of them are present in rGO/CoN-TNT which depicts the presence of pure anatase phase. A shoulder is observed in a peak present at 25.24º which depicts the presence of reduced graphene oxide as reduced graphene oxide has its characteristic peak at 24º.

In co-doped TiO_2 nanotubes broad peaks having low intensity at ~24.5º, ~28.9º and ~48.2 were observed with slight shifting in all samples. These peaks are characteristic peaks of titanate formation in hydrothermal process. Peak broadening is because of low crystallite size, low crystallinity and thin walled nanotubes formation. As according to many studies nanotubes show broad peaks of titanate having low intensity. There are many reports regarding the titanate nanotubes formation in hydrothermal process and there good catalytic performance [56,116]. Titanate can be easily converted to anatase phase by optimization of annealing temperature.

No nitrogen and cobalt derived peaks were observed because of low concentration and uniform distribution of dopants. Possibility of cobalt oxide coating was also ruled out in this way. Characteristic rutile peaks were also not observed.

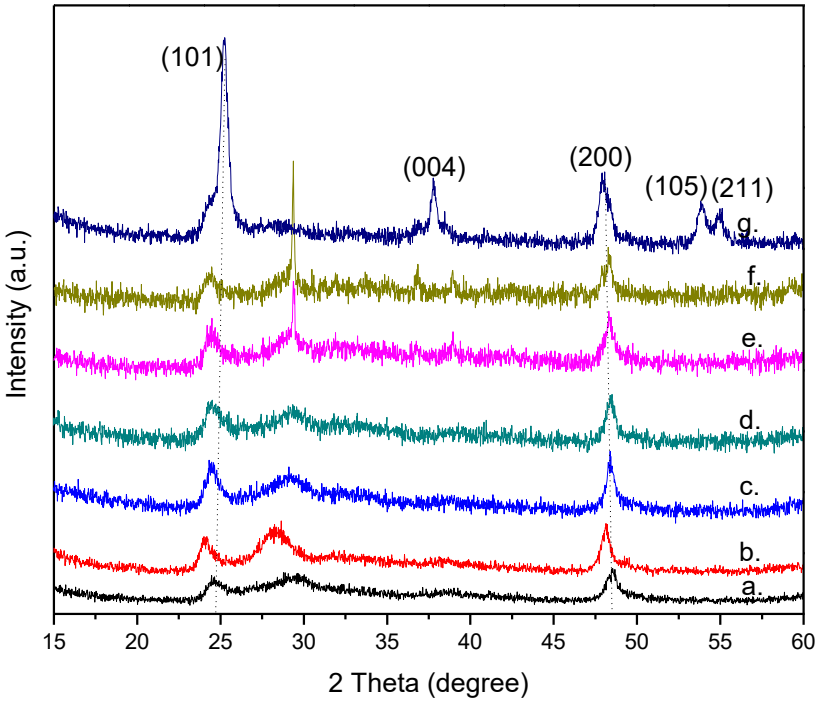

Figure 4.7 XRD spectras of prepared samples (a) TNT, (b) N-TNT, (c) 2-CoN-TNT, (d) 4-CoN-TNT, (e) 6-CoN-TNT, (f) 8-CoN-TNT and (g) rGO-CoN-TNT JCPDS card no. 21-1272 for anatase TiO_2

4.1.4. Brunauer Emmett-Teller (BET) surface area analysis

BET analyses of all the prepared samples were done and surface area was calculated. The surface area of the commercially available titania powder is very less and synthesized nanotubes show remarkable increase in the surface area. Maximum surface area was achieved by simple nanotubes and nitrogen doped nanotubes. As the concentration of cobalt was increased the surface area was decreased because after certain limit the addition of dopants may cause the pore blockage.

Graphene oxide is showing the minimum surface area because no exfoliation of graphene oxide was done and the stacked sheets are showing very less surface area. But in the case of rGO/CoN-TNT (composite of reduced graphene oxide and codoped nanotubes) we saw increase in surface area as compare to simple graphene oxide because in the synthesis route we have done exfoliation by probe sonicator at very high amplitude which causes the separation of layers and thus surface area was increased. The surface areas of all the catalysts are shown in the following table.

Table 4.2 BET surface area of different samples

Sample Code	BET Surface area (m^2/g)
TiO_2 Powder	11
GO	0.6
TNT	168
N-TNT	168
2-CoN-TNT	117
4-CoN-TNT	116
6-CoN-TNT	90
8-CoN-TNT	87
rGO/CoN-TNT	62.29

4.1.5. Diffuse reflectance spectroscopy and tauc plots

From the DRS spectras tauc plots were constructed and band gaps were calculated. TiO_2 in anatase form have band gap of 3.2 eV which is quite enough to make it UV light active only. For making titania visible light active band gap is reduced by doping. Band gaps of all prepared samples are shown in the table 4.8.

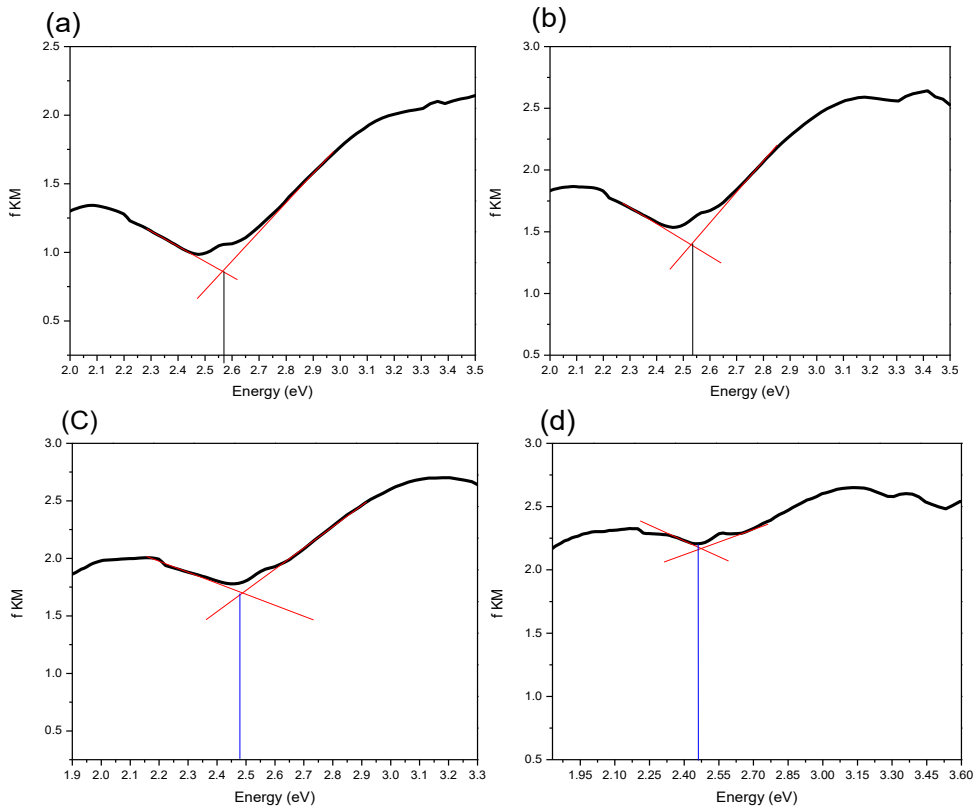

Figure 4.8 Tauc plots of (a) 2-CoN-TNT, (b) 4-CoN-TNT, (c) 6-CoN-TNT and (d) 8-CoN-TNT

Table 4.3 Band gaps of prepared samples

Sample code	Band gap (eV)
2-CoN-TNT	2.59
4-CoN-TNT	2.54
6-CoN-TNT	2.48
8-CoN-TNT	2.43

4.1.6. Fourier transform infrared spectroscopy (FT-IR)

FT-IR spectra of all the prepared samples are shown in figure 4.9 which conveys information about attached functional groups. Prominent peak at 500 cm^{-1} is seen in all titania samples. This peak is because of stretching vibrations of Ti-O-Ti bonds. Peaks at 3320 and 1630 cm^{-1} are because of the stretching and bending vibrations of adsorbed water molecules respectively.

A prominent peak at 1350 cm^{-1} is observed in all codoped samples. This characteristic peak is because of the presence of free nitrate ions as cobalt nitrate was used for cobalt doping. This peak is absent in nanocomposite rGO/CoN-TNT although codoped sample was used for nanocomposite formation. Excessive washing in the synthesis procedure of nanocomposite cause the removal of nitrate ions thus depicting no characteristic peak in particular sample.

GO has many oxygen containing functional groups attached that's why it shows many characteristic peaks. Broad peak at ~3200 -3500 cm^{-1} is representing stretching vibrations of –OH bond, peak at ~1720 cm^{-1} is because of -C=O stretching vibrations (most probably aldehydic group) and prominent peak at 1627 cm^{-1} is because of C=C stretching vibrations. In rGO/CoN-TNT peak at 3400 cm^{-1} is broader as compare to simple nanotubes because of the presence of –OH groups attached on reduced graphene oxide sheets but this peak is less broad as compare to graphene oxide, depicting the reduction of graphene oxide in the synthesis process of composite formation [120].

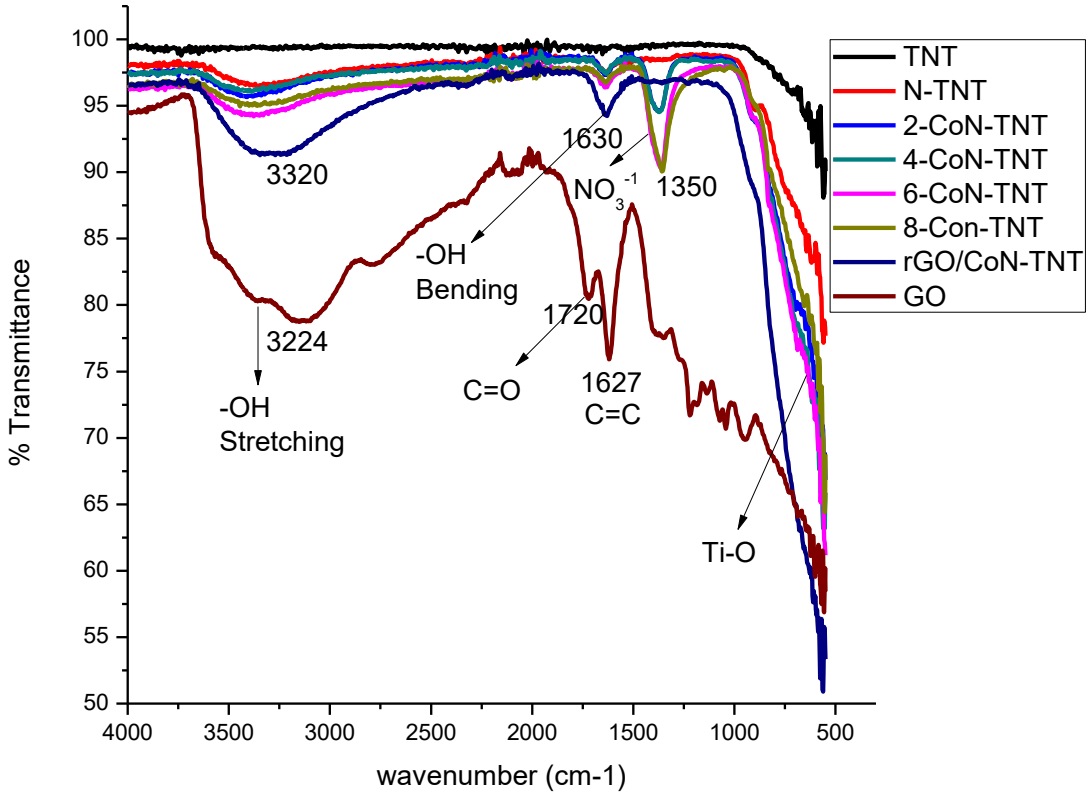

Figure 4.9 FT-IR spectra of as prepared samples

4.1.7 Thermo gravimetric analysis (TGA)

TGA provide us information about the thermal stability of samples. All samples were analyzed by 10 ºC increase in temperature per minute in nitrogen environment. Graphene oxide show mass loss in three stages. Mass loss below 100 ºC was due to the removal of physically adsorbed water on the surface of GO. Different functional groups containing oxygen and hydrogen are attached on graphene oxide sheets. These functional groups form hydrogen bonding with the trapped interlayer water molecules and other attached functional groups as shown in figure 1.19. Slight mass loss was observed between 100-200 ºC was because of the breakage of these hydrogen bonds and again water loss is the cause of this decrease in mass.

Near 200 ºC great mass loss was observed because of the decomposition of oxygen containing groups and formation of CO_2 and H_2O. Here water removal is because of covalent bonds cleavage of different functional groups attached. Mass loss near 600 ºC was observed due to the destruction of carbon double bonds of graphene. Whereas

composite, simple titania nanotubes and codoped titania nanotubes show good thermal stability. No mass loss was observed at 200ºC in rGO/CoN-TNT confirms the reduction of graphene oxide [121].

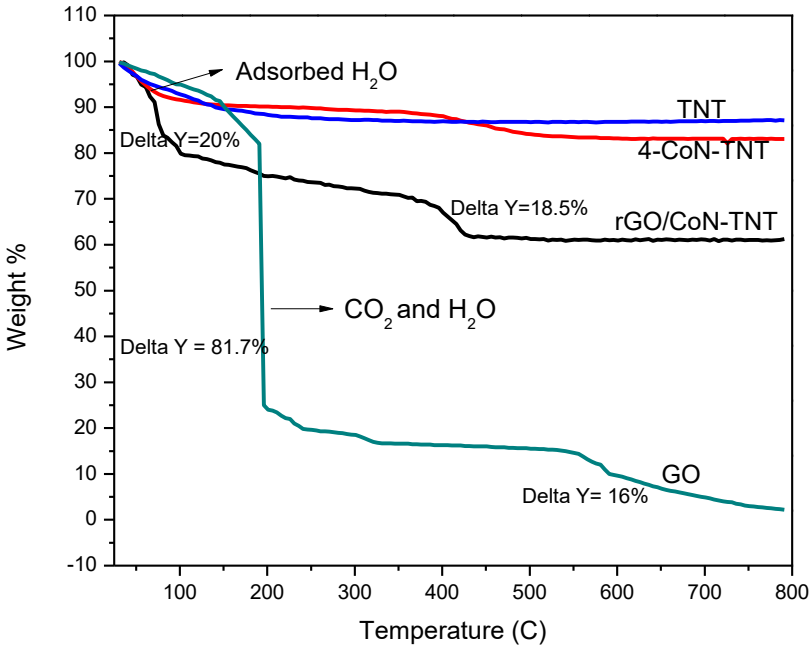

Figure 4.10 Thermogravimetric analysis graphs of samples

4.2. Investigation of the catalytic activity of the synthesized nanocatalysts against methyl orange

4.2.1. Degradation experiment

Degradation of methyl orange was studied to evaluate the activity of as prepared catalysts.

Methyl orange (Scharlau) was used. A solution of 0.1 mM of methyl orange was prepared in distilled water as stock solution and diluted to 0.01mM for photocatalytic study. Figure 4.11 show different concentration solutions of MO.

Figure 4.11 Different concentration solutions of methyl orange.
(a) 3 mM, (b) 0.1 mM, (c) 0.01 mM.

For the experiment about 50 ml solution of 0.01 mM concentration of MO was prepared and 50 mg catalyst was added. The samples was stirred in dark for two hours to ensure adsorption desorption equilibrium. Then 130 micro liters hydrogen peroxide was added as its addition cause the increment in the rate of degradation of dye [132]. Then samples were kept in the reactor chamber having 250 W energy saver under continuous shaking over a shaker at 150 rpm. After different time intervals aliquots were taken, centrifuged and examined from UV-vis spectrophotometer. MO have characteristic peak at 464 nm and decrease in the absorbance at this point indicates MO degradation.

4.2.1.1. Methyl Orange degradation

Each catalyst was checked against degradation of methyl orange. Following graphs and data show degradation of methyl orange against prepared catalysts.

First of all undoped as prepared titania nanotubes were studied. TiO_2 is UV light active and its activity against MO degradation is very less in visible region.

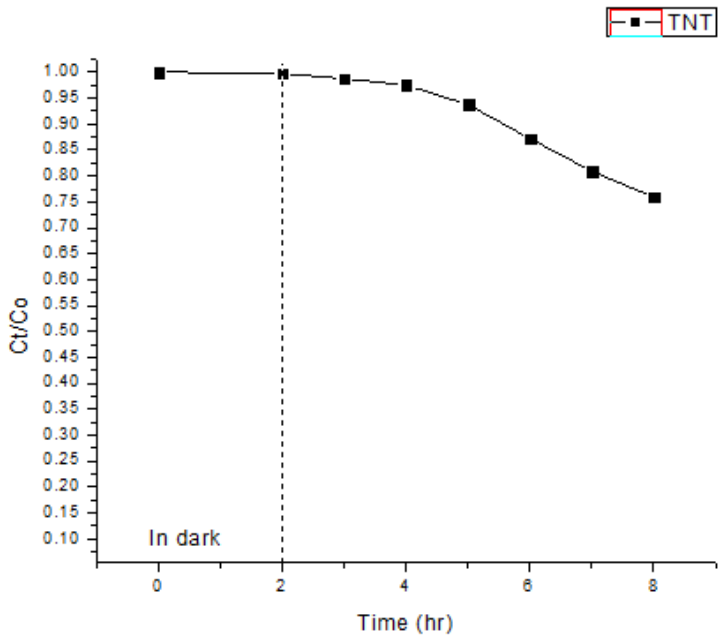

Figure 4.12 Activity of undoped TNT's against MO in visible region

Nitrogen doped TiO_2 nanotubes show better efficiency then undoped TNT's.

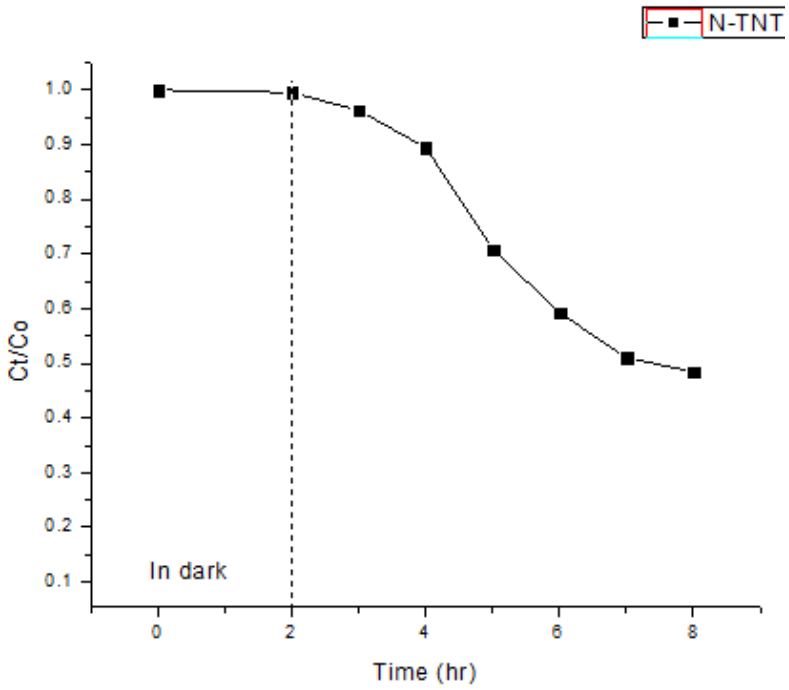

Figure 4.13 Activity of nitrogen doped TNT's against MO in visible region.

Cobalt and nitrogen co-doped TiO_2 nanotubes show better results. As the doped element concentration increases the activity should also increase but 4-CoN-TNT show best results, there are many factors involved due to which high efficiency of

particular catalyst was achieved. The reasons include (i) high surface area of 4-CoN-TNT, as we know that surface area have direct relation with degradation efficiency because more the surface area more will be the available active sights, (ii) concentration of dopant above particular value may also clog the pores or activation sights thus cause lowering in effeciency and (iii) as the dopant concentration was increased the color of catalyst became darker so penetration of light is quite difficult, so absence of light in the core cause poor activity of catalysts.

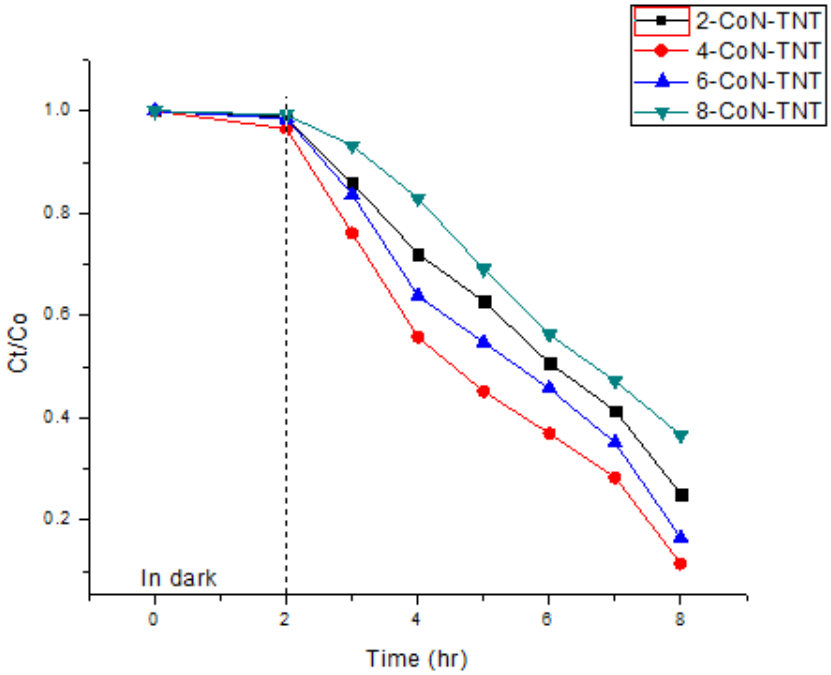

Figure 4.14 Activity of co-doped TNT's against MO degradation.

Best results for the degradation of MO were shown by a composite of reduced graphene oxide and 4-CoN-TNT.

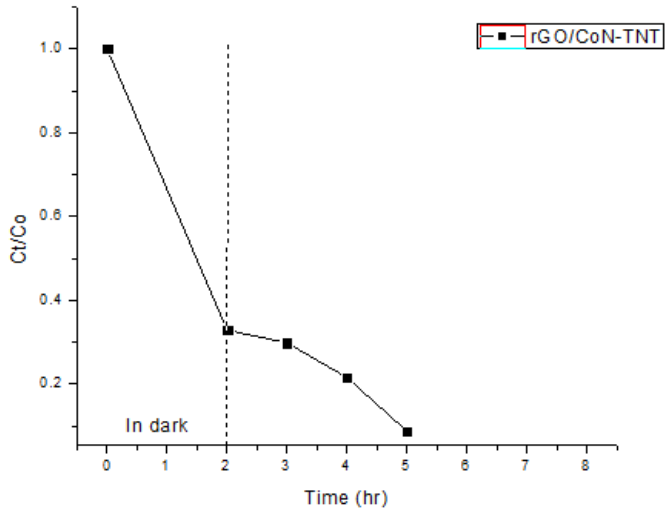

Figure 4.15 Activity of rGO/CoN-TNT against MO degradation.

Blank solutions were also run which show almost no degradation under visible light and conforms that degradation of methyl orange is caused by the as prepared catalysts.

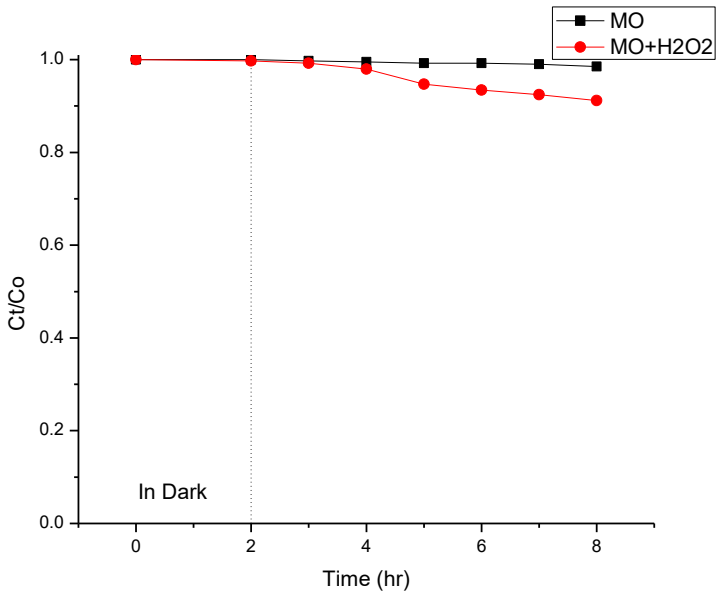

Figure 4.16 Blank run with MO and MO + H_2O_2

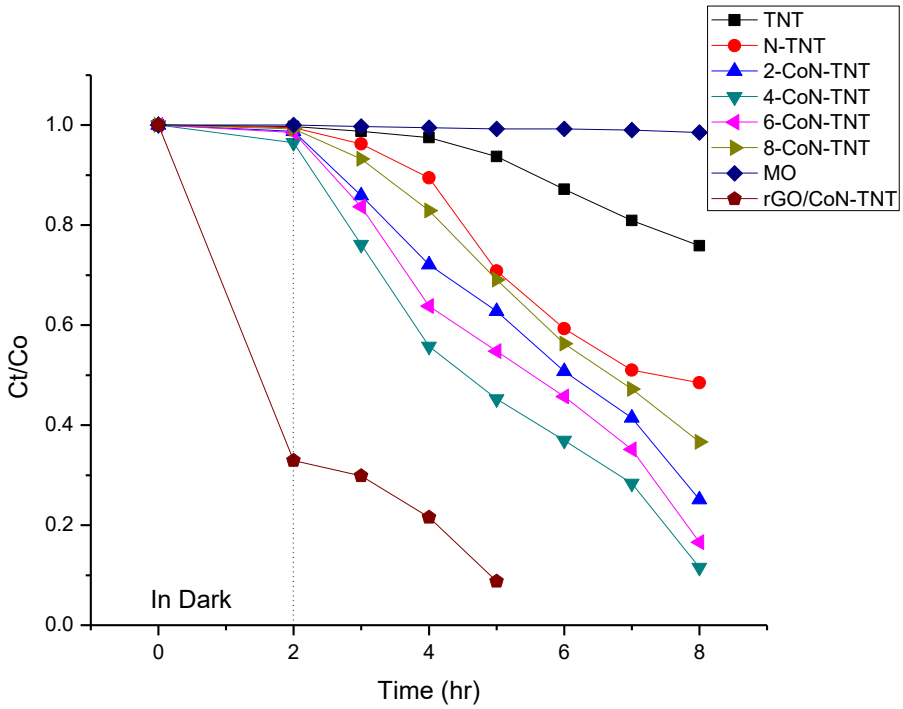

Figure 4.17 Activity of all prepared catalysts and blank run for MO degradation

Percentage efficiency of all catalysts is shown in the following graph;

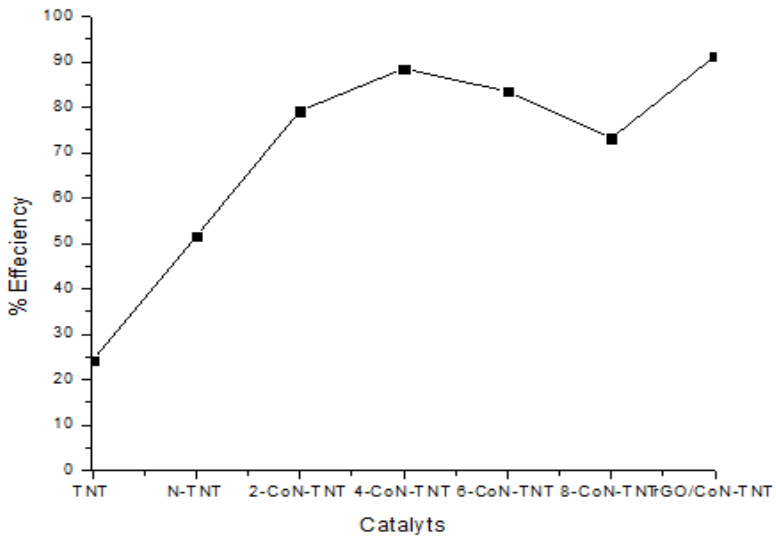

Figure 4.18 Comparison of percentage efficiency of all catalysts against MO

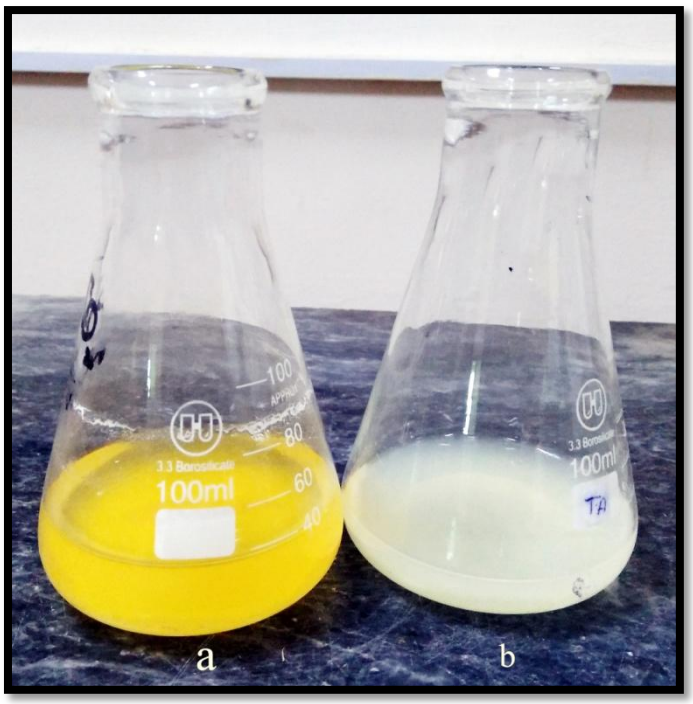

Figure 4.19 Methyl orange solution (a) before and (b) after degradation

The main objective of the study was to make titania visible light active and more efficient by using different techniques. Table 4.4 shows the findings of degradation of methyl orange.

Table 4.4 Degradation rate calculation for MO degradation under visible light

Catalysts	Time (hr)	Absorbance examined	C_t	C_o	C_t/C_o
TNT	2	0.396	0.010894	0.397	0.997525
	3	0.392	0.010784		0.987472
	4	0.387	0.010647		0.974905
	5	0.372	0.010235		0.937206
	6	0.346	0.009522		0.87186
	7	0.321	0.008835		0.809028
	8	0.301	0.008286		0.758762
N-TNT	2	0.395	0.010867	0.397	0.995012
	3	0.382	0.01051		0.962339
	4	0.355	0.009769		0.89448
	5	0.281	0.007737		0.708497
	6	0.235	0.006475		0.592885
	7	0.202	0.005569		0.509947
	8	0.192	0.005295		0.484814
2-CoN-TNT	2	0.392	0.010784	0.397	0.987472
	3	0.341	0.009384		0.859294
	4	0.265	0.007298		0.668284
	5	0.249	0.006859		0.628071
	6	0.201	0.005542		0.507433
	7	0.164	0.004526		0.414442
	8	0.082	0.002275		0.208352
4-CoN-TNT	2	0.383	0.010537	0.397	0.964852
	3	0.302	0.008314		0.761276
	4	0.205	0.005651		0.507433
	5	0.201	0.005542		0.517486
	6	0.187	0.005157		0.472247
	7	0.12	0.003318		0.303857
	8	0.045	0.00126		0.11536

6-CoN-TNT	2	0.391	0.010757	0.397	0.984958
	3	0.339	0.009329		0.854267
	4	0.235	0.006475		0.592885
	5	0.217	0.005981		0.547646
	6	0.194	0.00535		0.48984
	7	0.145	0.004005		0.366689
	8	0.065	0.001809		0.165626
8-CoN-TNT	2	0.394	0.010839	0.397	0.992498
	3	0.379	0.010427		0.954799
	4	0.329	0.009055		0.829134
	5	0.274	0.007545		0.690904
	6	0.223	0.006146		0.562726
	7	0.187	0.005157		0.472247
	8	0.106	0.002934		0.268671
rGO/C0N-TNT	2	0.13	0.003593	0.397	0.32899
	3	0.125	0.003456		0.316423
	4	0.085	0.002358		0.215892
	5	0.034	0.000958		0.087714

4.2.2. Reaction Kinetics

Reaction kinetics of the photocatalytic reaction depends on the catalyst concentration and concentration of the degrading component (methyl orange and dmmp). As the concentration of the catalyst is constant so the expression can be written as;

$$\ln C_t/C_o = -Kt$$

For finding the order of reaction a plot between ln Co/C_t vs time is given by the following figures;

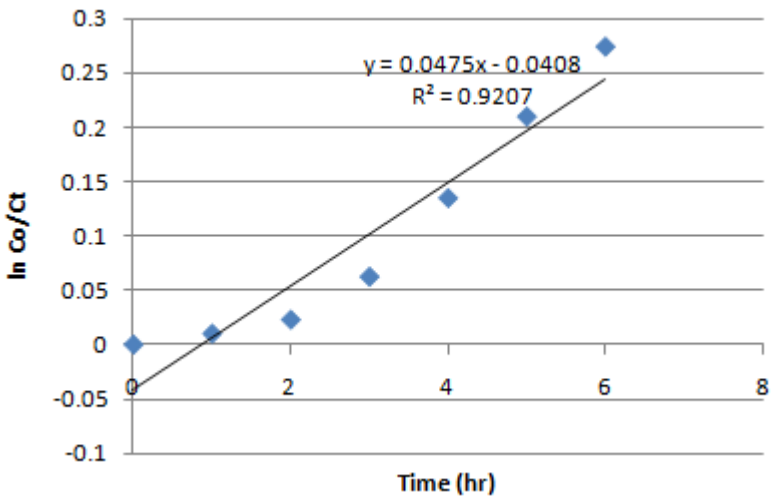

Fig Plot between ln C_o/C_t vs time for MO

The linearity of a graph shows the order of reaction is first order under pseudo condition. From the slope rate constant can be calculated.

Chapter 5: Conclusions and Future Plans

Cobalt and nitrogen co-doped TiO_2 nanotubes were synthesized efficiently from simple hydrothermal method. Conditions for hydrothermal method were same for all samples i.e. heating at 130ºC for 72 hours. Urea and $Co(NO_3)_2.6H_2O$ were used as precursors of nitrogen and cobalt dopants. Different ratios of $Co(NO_3)_2.6H_2O$ added gave different cobalt loading. All samples were characterized by FT-IR, UV-Vis DRS, SEM, TGA, BET, XRD and EDX.

FT-IR confirms some stretching and bending vibrations related to adsorbed water molecules and oxygen containing functional groups attached on graphene oxide. SEM confirms the tube like morphology. By using DRS data we have constructed tauc plots and are able to find band gaps. A decrease in band gap was observed after doping. TGA confirms the thermal stability of TiO_2 even at very high temperatures. The surface area was increased by many folds as compare to starting titania powder was justified by BET analysis.

Among all the synthesized catalysts 4-CoN-TNT show the best activity as its efficiency was nearly 88%. This catalyst was selected for the synthesis of composite with graphene oxide. In situ reduction of graphene oxide was reported and the composite formed have highest efficiency up to 93%.

In future these catalysts will be tested against different pesticides and war fare agent stimulants i.e DMMP. Recyclability of catalysts will be tested and effect of degradation on different properties of catalysts will be examined. As we are using one specific concentration of graphene oxide, we will also optimize it.

References

1. Diebold, Ulrike. "The surface science of titanium dioxide." *Surface science reports* 48, no. 5 (2003): 53-229.
2. Moellmann, Jonas, Stephan Ehrlich, Ralf Tonner, and Stefan Grimme. "A DFT-D study of structural and energetic properties of TiO_2 modifications." *Journal of physics: condensed matter* 24, no. 42 (2012): 424206.
3. Li, Ji-Guang, Takamasa Ishigaki, and Xudong Sun. "Anatase, brookite, and rutile nanocrystals via redox reactions under mild hydrothermal conditions: phase-selective synthesis and physicochemical properties." *The Journal of Physical Chemistry C* 111, no. 13 (2007): 4969-4976.
4. Tang, H., K. Prasad, R. Sanjines, P. E. Schmid, and F. Levy. "Electrical and optical properties of TiO2 anatase thin films." *Journal of applied physics* 75, no. 4 (1994): 2042-2047.
5. Popov, A. P., A. V. Priezzhev, J. Lademann, and R. Myllylä. "TiO_2 nanoparticles as an effective UV-B radiation skin-protective compound in sunscreens." *Journal of Physics D: Applied Physics* 38, no. 15 (2005): 2564.
6. Jaroenworaluck, A., W. Sunsaneeyametha, N. Kosachan, and R. Stevens. "Characteristics of silica-coated TiO2 and its UV absorption for sunscreen cosmetic applications." *Surface and Interface Analysis* 38, no. 4 (2006): 473-477.
7. Braun, Juergen H., Andrejs Baidins, and Robert E. Marganski. "TiO_2 pigment technology: a review." *Progress in organic coatings* 20, no. 2 (1992): 105-138.
8. Zhao, Xiujian, Qingnan Zhao, Jiaguo Yu, and Baoshun Liu. "Development of multifunctional photoactive self-cleaning glasses." *Journal of Non-Crystalline Solids* 354, no. 12 (2008): 1424-1430.
9. Guan, Kaishu. "Relationship between photocatalytic activity, hydrophilicity and self-cleaning effect of TiO_2/SiO_2 films." *Surface and Coatings Technology* 191, no. 2 (2005): 155-160.
10. Benedix, Roland, Frank Dehn, Jana Quaas, and Marko Orgass. "Application of titanium dioxide photocatalysis to create self-cleaning building materials." *Lacer* 5 (2000): 157-168.
11. Tian, Wei-Cheng, Yu-Hsuan Ho, Chao-Hao Chen, and Chun-Yen Kuo. "Sensing performance of precisely ordered TiO_2 nanowire gas sensors fabricated by electron-beam lithography." *Sensors* 13, no. 1 (2013): 865-874.
12. Traversa, Enrico, Maria Luisa Di Vona, Silvia Licoccia, Michele Sacerdoti, Maria Cristina Carotta, Luigi Crema, and Giuliano Martinelli. "Sol-gel processed TiO_2-based nano-sized powders for use in thick-film gas sensors for atmospheric pollutant monitoring." *Journal of sol-gel science and technology* 22, no. 1 (2001): 167-179.
13. Shen, Jing, Zhanqian Song, Xueren Qian, and Yonghao Ni. "A review on use of fillers in cellulosic paper for functional applications." *Industrial & Engineering Chemistry Research* 50, no. 2 (2010): 661-666.
14. Yu, Jiaguo, Lifang Qi, and Mietek Jaroniec. "Hydrogen production by photocatalytic water splitting over Pt/TiO_2 nanosheets with exposed (001) facets." *The Journal of Physical Chemistry C* 114, no. 30 (2010): 13118-13125.

15. Bhatkhande, Dhananjay S., Sanjay P. Kamble, Sudhir B. Sawant, and Vishwas G. Pangarkar. "Photocatalytic and photochemical degradation of nitrobenzene using artificial ultraviolet light." *Chemical Engineering Journal*102, no. 3 (2004): 283-290.
16. Cardoso, Juliano Carvalho, Thiago Mescoloto Lizier, and Maria Valnice Boldrin Zanoni. "Highly ordered TiO_2 nanotube arrays and photoelectrocatalytic oxidation of aromatic amine." *Applied Catalysis B: Environmental* 99, no. 1 (2010): 96-102.
17. Chen, Wen-Shing, and Shu-Chi Huang. "Sonophotocatalytic degradation of dinitrotoluenes and trinitrotoluene in industrial wastewater." *Chemical engineering journal* 172, no. 2 (2011): 944-951.
18. Surolia, Praveen K., and Raksh V. Jasra. "Photocatalytic degradation of p-nitrotoluene (PNT) using TiO_2-modified silver-exchanged NaY zeolite: kinetic study and identification of mineralization pathway." *Desalination and Water Treatment* 57, no. 46 (2016): 22081-22098.
19. Nakata, Kazuya, and Akira Fujishima. "TiO_2 photocatalysis: design and applications." *Journal of Photochemistry and Photobiology C: Photochemistry Reviews* 13, no. 3 (2012): 169-189.
20. Yang, Hua Gui, and Hua Chun Zeng. "Preparation of hollow anatase TiO_2 nanospheres via Ostwald ripening." *The Journal of Physical Chemistry B*108, no. 11 (2004): 3492-3495.
21. Li, Jing, and Hua Chun Zeng. "Hollowing Sn-doped TiO_2 nanospheres via Ostwald ripening." *Journal of the American Chemical Society* 129, no. 51 (2007): 15839-15847.
22. Kasuga, Tomoko, Masayoshi Hiramatsu, Akihiko Hoson, Toru Sekino, and Koichi Niihara. "Formation of titanium oxide nanotube." *Langmuir* 14, no. 12 (1998): 3160-3163.
23. Wong, Chung Leng, Yong Nian Tan, and Abdul Rahman Mohamed. "A review on the formation of titania nanotube photocatalysts by hydrothermal treatment." *Journal of environmental management* 92, no. 7 (2011): 1669-1680.
24. Tsai, Chien-Cheng, and Hsisheng Teng. "Regulation of the physical characteristics of titania nanotube aggregates synthesized from hydrothermal treatment." *Chemistry of Materials* 16, no. 22 (2004): 4352-4358.
25. Xing, Jun, Hua Gui Yang, and Gao Qing Max Lu. "Enhanced solar water splitting by surface engineering of titanium dioxide." *Nanotechnology, SPIE Newsroom* 3894 (2011): 1-3.
26. Shichi, T., and K-I. Katsumata. "Development of photocatalytic self-cleaning glasses utilizing metal oxide nanosheets." *Hyomen Gijutsu* 61 (2010): 30-35.
27. Cai, Hongyuan, Xiaoxu Chen, Qinghua Li, Benlin He, and Qunwei Tang. "Enhanced photocatalytic activity from Gd, la codoped TiO 2 nanotube array photocatalysts under visible-light irradiation." *Applied Surface Science* 284 (2013): 837-842.
28. Zhang, Shengsen, Feng Peng, Hongjuan Wang, Hao Yu, Shanqing Zhang, Jian Yang, and Huijun Zhao. "Electrodeposition preparation of Ag loaded N-doped TiO 2 nanotube arrays with enhanced visible light photocatalytic performance." *Catalysis Communications* 12, no. 8 (2011): 689-693.

29. Shankar, Karthik, Gopal K. Mor, Haripriya E. Prakasam, Sorachon Yoriya, Maggie Paulose, Oomman K. Varghese, and Craig A. Grimes. "Highly-ordered TiO_2 nanotube arrays up to 220 µm in length: use in water photoelectrolysis and dye-sensitized solar cells." *Nanotechnology* 18, no. 6 (2007): 065707.
30. Galstyan, Vardan, Elisabetta Comini, Guido Faglia, and Giorgio Sberveglieri. "TiO2 nanotubes: recent advances in synthesis and gas sensing properties." *Sensors* 13, no. 11 (2013): 14813-14838.
31. Qiu, Jijun, Weidong Yu, Xiangdong Gao, and Xiaomin Li. "Sol–gel assisted ZnO nanorod array template to synthesize TiO_2 nanotube arrays." *Nanotechnology* 17, no. 18 (2006): 4695.
32. Iijima, Sumio. "Helical microtubules of graphitic carbon." *nature* 354, no. 6348 (1991): 56.
33. Ogihara, Hitoshi, Masahiro Sadakane, Yoshinobu Nodasaka, and Wataru Ueda. "Shape-controlled synthesis of ZrO_2, Al_2O_3, and SiO_2 nanotubes using carbon nanofibers as templates." *Chemistry of materials* 18, no. 21 (2006): 4981-4983.
34. Bastakoti, Bishnu Prasad, Masataka Imura, Yoshihiro Nemoto, and Yusuke Yamauchi. "Synthesis of MoO_3 nanotubes by thermal mesostructural transition of spherical triblock copolymer micelle templates." *Chemical Communications* 48, no. 99 (2012): 12091-12093.
35. Mohan, V. M., Bin Hu, Weiliang Qiu, and Wen Chen. "Synthesis, structural, and electrochemical performance of V_2O_5 nanotubes as cathode material for lithium battery." *Journal of applied electrochemistry* 39, no. 10 (2009): 2001.
36. Xiao, Yaoming, Jihuai Wu, Gentian Yue, Guixiang Xie, Jianming Lin, and Miaoliang Huang. "The preparation of titania nanotubes and its application in flexible dye-sensitized solar cells." *Electrochimica Acta* 55, no. 15 (2010): 4573-4578.
37. Hsieh, Chien-Te, Wen-Syuan Fan, Wei-Yu Chen, and Jia-Yi Lin. "Adsorption and visible-light-derived photocatalytic kinetics of organic dye on Co-doped titania nanotubes prepared by hydrothermal synthesis." *Separation and Purification Technology* 67, no. 3 (2009): 312-318.
38. Kasuga, Tomoko, Masayoshi Hiramatsu, Akihiko Hoson, Toru Sekino, and Koichi Niihara. "Titania nanotubes prepared by chemical processing." *Advanced Materials* 11, no. 15 (1999): 1307-1311.
39. Kamat, Prashant V. "Meeting the clean energy demand: nanostructure architectures for solar energy conversion." *The Journal of Physical Chemistry C* 111, no. 7 (2007): 2834-2860.
40. Chen, Xiaobo, Can Li, Michaël Grätzel, Robert Kostecki, and Samuel S. Mao. "Nanomaterials for renewable energy production and storage." *Chemical Society Reviews* 41, no. 23 (2012): 7909-7937.
41. Romeas, Virginie, Pierre Pichat, Chantal Guillard, Thierry Chopin, and Corinne Lehaut. "Testing the efficacy and the potential effect on indoor air quality of a transparent self-cleaning TiO_2-coated glass through the degradation of a fluoranthene layer." *Industrial & engineering chemistry research* 38, no. 10 (1999): 3878-3885.
42. Paz, Y., Z. Luo, L. Rabenberg, and A. Heller. "Photooxidative self-cleaning transparent titanium dioxide films on glass." *Journal of Materials Research*10, no. 11 (1995): 2842-2848.

43. Thu, Hoai Bui, Maithaa Karkmaz, Eric Puzenat, Chantal Guillard, and Jean-Marie Herrmann. "From the fundamentals of photocatalysis to its applications in environment protection and in solar purification of water in arid countries." *Research on chemical intermediates* 31, no. 4 (2005): 449-461.
44. Zhang, Yanrong, Jing Wan, and Youqing Ke. "A novel approach of preparing TiO_2 films at low temperature and its application in photocatalytic degradation of methyl orange." *Journal of Hazardous Materials* 177, no. 1 (2010): 750-754.
45. Linsebigler, Amy L., Guangquan Lu, and John T. Yates Jr. "Photocatalysis on TiO_2 surfaces: principles, mechanisms, and selected results." *Chemical reviews* 95, no. 3 (1995): 735-758.
46. *Photocatalysis*. The Parashant kamat Laboratory. Available from: https://www3.nd.edu/~kamatlab/research_photocatalysis.html
47. Seery, M., *Metal Oxide Photocatalysis.* 2009. Available from: https://photochemistry.wordpress.com/2009/09/30/metal-oxide-photocatalysis/
48. Zhang, Liwu, and Yongfa Zhu. "A review of controllable synthesis and enhancement of performances of bismuth tungstate visible-light-driven photocatalysts." *Catalysis Science & Technology* 2, no. 4 (2012): 694-706.
49. Doong, Ruey-an, and Chun-Yi Liao. "Enhanced visible-light-responsive photodegradation of bisphenol A by Cu, N-codoped titanate nanotubes prepared by microwave-assisted hydrothermal method." *Journal of hazardous materials* 322 (2017): 254-262.
50. Tokudome, Hiromasa, and Masahiro Miyauchi. "N-doped TiO_2 nanotube with visible light activity." *Chemistry Letters* 33, no. 9 (2004): 1108-1109.
51. Zhao, Xiao, Zhengqing Cai, Ting Wang, S. E. O'Reilly, Wen Liu, and Dongye Zhao. "A new type of cobalt-deposited titanate nanotubes for enhanced photocatalytic degradation of phenanthrene." *Applied Catalysis B: Environmental* 187 (2016): 134-143.
52. Wang, Jung-Pin, Hsi-Chi Yang, and Chien-Te Hsieh. "Visible-light photodegradation of dye on Co-doped Titania nanotubes prepared by hydrothermal synthesis." *International Journal of Photoenergy* 2012 (2011).
53. Liang, Jicai, Cuiyu Hao, Kaifeng Yu, and Yi Li. "Excellent photocatalytic performance of cobalt-doped titanium dioxide nanotubes under ultraviolet light." *Nanomaterials and Nanotechnology* 6 (2016): 1847980416680808.
54. Dong, Fan, Weirong Zhao, and Zhongbiao Wu. "Characterization and photocatalytic activities of C, N and S co-doped TiO_2 with 1D nanostructure prepared by the nano-confinement effect." *Nanotechnology* 19, no. 36 (2008): 365607.
55. Chai, Yuchao, Lin Lin, Ke Zhang, Bin Zhao, and Dannong He. "Efficient visible-light photocatalysts from Gd–La codoped TiO_2 nanotubes." *Ceramics International* 40, no. 2 (2014): 2691-2696.
56. Parayil, Sreenivasan Koliyat, Abdul Razzaq, Seung-Min Park, Hye Rim Kim, Craig A. Grimes, and Su-Il In. "Photocatalytic conversion of CO_2 to hydrocarbon fuel using carbon and nitrogen co-doped sodium titanate nanotubes." *Applied Catalysis A: General* 498 (2015): 205-213.
57. Fan, Jinmin, Zhihuan Zhao, Jianye Wang, and Lixiao Zhu. "Synthesis of Cr, N-codoped titania nanotubes and their visible-light-driven photocatalytic properties." *Applied Surface Science* 324 (2015): 691-697.

58. Behnajady, Mohammad A., and Hamed Eskandarloo. "Characterization and photocatalytic activity of Ag–Cu/TiO_2 nanoparticles prepared by sol–gel method." *Journal of nanoscience and nanotechnology* 13, no. 1 (2013): 548-553.
59. Li, Guangshe, Liping Li, Juliana Boerio-Goates, and Brian F. Woodfield. "High purity anatase TiO_2 nanocrystals: near room-temperature synthesis, grain growth kinetics, and surface hydration chemistry." *Journal of the American Chemical Society* 127, no. 24 (2005): 8659-8666.
60. Lee, Soo-Keun, and Andrew Mills. "Detoxification of water by semiconductor photocatalysis." *Journal of Industrial and Engineering Chemistry* 10, no. 2 (2004): 173-187.
61. Sobczyński, A., and A. Dobosz. "Water purification by photocatalysis on semiconductors." *Polish journal of environmental studies* 10, no. 4 (2001): 195-205.
62. Stothers, J.B., *Dye*. Encyclopædia Britannica, inc.: Encyclopædia Britannica. Available from: https://www.britannica.com/technology/dye
63. *What is Dye*, in *dye-pigments.standardcon*. Available from: dyes-pigments.standardcon.com/what-is-dye.html
64. *Classification of Dyes*. Available from: https://textlnfo.wordpress.com/2011/12/04/classification-of-dyes/.
65. *Problems Caused by Textile Dyes in the Environment*. 2017: Textile Learner. Available from: http://textilelearner.blogspot.com/2011/04/problems-of-textile-dyes-in-environment_4787.html
66. *Environmental Chemistry of Dyes and Pigments*. 1996, United states of America: A Wiley-Interscience Publications.
67. Sandberg, Richard G., Gary H. Henderson, Robert D. White, and Edward M. Eyring. "Kinetics of acid dissociation-ion recombination of aqueous methyl orange." *The Journal of Physical Chemistry* 76, no. 26 (1972): 4023-4025.
68. Ajmal, Anila, Imran Majeed, Riffat Naseem Malik, Hicham Idriss, and Muhammad Amtiaz Nadeem. "Principles and mechanisms of photocatalytic dye degradation on TiO_2 based photocatalysts: a comparative overview." *Rsc Advances* 4, no. 70 (2014): 37003-37026.
69. Wu, Chun-Hsing, and Jia-Ming Chern. "Kinetics of photocatalytic decomposition of methylene blue." *Industrial & engineering chemistry research* 45, no. 19 (2006): 6450-6457.
70. Dyro, F.M., *Organophosphates.* Medscape, 2017. Available from: emedicine.medscape.com/article/1175139-overview
71. Ganesan, K., S. K. Raza, and R. Vijayaraghavan. "Chemical warfare agents." *Journal of pharmacy and bioallied sciences* 2, no. 3 (2010): 166.
72. Chauhan, S., R. D'cruz, S. Faruqi, K. K. Singh, S. Varma, M. Singh, and V. Karthik. "Chemical warfare agents." *Environmental toxicology and pharmacology* 26, no. 2 (2008): 113-122.
73. Panayotov, Dimitar A., and John R. Morris. "Thermal decomposition of a chemical warfare agent simulant (DMMP) on TiO_2: Adsorbate reactions with lattice oxygen as studied by infrared spectroscopy." *The Journal of Physical Chemistry C* 113, no. 35 (2009): 15684-15691.
74. Zheng, Qi, Yong-chun Fu, and Jia-qiang Xu. "Advances in the chemical sensors for the detection of DMMP—A simulant for nerve agent sarin." *Procedia Engineering* 7 (2010): 179-184.

75. Smalley, Richard E. "Discovering the fullerenes." *Reviews of Modern Physics*69, no. 3 (1997): 723.
76. Novoselov, Kostya S., Andre K. Geim, Sergei V. Morozov, D. Jiang, Y_ Zhang, Sergey V. Dubonos, Irina V. Grigorieva, and Alexandr A. Firsov. "Electric field effect in atomically thin carbon films." *science* 306, no. 5696 (2004): 666-669.
77. Geim, A. K., and K. S. Novoselov. "The rise of graphene. naturematerials, 6: 183–191." (2007).
78. Dreyer, Daniel R., Sungjin Park, Christopher W. Bielawski, and Rodney S. Ruoff. "The chemistry of graphene oxide." *Chemical Society Reviews* 39, no. 1 (2010): 228-240.
79. Lee, Changgu, Xiaoding Wei, Jeffrey W. Kysar, and James Hone. "Measurement of the elastic properties and intrinsic strength of monolayer graphene." *science* 321, no. 5887 (2008): 385-388.
80. Teo, P. S., H. N. Lim, N. M. Huang, Chin Hua Chia, and I. Harrison. "Room temperature in situ chemical synthesis of Fe 3 O 4/graphene." *Ceramics International* 38, no. 8 (2012): 6411-6416.
81. Dong, Xiaochen, Wei Huang, and Peng Chen. "In situ synthesis of reduced graphene oxide and gold nanocomposites for nanoelectronics and biosensing." *Nanoscale Res Lett* 6, no. 1 (2011): 60.
82. Lu, Ting, Likun Pan, Haibo Li, Guang Zhu, Tian Lv, Xinjuan Liu, Zhuo Sun, Ting Chen, and Daniel HC Chua. "Microwave-assisted synthesis of graphene–ZnO nanocomposite for electrochemical supercapacitors." *Journal of Alloys and Compounds* 509, no. 18 (2011): 5488-5492.
83. Song, Shuyan, Wei Gao, Xiao Wang, Xiyan Li, Dapeng Liu, Yan Xing, and Hongjie Zhang. "Microwave-assisted synthesis of BiOBr/graphene nanocomposites and their enhanced photocatalytic activity." *Dalton Transactions* 41, no. 34 (2012): 10472-10476.
84. Mai, Y. J., X. L. Wang, J. Y. Xiang, Y. Q. Qiao, D. Zhang, C. D. Gu, and J. P. Tu. "CuO/graphene composite as anode materials for lithium-ion batteries." *Electrochimica Acta* 56, no. 5 (2011): 2306-2311.
85. Li, Baojun, and Huaqiang Cao. "ZnO@ graphene composite with enhanced performance for the removal of dye from water." *Journal of Materials Chemistry* 21, no. 10 (2011): 3346-3349.
86. Zhang, Ming, Danni Lei, Zhifeng Du, Xiaoming Yin, Libao Chen, Qiuhong Li, Yangguo Wang, and Taihong Wang. "Fast synthesis of SnO_2/graphene composites by reducing graphene oxide with stannous ions." *Journal of Materials Chemistry* 21, no. 6 (2011): 1673-1676.
87. He, Qiyuan, Shixin Wu, Zongyou Yin, and Hua Zhang. "Graphene-based electronic sensors." *Chemical Science* 3, no. 6 (2012): 1764-1772.
88. Yuan, Wenjing, and Gaoquan Shi. "Graphene-based gas sensors." *Journal of Materials Chemistry A* 1, no. 35 (2013): 10078-10091.
89. Gutés, Albert, Ben Hsia, Allen Sussman, Willi Mickelson, Alex Zettl, Carlo Carraro, and Roya Maboudian. "Graphene decoration with metal nanoparticles: towards easy integration for sensing applications." *Nanoscale*4, no. 2 (2012): 438-440.
90. Zou, Rujia, Guanjie He, Kaibing Xu, Qian Liu, Zhenyu Zhang, and Junqing Hu. "ZnO nanorods on reduced graphene sheets with excellent field emission, gas sensor and photocatalytic properties." *Journal of Materials Chemistry A* 1, no. 29 (2013): 8445-8452.

91. Song, Hongjie, Lichun Zhang, Chunlan He, Ying Qu, Yunfei Tian, and Yi Lv. "Graphene sheets decorated with SnO_2 nanoparticles: in situ synthesis and highly efficient materials for cataluminescence gas sensors." *Journal of Materials Chemistry* 21, no. 16 (2011): 5972-5977.
92. Wang, Da-Wei, Aijun Du, Elena Taran, Gao Qing Max Lu, and Ian R. Gentle. "A water-dielectric capacitor using hydrated graphene oxide film." *Journal of Materials Chemistry* 22, no. 39 (2012): 21085-21091.
93. Becker, H.I., *Low voltage electrolytic capacitor*. 1957, Google Patents.
94. Salari, Maryam, Seyed Hamed Aboutalebi, Konstantin Konstantinov, and Hua Kun Liu. "A highly ordered titania nanotube array as a supercapacitor electrode." *Physical Chemistry Chemical Physics* 13, no. 11 (2011): 5038-5041.
95. Xie, Yibing, Chuanjun Huang, Limin Zhou, Yang Liu, and Haitao Huang. "Supercapacitor application of nickel oxide–titania nanocomposites." Composites Science and Technology 69, no. 13 (2009): 2108-2114.
96. Lu, Linghong, Yudan Zhu, Fujun Li, Wei Zhuang, Kwong Yu Chan, and Xiaohua Lu. "Carbon titania mesoporous composite whisker as stable supercapacitor electrode material." *Journal of Materials Chemistry* 20, no. 36 (2010): 7645-7651.
97. *Facts about Water*. 2016; Available from: https://thewaterproject.org/water-scarcity/water_stats.
98. Xiang, Quanjun, Jiaguo Yu, and Mietek Jaroniec. "Graphene-based semiconductor photocatalysts." *Chemical Society Reviews* 41, no. 2 (2012): 782-796.
99. Fujishima, Akira, Xintong Zhang, and Donald A. Tryk. "TiO_2 photocatalysis and related surface phenomena." *Surface Science Reports* 63, no. 12 (2008): 515-582.
100. Gong, Dawei, Craig A. Grimes, Oomman K. Varghese, Wenchong Hu, R. S. Singh, Zhi Chen, and Elizabeth C. Dickey. "Titanium oxide nanotube arrays prepared by anodic oxidation." *Journal of Materials Research* 16, no. 12 (2001): 3331-3334.
101. Li, Qi, and Jian Ku Shang. "Self-organized nitrogen and fluorine co-doped titanium oxide nanotube arrays with enhanced visible light photocatalytic performance." *Environmental science & technology* 43, no. 23 (2009): 8923-8929.
102. Maiyalagan, T., B. Viswanathan, and U. V. Varadaraju. "Fabrication and characterization of uniform TiO_2 nanotube arrays by sol--gel template method." *Bulletin of Materials Science* 29, no. 7 (2006).
103. Cheng, Zhuowei, Zhiqi Gu, Jianmeng Chen, Jianming Yu, and Lingjun Zhou. "Synthesis, characterization, and photocatalytic activity of porous La–N–co-doped TiO_2 nanotubes for gaseous chlorobenzene oxidation." *Journal of Environmental Sciences* 46 (2016): 203-213.
104. Du, G. H., Q. Chen, R. C. Che, Z. Y. Yuan, and L-M. Peng. "Preparation and structure analysis of titanium oxide nanotubes." *Applied Physics Letters* 79, no. 22 (2001): 3702-3704.
105. Sun, Xiaoming, and Yadong Li. "Synthesis and characterization of ion-exchangeable titanate nanotubes." *Chemistry-A European Journal* 9, no. 10 (2003): 2229-2238.

106. Tsai, Chien-Cheng, and Hsisheng Teng. "Regulation of the physical characteristics of titania nanotube aggregates synthesized from hydrothermal treatment." *Chemistry of Materials* 16, no. 22 (2004): 4352-4358.

107. Bavykin, Dmitry V., Valentin N. Parmon, Alexei A. Lapkin, and Frank C. Walsh. "The effect of hydrothermal conditions on the mesoporous structure of TiO_2 nanotubes." *Journal of Materials Chemistry* 14, no. 22 (2004): 3370-3377.

108. Poudel, B., W. Z. Wang, C. Dames, J. Y. Huang, S. Kunwar, D. Z. Wang, D. Banerjee, G. Chen, and Z. F. Ren. "Formation of crystallized titania nanotubes and their transformation into nanowires." *Nanotechnology* 16, no. 9 (2005): 1935.

109. Razali, Mohd Hasmizam, Ahmad-Fauzi Mohd Noor, Abdul Rahman Mohamed, and Srimala Sreekantan. "Morphological and structural studies of titanate and titania nanostructured materials obtained after heat treatments of hydrothermally produced layered titanate." *Journal of Nanomaterials* 2012 (2012): 18.

110. Natarajan, Kalithasan, Rukshana I. Kureshy, Hari C. Bajaj, and Rajesh J. Tayade. "Photocatalytic Degradation of Indigo Carmine Dye Using Hydrothermally Synthesized Anatase TiO_2 Nanotubes under Ultraviolet Light Emitting Diode Irradiation." In *Materials Science Forum*, vol. 855, pp. 45-57. Trans Tech Publications, 2016.

111. Geng, Jiaqing, Dong Yang, Juhong Zhu, Daimei Chen, and Zhongyi Jiang. "Nitrogen-doped TiO_2 nanotubes with enhanced photocatalytic activity synthesized by a facile wet chemistry method." *Materials Research Bulletin*44, no. 1 (2009): 146-150.

112. Lin, D. O. N. G., Guo-Xi Cao, M. A. Ying, Xiao-Lin Jia, Guo-Tian Ye, and Shao-Kang Guan. "Enhanced photocatalytic degradation properties of nitrogen-doped titania nanotube arrays." *Transactions of Nonferrous Metals Society of China* 19, no. 6 (2009): 1583-1587.

113. Lai, Yue-Kun, Jian-Ying Huang, Hui-Fang Zhang, Vishnu-Priya Subramaniam, Yu-Xin Tang, Dang-Guo Gong, Latha Sundar, Lan Sun, Zhong Chen, and Chang-Jian Lin. "Nitrogen-doped TiO_2 nanotube array films with enhanced photocatalytic activity under various light sources." *Journal of Hazardous Materials* 184, no. 1 (2010): 855-863.

114. Xu, Jingjing, Yanhui Ao, Mindong Chen, and Degang Fu. "Photoelectrochemical property and photocatalytic activity of N-doped TiO 2 nanotube arrays." *Applied Surface Science* 256, no. 13 (2010): 4397-4401.

115. Antony, Rajini P., Tom Mathews, Kalpataru Panda, B. Sundaravel, S. Dash, and A. K. Tyagi. "Enhanced field emission properties of electrochemically synthesized self-aligned nitrogen-doped TiO_2 nanotube array thin films." *The Journal of Physical Chemistry C* 116, no. 31 (2012): 16740-16746.

116. Hu, Cheng-Ching, Tzu-Chien Hsu, and Shan-Yu Lu. "Effect of nitrogen doping on the microstructure and visible light photocatalysis of titanate nanotubes by a facile cohydrothermal synthesis via urea treatment." *Applied Surface Science* 280 (2013): 171-178.

117. Ferreira, V. C., M. R. Nunes, A. J. Silvestre, and O. C. Monteiro. "Synthesis and properties of Co-doped titanate nanotubes and their optical sensitization with methylene blue." *Materials Chemistry and Physics* 142, no. 1 (2013): 355-362.

118. Doong, Ruey-an, and Chun-Yi Liao. "Enhanced visible-light-responsive photodegradation of bisphenol A by Cu, N-codoped titanate nanotubes prepared by microwave-assisted hydrothermal method." *Journal of hazardous materials* 322 (2017): 254-262.
119. Song, Peng, Xiaoyan Zhang, Mingxuan Sun, Xiaoli Cui, and Yuehe Lin. "Graphene oxide modified TiO_2 nanotube arrays: enhanced visible light photoelectrochemical properties." *Nanoscale* 4, no. 5 (2012): 1800-1804.
120. Liu, Wei, Xinzhi Wang, Jianguo Song, Qian Zhang, and Chang-Tang Chang. "Synthesis and visible catalytic applications of graphene–titania dioxide nanotube composites." *Materials Science in Semiconductor Processing* 27 (2014): 273-279.
121. Tao, Hong, Xiao Liang, Qian Zhang, and Chang-Tang Chang. "Enhanced photoactivity of graphene/titanium dioxide nanotubes for removal of Acetaminophen." *Applied Surface Science* 324 (2015): 258-264.
122. Wan, Junmin, Meng Wei, Zhiwen Hu, Zhiqin Peng, Bing Wang, Daoyan Feng, and Yuewei Shen. "Ternary composites of TiO_2 nanotubes with reduced graphene oxide (rGO) and meso-tetra (4-carboxyphenyl) porphyrin for enhanced visible light photocatalysis." *International Journal of Hydrogen Energy* 41, no. 33 (2016): 14692-14703.
123. Lai, Qi, Xue-ping Luo, and Shi-fu Zhu. "Titania nanotube-graphene oxide hybrids with excellent photocatalytic activities." *New Carbon Materials* 31, no. 2 (2016): 121-128.
124. Liu, Huidi, Yaling Wang, Lei Shi, Ruopeng Xu, Langhuan Huang, and Shaozao Tan. "Utilization of reduced graphene oxide for the enhancement of photocatalytic property of TiO_2 nanotube." *Desalination and Water Treatment*57, no. 28 (2016): 13263-13272.
125. O'shea, K. E., I. Garcia, and M. Aguilar. "TiO_2 photocatalytic degradation of dimethyl-and diethyl-methylphosphonate, effects of catalyst and environmental factors." *Research on chemical intermediates* 23, no. 4 (1997): 325-339.
126. Obee, Timothy N., and Sunita Satyapal. "Photocatalytic decomposition of DMMP on titania." *Journal of Photochemistry and Photobiology A: Chemistry*118, no. 1 (1998): 45-51.
127. Chen, Yi-Chuan, Alexandre V. Vorontsov, and Panagiotis G. Smirniotis. "Enhanced photocatalytic degradation of dimethyl methylphosphonate in the presence of low-frequency ultrasound." *Photochemical & Photobiological Sciences* 2, no. 6 (2003): 694-698.
128. Leonard, D.N., G.W. Chandler, and S. Seraphin, *Scanning Electron Microscopy*, in *Characterization of Materials*. 2002, John Wiley & Sons, Inc.
129. Wittke, J.H. *Scanning Electron Microscope*. 2008; Available from: http://saturno.fmc.uam.es/web/superficies/instrumentacion/Instrumentation.htm.
130. Lavina, Barbara, Przemyslaw Dera, and Robert T. Downs. "Modern X-ray diffraction methods in mineralogy and geosciences." *Reviews in Mineralogy and Geochemistry* 78, no. 1 (2014): 1-31.
131. Nina Hwang, A.R.B. *BET Surface Area Analysis of Nanoparticles*. Available from: http://cnx.org/contents/9cBY4EHy@1/BET-Surface-Area-Analysis-of-N.

132. Bansal, Palak, Anoop Verma, Kashish Aggarwal, Amanjit Singh, and Saurabh Gupta. "Investigations on the degradation of an antibiotic Cephalexin using suspended and supported TiO_2: Mineralization and durability studies." *The Canadian Journal of Chemical Engineering* 94, no. 7 (2016): 1269-1276.